INTERNATIONAL SCIENTIFIC JOURNAL

INDUSTRY 4.0

ISSN (PRINT) 2534-8582
ISSN (WEB) 2534-997X

YEAR VI ISSUE 1/2021

PUBLISHED BY
SCIENTIFIC TECHNICAL UNION OF MECHANICAL ENGINEERING
“INDUSTRY 4.0”, BULGARIA

INTERNATIONAL SCIENTIFIC JOURNAL

INDUSTRY 4.0

YEAR VI, ISSUE 1 / 2021

ISSN (PRINT) 2534-8582, ISSN (WEB) 2534-997X

PUBLISHER

SCIENTIFIC TECHNICAL UNION OF MECHANICAL ENGINEERING "INDUSTRY 4.0"

108, Rakovski Str., 1000 Sofia, Bulgaria
tel. (+359 2) 987 72 90,
tel./fax (+359 2) 986 22 40,
office@stumejournals.com
WWW.STUMEJOURNALS.COM

C O N T E N T S

Generation of test sequences with a given switching activity

Mikalai Shauchenka
Weird Science Club, Lichtenbergschule Darmstadt
Ludwigshöhstraße 105, 64285 Darmstadt, Germany
nik.sh.de@gmail.com

Abstract: *The Proposed study is based on the universal method of quasi-random Sobol sequences generation, efficiently used for address test sequence formation. As the mathematical model, a modification of the economical method of Antonov and Saleev is used. The main idea of the suggested approach is the use of generating matrixes with not necessarily the maximum rank for the procedure of generating test patterns. The proposed approach allows the generation of significantly more different sequences with different switching activities of the individual bits as well as the sequences itself. Mathematical expressions are obtained that make it possible to estimate the limiting values of the switching activity, both of the test sequence itself and the individual bits. Examples of the application of the proposed methods are considered.*

Keywords*: COMPUTER SYSTEM TESTING, ADDRESS TEST SEQUENCES, SWITCHING ACTIVITY, MULTIPLE TESTING, MODIFIED SOBOL SEQUENCES*

1. Introduction

The testing of modern computing systems such as embedded systems, systems on a chip, and nets on a chip is important and is in demand at the present time [1, 2, 3]. There are numerous approaches and new solutions aimed to increase efficiency of modern computer system testing. Among them the deterministic tests play a crucial role, such as the *counting sequences*, *Gray sequences*, *anti-Gray sequences*, sequences with *maximal Hamming distance*, and many others [4, 5]. Such sequences are usually periodic and are often called *enumeration sequences*, *de Bruijn sequences*, or sequences of *maximum length* [5]. There are many kinds of maximum length sequences. Each of these test sequences is described by its unique algorithm that suggests a specific implementation and has characteristics that are common with the other sequences. As the general characteristic of a test sequence, the most commonly used one is the so-called *switching activity*, which affects the switching activity of the tested computer systems [4–8].

Address sequences as subset of periodic tests have been investigated within the framework of the memory built-in self-testing [9–13], and multi-run memory testing [14–16]. The main feature of this kind sequence is that it consists of the entire set of binary vectors including all possible 2^m binary combinations, where m is the address length in bit. The task of generating the desired address sequence can therefore be regarded as the generation of m-dimensional binary vectors in binary space.

There is no doubt that the efficiency of the test is a major design issue. To achieve higher efficiency, a characteristic like the switching activity very often plays the crucial role. At the same time, the restriction on the set of the patterns (which is always 2^m) in address sequences may reduce the efficiency of the memory test procedures. To overcome this tradeoff the new approach as the extension of the idea of address sequences generation for a general case of the test sequences with specified values of switching activities is proposed and analyzed in this paper. The motivation for this work is to design an efficient test sequence generator, which allows to generate significantly more different sequences with different switching activities of the individual bits of an address and of the whole sequence itself.

2. Mathematical Model

To significantly reduce hardware overhead needed to generate many different address sequences, a mathematical model of a universal generator was considered and investigated [15]. An address sequence is an ordered sequence of m-bit binary vectors $A(n) = a_{m-1}(n)\, a_{m-2}(n)a_{m-3}(n) \ldots a_1(n)a_0(n)$, $a_i(n)\in\{0, 1\}$, $i\in\{0, 1, 2, \ldots, m-1\}$ and $n\in\{0, 1, 2, \ldots, 2^m-1\}$ where the vectors take all possible values $\{0, 1, 2, ..., 2^m-1\}$ exactly once. As the basis of this model, a modified method of *Sobol sequence* generation is used [11, 16, 18]. According to this model, the nth element $A(n) = a_{m-1}(n)a_{m-2}(n)a_{m-3}(n) \ldots a_1(n)a_0(n)$, of the *Sobol* sequence is formed in accordance with the following recurrence relation

$$A(n) = A(n-1) \oplus v_i, \quad n = \overline{0, 2^m-1}, i = \overline{0, m-1}, \qquad (1)$$

in which only one modified direction number $v_i = \beta_{m-1}(i)\beta_{m-2}(i)\beta_{m-3}(i) \ldots \beta_1(i)\beta_0(i)$, $i\in\{0, 1, 2, ..., m-1\}$ is added to the previous element $A(n-1)$ of the *Sobol* sequence [15]. The value of the index i of the direction number v_i that is used in expression (1) as a term depends on the so-called *switching sequence* T_{m-1} of the *reflected Gray code* [15, 18]. For example, for $m = 4$, the switching sequence has the form T_3 = 0, 1, 0, 2, 0, 1, 0, 3, 0, 1, 0, 2, 0, 1, 0, which represents the sequence of indices $i\in\{0, 1, 2, 3\}$ that are used for the generation of the sequence $A(n) = a_3(n)a_2(n)a_1(n)a_0(n)$ for $m = 4$ according to (1). Using an arbitrary initial value $A(0)\in\{0, 1, 2, ..., 2^m-1\}$, the recurrence relation (1) allows to obtain all other $2^m - 1$ values of $A(n)$ [15, 18]. This mathematical model was generalized for the case of sequences that are related to not only the set of quasi-random test sets [18]. In a general case, any binary square matrix of dimension $m \times m$ can be used as a generating matrix V consisting of direction numbers v_i, $i\in\{0, 1, 2, ..., m-1\}$

$$V = \begin{vmatrix} \beta_{m-1}(0) & \beta_{m-2}(0) & \beta_{m-3}(0) & \ldots & \beta_0(0) \\ \beta_{m-1}(1) & \beta_{m-2}(1) & \beta_{m-3}(1) & \ldots & \beta_0(1) \\ \beta_{m-1}(2) & \beta_{m-2}(2) & \beta_{m-3}(2) & \ldots & \beta_0(2) \\ \ldots & \ldots & \ldots & \ldots & \ldots \\ \beta_{m-1}(m-1) & \beta_{m-2}(m-1) & \beta_{m-3}(m-1) & \ldots & \beta_0(m-1) \end{vmatrix}, \qquad (2)$$

constructed from m linearly independent binary vectors $v_i = \beta_{m-1}(i)\beta_{m-2}(i)\beta_{m-3}(i) \ldots \beta_1(i)\beta_0(i)$, $i = \overline{0, m-1}$. Linear independence is a necessary condition to generate all entries of the address sequence. In this case the matrix (2) has the maximal rank.

To evaluate the properties of modified *Sobol* sequences $A(n) = a_{m-1}(n)a_{m-2}(n)a_{m-3}(n) \ldots a_1(n)a_0(n)$ when used as a test sequence, the metric $F(a_j)$, $j\in\{0, 1, 2, ..., m-1\}$, which determines the number of switches (changes) of the jth digit a_j of the sequence $A(n)$ has been proposed and analyzed in [15]. This metric $F(a_j)$ is called *switching activity* [6, 8, 18] and determines the total number of switches of the jth digit of the test patterns $A(n)$ when all 2^m patterns are generated.

3. Proposed method

As was shown earlier [11, 15–16, 18], the use of generating matrices (2) of maximum rank allows to generate a wide range of sequences having a maximum length of 2^m. Such sequences were often called address sequence because they are composed from the whole set of non-repeating binary *m*-bit patterns. The requirement of maximizing the rank of the generating matrix *V* allows to obtain all 2^m binary combinations in the generated sequence $A(n)$ (1), however, they impose several restrictions on the properties of such sequences [18].

The proposed solution is based on the extension of the mathematical model (1) in terms of generating matrix *V*, which in this case does not have to have the maximal rank. This modification will allow to generate a wider spectrum of test sequences with a desired switching activity than the known solutions [15, 18]. As the examples of such an approach, Table 1 contains some sequences $A(n)$ obtained according to (1) with multiple generating matrixes *V* for $m = 4$ with the ranks less than 4.

The first (V_1) is the trivial solution to generate the sequence $A(n)$ with the maximum switching activity $F_{av}(A) = 4$, which equals *m* for general case. It should be mentioned that the sequence $A(n)$ consists from two patterns, namely arbitrary $A(0)$ and its negation, as presented in Table 1, where $A(0) = 0\ 1\ 0\ 0$ and $\overline{A(0)} = 1\ 0\ 1\ 1$. The rank of the matrix V_1 equals to 1, matrix V_2 has rank 1, and matrix V_3 has rank 3. In all these cases the test sequence $A(n)$ is a periodic sequence with the period being less than $2^m = 2^4$. At the same time the matrix V_4 with rank 2 used in (1) for test sequence generation provides the output sequence with the maximum period of 2^4 but does not include all possible 4-bit binary combinations.

A brief analysis of the examples presented in Table 1, allows to make conclude that in a case of a random matrix *V* with an arbitrary rank there are different types of test sequences $A(n)$ generated by equation (1). The type of test sequences called address sequence in

V	V_1	V_2	V_3	V_4	V_5
$\beta_3(0)\beta_2(0)\beta_1(0)\beta_0(0)$ $\beta_3(1)\beta_2(1)\beta_1(1)\beta_0(1)$ $\beta_3(2)\beta_2(2)\beta_1(2)\beta_0(2)$ $\beta_3(3)\beta_2(3)\beta_1(3)\beta_0(3)$	1 1 1 1 1 1 1 1 1 1 1 1 1 1 1 1	1 1 1 1 0 0 0 0 0 0 0 0 0 0 0 0	0 0 1 0 1 0 0 0 1 1 1 1 1 1 1 1	0 0 0 0 0 0 0 0 1 0 0 1 0 1 0 1	0 1 1 0 1 1 0 0 0 1 1 0 1 1 0 0
$A(0)$	0 1 0 0	0 0 0 0	0 0 0 0	0 0 0 0	0 0 0 0
$A(1) = A(0) \oplus v_0$	1 0 1 1	1 1 1 1	0 0 1 0	0 0 0 0	0 1 1 0
$A(2) = A(1) \oplus v_1$	0 1 0 0	1 1 1 1	1 0 1 0	0 0 0 0	1 0 1 0
$A(3) = A(2) \oplus v_0$	1 0 1 1	0 0 0 0	1 0 0 0	0 0 0 0	1 1 0 0
$A(4) = A(3) \oplus v_2$	0 1 0 0	0 0 0 0	0 1 1 1	1 0 0 1	1 0 1 0
$A(5) = A(4) \oplus v_0$	1 0 1 1	1 1 1 1	0 1 0 1	1 0 0 1	1 1 0 0
$A(6) = A(5) \oplus v_1$	0 1 0 0	1 1 1 1	1 1 0 1	1 0 0 1	0 0 0 0
$A(7) = A(6) \oplus v_0$	1 0 1 1	0 0 0 0	1 1 1 1	1 0 0 1	0 1 1 0
$A(8) = A(7) \oplus v_3$	0 1 0 0	0 0 0 0	0 0 0 0	1 1 0 0	1 0 1 0
$A(9) = A(8) \oplus v_0$	1 0 1 1	1 1 1 1	0 0 1 0	1 1 0 0	1 1 0 0
$A(10) = A(9) \oplus v_1$	0 1 0 0	1 1 1 1	1 0 1 0	1 1 0 0	0 0 0 0
$A(11) = A(10) \oplus v_0$	1 0 1 1	0 0 0 0	1 0 0 0	1 1 0 0	0 1 1 0
$A(12) = A(11) \oplus v_2$	0 1 0 0	0 0 0 0	0 1 1 1	0 1 0 1	0 0 0 0
$A(13) = A(12) \oplus v_0$	1 0 1 1	1 1 1 1	0 1 0 1	0 1 0 1	0 1 1 0
$A(14) = A(13) \oplus v_1$	0 1 0 0	1 1 1 1	1 1 0 1	0 1 0 1	1 0 1 0
$A(15) = A(14) \oplus v_0$	1 0 1 1	0 0 0 0	1 1 1 1	0 1 0 1	1 1 0 0

a case of maximal rank matrix *V*, have been thoroughly investigated in [11, 15–16, 18]. Therefore, further analysis will be focused on the general case of the sequences $A(n)$ obtained by (1) using any generating matrix *V* regardless of its rank.

First, let us to formulate the property of the sequences $A(n)$ generated based on relation (1) using a random generating matrix *V* (2).

The switching activity $F(a_j)$, for the *j*th $j \in \{0, 1, 2, ..., m-1\}$ digit a_j of the sequence $A(n) = a_{m-1}(n)\ a_{m-2}(n)a_{m-3}(n)\ ...\ a_1(n)a_0(n)$ generated according to (1) takes values in the range from 0 to $2^m - 1$. The value of this switching activity $F(a_j) = 0$ for the *j*th bit of the $A(n)$ generated according to (1) is provided by the *j*th all zero column in the generating matrix *V*, as it was shown in Table 1 (see V_4 and V_5). Maximal switching activity $F(a_j) = 2^m - 1$ for the *j*th bit of the $A(n)$ corresponds to all ones within *j*th column in matrix *V* as it is for the cases of V_1 and V_5, shown in Table 1.

The switching activity $F(A)$ of the sequence $A(n)$, takes the minimum value $F(A) = 0$ in the case of an all zero generating matrix *V*. The maximum value of the switching activity $F(A) = m\times(2^m - 1)$ is achieved with the all ones matrix *V* (see V_1 in Table 1). The ranges of values of average switching activity values $F_{av}(A)$ and $F_{av}(a_j)$ are presented below (3).

$$\begin{aligned}
&\min\ F_{av}(a_j) = \min\ F(a_j)/(2^m - 1) = 0;\\
&\max\ F_{av}(a_j) = \max\ F(a_j)/(2^m - 1) = 1;\\
&\min\ F_{av}(A) = \min\ F(A)/(2^m - 1) = 0;\\
&\max\ F_{av}(A) = \max\ F(A)/(2^m - 1) = m.
\end{aligned} \tag{3}$$

A wide range of possible values of switching activity (3), as well as the absence of many restrictions on their mutual relationship allows us to generate a significantly larger number of test sequences with specified values of switching activities.

4. Maximal Length Test Sequences

As the test sequence $A(n) = a_{m-1}(n)a_{m-2}(n)a_{m-2}(n)\ \ldots\ a_1(n)a_0(n)$, where $a_i(n) \in \{0, 1\}$, $i \in \{0, 1, 2, \ldots, m-1\}$, and $n \in \{0, 1, 2, \ldots, 2^m - 1\}$, *m*-dimensional binary vectors in binary space were considered [18]. The generation of the specified test sequence has been regarded as the generation of *m*-dimensional binary vectors in binary space. The set of linearly independent vectors $v_i^* = \beta_{m-1}^*(i)\beta_{m-2}^*(i)\beta_{m-3}^*(i)\ \ldots\ \beta_1^*(i)\beta_0^*(i)$, $i \in \{0, 1, 2, ..., m-1\}$, generates the *m*-dimensional binary vectors $A(n)$ through all their possible linear combinations [19, 20]:

$$A^*(n) = v_0^* \times b_0(n) \oplus v_1^* \times b_1(n) \oplus v_2^* \times b_2(n) \oplus ... \oplus v_{m-1}^* \times b_{m-1}(n). \tag{4}$$

$B(n) = b_{m-1}(n)b_{m-2}(n)b_{m-3}(n)\ \ldots\ b_1(n)b_0(n)$; $b_i(n) \in \{0, 1\}$, $i \in \{0, 1, 2, \ldots, m-1\}$ is any binary vector set consisting of all possible 2^m binary combinations. Then the vector space $A^*(n)$ formed according to (4) is of dimension *m* and consists of all 2^m vectors, and that is why vectors $A^*(n)$ can be used as an address sequence [18]. For further investigations, the set of vectors $B(n)$ is regarded as the *Linear sequence* or simply the binary *Up-counter* sequence.

Application of the Gray code sequence in (4) was the productive idea for recursive generation of the quasi-random *Sobol* sequences according to (1) [21]. Relation between the output sequence $A^*(n)$ and $A(n)$ generated based on linear sequence (4) and Gray sequence (1) can be described in terms of corresponding generation matrixes V^* and *V*.

For this sequences $A^*(n)$ and $A(n)$ the next statement is true.

Statement 1. Sequence $A^*(n)$ generated as *m*-dimensional binary vectors according to (4) based on any generating *m* by *m* matrix *V** can also be obtained from the recursive relation (1) ($A(n) = A^*(n)$) with matrix *V* obtained from (7), and vice versa.

$$V=\begin{vmatrix} v_0 \\ v_1 \\ v_2 \\ \dots \\ v_{m-2} \\ v_{m-1} \end{vmatrix}=\begin{vmatrix} v_0^* \\ v_0^*\oplus v_1^* \\ v_0^*\oplus v_1^*\oplus v_2^* \\ \dots \\ v_0^*\oplus v_1^*\oplus v_2^*\oplus\dots\oplus v_{m-2}^* \\ v_0^*\oplus v_1^*\oplus v_2^*\oplus\dots\oplus v_{m-1}^* \end{vmatrix};\quad V^*=\begin{vmatrix} v_0^* \\ v_1^* \\ v_2^* \\ \dots \\ v_{m-2}^* \\ v_{m-1}^* \end{vmatrix}=\begin{vmatrix} v_0 \\ v_0\oplus v_1 \\ v_1\oplus v_2 \\ \dots \\ v_{m-3}\oplus v_{m-2} \\ v_{m-2}\oplus v_{m-1} \end{vmatrix}. \quad (5)$$

For example, corresponding matrix V_5^* for the matrix V_5, shown in Table 1 has the form

$$V_5^* == \begin{vmatrix} 0 & 1 & 1 & 0 \\ 1 & 0 & 1 & 0 \\ 1 & 0 & 1 & 0 \\ 1 & 0 & 1 & 0 \end{vmatrix},$$

and it is obvious that the sequence $A^*(n)$ (4) generated based on V_5^* is identical to the sequence $A(n)$ (1) generated according to V_5.

Statement 1 allows to make the conclusion that the resulting sequence $A(n)$ obtained from the recursive relation (1) is the linear combination of the binary sequences $b_i(n)\in\{0,1\}$, $i\in\{0, 1, 2, \dots, m-1\}$ representing the counter sequence $B(n)$. The sequence $b_i(n)$ has period equals to 2^{i+1}, that is why the period of $A^*(n)$ will be equal to the maximal period when linear sum (4) includes $b_{m-1}(n)$, what follows from next statement [19].

Statement 2. The sum $A^*(n)$ (4) of the periodic binary counting sequences $b_i(n)\in\{0, 1\}$, $i\in\{0, 1, 2, \dots, m-1\}$ has the period 2^{j+1}, where j is the maximal index of the nonzero values of v_i^*.

Based on the last statement, it is easy to obtain a condition for the formation of a sequence $A(n)$ with the maximal period which consists in the fulfillment of the inequality $v_{m-2} \neq v_{m-1}$. This inequality follows from the following affirmation. According to statement the maximal length sequence $A^*(n)$ will be obtained in a case when $v_{m-1}^* \neq 0$. Then to get the sequence $A(n) = A^*(n)$ the next condition should be accomplished $v_{m-2}\oplus v_{m-1} \neq 0$ (see (5)).

Table 1 contains two examples of $A(n)$ with the maximal period 2^4 for the case of two generating matrixes V_4 and V_5, due to for both matrixes $v_2 \neq v_3$. There are three matrixes V_1, V_2 and V_3 in Table 1 with $v_2 = v_3$, which correspond to the sequences with a period less than 2^4.

5. Generation of Test Sequences with Specified Switching Activities

Considering the wide range of applications of test sequences with specified values of switching activities $A(n)$ [5–10, 18], the problems of finding a generator for such sequences can be formulated as follows:

Find the generating matrix V (2), which provides the required values of $F_{av}(A)$ and $F_{av}(a_i)$ of the sequence $A(n) = a_{m-1}(n)a_{m-2}(n)a_{m-3}(n) \dots a_1(n)a_0(n)$, $a_i(n)\in\{0, 1\}$, $i\in\{0, 1, 2, \dots, m-1\}$ and $n\in\{0, 1, 2, \dots, 2^m-1\}$, where the desired values $F_{av}(A)$ and $F_{av}(a_i)$ do not exceed their bounds (3).

There are three cases of this design problem. The first case is the test sequence with a desired $F_{av}(A)$ and the second is specified $F_{av}(a_i)$ for $k \leq m$ digits $a_{\alpha1}, a_{\alpha2}, a_{\alpha3}, \dots, a_{\alpha k}$, $\alpha i\in\{0, 1, 2, \dots, m-1\}$ $i=\overline{1,k}$, of the sequence $A(n)$. The third case is the union of the first two.

Let´s show the solutions for all those three types of problems using the algorithm of partition of a positive integer number $F(A) = (2^m-1)\times F_{av}(A)$, that is the basis for matrix V construction as it was shown in [18].

Algorithm for partitioning an integer into terms:

Input data: An integer $F(A)$ belonging to the range from 0 to $m\times(2^m-1)$; The terms should belong to the set of in integer values 2^i, where $i\in\{0, 1, 2, \dots, m-1\}$ to obtain a partition of the integer $F(A)$.

1. Initially, the sum of all terms 2^i is formed, which is equal to the maximum m-bit binary number 2^m-1.

2. The division operation $F(A)$ by 2^m-1 is performed. The resulting quotient q determines the minimum amount of use of each of the terms 2^i in the partition of the integer $F(A)$. If the remainder r of the division operation is zero, the quotient q is the number of uses of each of the terms 2^i in the partition $F(A)$, and at this step the partition algorithm ends. Otherwise, the next step is performed.

3. The remainder $0 < r < 2^m-1$ from the division operation performed in the previous step is represented in the binary code $r = b_{m-1}\times2^{m-1} + b_{m-2}\times2^{m-2} + b_{m-3}\times2^{m-3} + \dots + b_0\times2^0$, $b_i\in\{0, 1\}$.

4. The partition of the integer $F(A)$ into terms 2^i is constructed, where $i\in\{0, 1, 2, \dots, m-1\}$, each of the terms is included in the partition $q + b_{m-1-i}$ times. The quantity $q + b_{m-1-i}$ determines the value of the Hamming weight $w(v_i)$ of the binary vector $v_i = \beta_{m-1}(i)\beta_{m-2}(i)\beta_{m-3}(i) \dots \beta_1(i)\beta_0(i)$, which is the result of applying this algorithm.

Problem 1. Find the generating matrix V for the sequence $A(n)$ for a given value of m and the desired value of $F_{av}(A)$.

The solution of the problem 1 will be as follows: obtaining $F(A) = \mathrm{int}[2^m\times F_{av}(A)]$; partitioning the integer $F(A)$ into terms [18]; obtaining the values of the row weights $w(v_i)$ of the desired generating matrix V and finding the matrix with maximal rank corresponding to the given values of m and $w(v_i)$. The matrix with maximal rank is chosen from the matrix with the restriction that $v_{m-1} \neq v_m$, which guarantees the maximal length of the sequence $A(n)$. The maximal rank of the matrix V is the requirement to get maximal number of binary combinations $a_{m-1}(n)a_{m-2}(n)a_{m-3}(n) \dots a_1(n)a_0(n)$ within $A(n)$ [19].

*Problem 2***.** For a given value m find the generating matrix V for sequence $A(n)$, in which specified $F_{av}(a_j)$ for $k \leq m$ digits $a_{\alpha1}, a_{\alpha2}, a_{\alpha3}, \dots, a_{\alpha k}$, $\alpha j\in\{0, 1, 2, \dots, m-1\}$ $j=\overline{1,k}$, are determined.

Initially, as in the case of Problem 1, the average values $F_{av}(a_{\alpha1})$, $F_{av}(a_{\alpha2})$, $F_{av}(a_{\alpha3})$, …, $F_{av}(a_{\alpha k})$ of switching activities are represented as total values of the number of switching bits $a_{\alpha1}, a_{\alpha2}, a_{\alpha3}, \dots, a_{\alpha k}$ of $A(n)$. These values $F(a_{\alpha1})$, $F(a_{\alpha2})$, $F(a_{\alpha3})$, …, $F(a_{\alpha k})$ are determined according to the relation $F(a_{\alpha j}) = \mathrm{int}\,[F_{av}(a_{\alpha j})\times(2^m-1)]$. Then, $F(a_{\alpha j})$ is converted to an m-bit code represented in the binary number system $F(a_{\alpha j})_{(10)} = F(a_{\alpha j})_{(2)} = \beta_{\alpha j}(0)\times2^{m-1} + \beta_{\alpha j}(1)\times2^{m-2} + \beta_{\alpha j}(2)\times2^{m-3} + \dots + \beta_{\alpha j}(m-1)\times2^0$. The values of all $k \leq m$ columns of the matrix V are calculated, which provides the switching activities $F_{av}(a_{\alpha1})$, $F_{av}(a_{\alpha2})$, $F_{av}(a_{\alpha3})$, …, $F_{av}(a_{\alpha k})$. The next step in solving Problem 2 is to randomly (equally likely and independently) generate the remaining columns of the binary matrix V. From the resulting matrixes, the matrix with the highest rank must be selected.

Problem 3. For a given value m find the generating matrix V for sequence $A(n)$, in which specified $F_{av}(a_j)$ for $k \leq m$ digits $a_{\alpha1}, a_{\alpha2}, a_{\alpha3}, \dots, a_{\alpha k}$, $\alpha j\in\{0, 1, 2, \dots, m-1\}$ $j=\overline{1,k}$, are determined, and the switching activity $A(n)$ equals $F_{av}(A)$.

The correct formulation of Problem 3 assumes that $F_{av}(a_{\alpha1}) + F_{av}(a_{\alpha2}) + F_{av}(a_{\alpha3}) + \dots + F_{av}(a_{\alpha k}) < F_{av}(A) \leq m$. At the initial stage, the solution of Problem 3 repeats the solution to Problem 2. Next, the steps of the procedure for solving Problem 1 are performed. The difference is the partition on the terms have to be performed on the integer $F^*(A) = \text{int}[F_{av}(A) \times (2^m - 1)] - \text{int}[F_{av}(a_{\alpha 1}) \times (2^m - 1)] - \text{int}[F_{av}(a_{\alpha 2}) \times (2^m - 1)] - ... - \text{int}[F_{av}(a_{\alpha k}) \times (2^m - 1)]$. In addition, when obtaining the row weights $w(v_i)$ of the desired generating matrix V, it is necessary to consider the row weights of the previously generated k columns.

The partition of the integer $F^*(A)$ into terms 2^i is constructed, where each term is included in the partition $q + b_{m-1-i} = 1 + 0$ times. Since $r = 0000$, the terms 2^3, 2^2, 2^1 are included in the partition of 15 only once. The value $q + b_{m-1-i}$ determines the Hamming weight of the rows of the desired matrix V, consisting of four rows and four columns, excluding the first and third columns. Then, randomly generated values of six two-digit binary vectors with Hamming weights equal to $w(v_0) = w(v_1) = w(v_2) = w(v_3) = 1$, which will be determine the values of the remaining columns (except the first and third) of the desired matrix. For the matrixes thus obtained, the maximal of its rank is determined. One of the possible solutions of this example may be the matrix V_5, shown in Table 1.

6. Conclusion

The use of a modified mathematical model for the *Sobol* sequences generation has allowed to expand the capabilities of the test sequence generator in terms of a significant increase in the number of different types of such sequences. The paper describes a method for constructing a test sequences with given values of switching activity, of the test patterns and the activity of their bits. The essence of the method consists in the synthesis of the required generating matrix providing specified values of switching activity. The limitations of the previously proposed and investigated techniques associated with possible conflicting requirements for the values of the weights of the rows of the matrix and their linear independence are shown. The main idea that distinguishes the results obtained in this article is the use of arbitrary matrices for which the condition that ensures the maximum period of the test sequence is fulfilled. Of the many matrices for which this condition is satisfied, it is necessary to use matrices with a maximum rank. In this case, not only the required values of the switching activity are provided, but also a larger number of test patterns in the sequence. Examples of the use of such sequences for the purpose of constructing a test pattern generator are considered.

7. References

[1] M.L. Bushnell and V.D. Agrawal, New York: Kluwer Academic Publishers, *Essentials of Electronic Testing for Digital, Memory & Mixed-Signal VLSI Circuits* (2000).

[2] L.-T. Wang, C.-W. Wu and X. Wen, New York: Elsevier Inc. *VLSI Test Principles and Architectures: Design for Testability*. (2006).

[3] I. A. Grout, Springer-Verlag, *Integrated Circuit Test Engineering. Modern Techniques* (2006).

[4] E.J. Marinissen, B. Prince, D. Keitel-Schulz and Y. Zorian, Proc. of Design, Automation and Test in Europe Conference and Exhibition, Munich, Germany, *Challenges in Embedded Memory Design and Test*, pp. 722–727 (2005).

[5] V.N. Yarmolik, Bestprint, *Kontrol' I diagnostika vuchislitel'nuh system* (2019).

[6] I. Pomeranz, IEEE Trans. Comput., *An Adjacent Switching Activity Metric under Functional Broadside Tests*, **vol. 62**, **№ 4**, pp. 404–410 (2013).

[7] P.A Girard, L. Guiller, C. Landrault, and S. Pravossondovitch, Proc. Ninth Great Lakes Symposium on VLSI, *A test vector ordering technique for switching activity reduction during test operation*, pp. 24–27 (1999).

[8] S. Wang and S.K. Gupta, IEEE Trans. Comput.-Aided Design of Integr. Circuits and Systems, *An automatic test pattern generator for minimizing switching activity during scan testing activity*, **vol. 21**, **№ 8**, pp. 954–968 (2002).

[9] S. Saravanan, M. Hailu, G.M. Gouse, M. Lavanya, and R. Vijaysai, Proc. of 6th EAI International Conference, ICAST, Bahir Dar, Ethiopia, *Design and Analysis of Low-Transition Address Generator* (2018).

[10] P.A. Pavani, G. Anitha, J. Bhavana, and J.P. Raj, Inter. J. of Scien. & Eng. Research, *Novel Architecture Design of Address Generators for BIST Algorithms*, **vol. 7**, **№ 2**, pp. 1484–1488 (2016).

[11] V.N. Yarmolik, and S.V. Yarmolik, Autom. Control Comput. Sci, *Address sequences*, pp. 207–213, **vol. 48**, **№ 4** (2014).

[13] B. Singh, S. Narang, and A. Khosla, IJCSI Int. J. Comput Sci. Issues, *Address Counter / Generators for Low Power Memory BIST*, **vol. 8**, **Issue 4**, **№ 1**, pp. 561–567 (2011)

[14] I. Mrozek and V.N. Yarmolik, Journal of Electronic Testing: Theory and Applications, *Iterative Antirandom Testing*, **vol. 9**, **№ 3**, pp. 251–266

[15] Yarmolik, V.N. and Yarmolik, S.V., Generating Modified Sobol Sequences for Multiple Run March Memory Test, *Autom. Control Comput. Sci*, vol. 47, № 5, pp. 242–247 (2013).

[16] V.N. Yarmolik, and S.V. Yarmolik, Autom. Control Comput. Sci, *Address sequences for multiple-run March tests of random-access memory*, **vol. 40**, **№ 5**, pp. 42–49. (2006)

[17] A.J. Goor, H. Kukner, and S. Hamdioui, , Proc. of 2011 6th Int. Conf. on Design & Tech. of Integrated Systems in Nanoscale Era, *Optimizing memory BIST Address Generator implementations*, pp. 572–576 (2011).

[18] V.N. Yarmolik, and M.A. Shauchenka, Informatics, *Generation of address sequences with a given switching activity* **vol. 17**, **№ 1**, pp. 47–62 (2020).

[19] S. Boyd, Cambridge, UK: University Printing House, *Introduction to Applied Linear Algebra: Vectors, Matrices, and Least Squares* (2018).

[20] P. Ferreira, B. Jesus, J. Vieira, and A.J. Pinho, IEEE Communic. Let., *The Rank of Random Binary Matrices and Distributed Storage Applications*, **vol. 17**, **№ 1**, pp. 151–154 (2013).

[21] I.A. Antonov, and V.M. Saleev, Zh. Vychisl. Matem. Mat. Fiz, *Economical method of LP sequences calculation*, **vol. 19**, pp. 243–245 (1979).

On the acoustic unit choice for the keyword spotting problem

Aliaksei Kolesau[1,*], Dmitrij Šešok[1]
Department of Information Technologies, Vilnius Gediminas Technical University, Saulėtekio al. 11, LT-10223 Vilnius, Lithuania[1]
aliaksei.kolesau@vilniustech.lt

Abstract: *In this paper we examine the results of using different acoustic units for the building of keyword spotting system. The choice of the acoustic unit greatly influences the quality of the resulting system given the dataset and the model complexity. Decomposing the keyword into simple acoustic units requires the prior knowledge. This knowledge might make the task easier (so the resulting accuracy will be higher), but on the other hand even slightly incorrect priors could mislead the model so the quality might drop significantly. We compare using phonemes, syllables, words and several synthetic acoustic units for Russian language. We show that for modern keyword spotting systems phonemes is a robust and high quality choice, especially in low-resource setting.*
Keywords*: KEYWORD SPOTTING, VOICE ACTIVATION, ACOUSTIC UNIT*

1. Introduction

Voice control is used in a large number of modern mobile and embedded devices. Nevertheless the speech recognition of the whole audio stream is not possible because of both privacy and resource consumption reasons. In order to initiate a voice control most devices use a voice activation system. Its task is to find the specified keyword (e.g. “Alexa”) or keyphrase (“Ok, Google”) in the audio stream and pass the control for more high-level system. Because of the embedded usage keyword spotting system must have a high accuracy, work in real-time and consume a small amount of CPU and RAM.

The keyword spotting task has been attracting both research [1], [2] and industry [3], [4] for several decades. Since the task of formulating an algorithm for determining whether a code phrase has been uttered in an audio stream is difficult to formulate, it is not surprising that heuristic algorithms and machine learning methods have long been used for the voice activation problem [5].

The requirements of working in real-time fashion and consuming a small amount of CPU make a restriction on the size of the keyword spotting model. This in turn limits the complexity and the modeling power of the model. In order to solve the hard problem of finding the keyphrase we can decompose the problem into detecting simpler acoustic events such as syllables or phonemes. The linguistic prior knowledge of how the keyword is decomposed in the smaller parts might greatly improve the quality of the system and make it more interpretable. On the other hand such decompositions are only the approximations of the real world. Building end-to-end model might be more profitable when a large dataset and a big model are available.

This paper examines using the phonemes, syllables, words, uniform and adaptive splitting of the words as target acoustic events. Also we investigate the question of using as targets the events that happen only inside the keyword or all the events of the given type (e.g. phoneme “g” happens not only in “Google”, but also, for example, in ”great” – should we use it as a target during the learning of the model?).

2. Typical voice activation system

Most of modern voice activation systems consist of the following parts [5]:

- feature extraction,
- acoustic model,
- decoding.

Feature extraction is the part of converting the source audio stream into acoustic features. Usually it is done by segmenting the audio and computing some signal processing transformation for each segment (frame) separately. In this paper we compute 80 log-mel filterbanks for the frames of 25 ms length and 10 ms offset.

Acoustic model is a system that generally computes the probability of acoustic observations, which often comes down to computing $P(u \mid O)$, where u is an acoustic unit and O are acoustic observations).

The decoding is the process of determining the state sequence with the reference to acoustic observation and acoustic model in order to determine whether a keyword has been uttered or not.

We follow the example of [3], where authors apply an acoustic model in a form of deep neural network to extracted log-mel filterbanks (feature extraction) and decide whether the keyword was uttered by aggregating deep neural network outputs and comparing them with a threshold (decoding). See Fig. 1 for the illustration.

The aggregation of the acoustic model outputs consists of the two following steps.

Raw posteriors from the neural network are noisy, so we smooth the posteriors over a fixed time window of size W (frames). Let's denote by $p_{f,i}$ the i-th output of the neural network at the frame f. Then the smoothed output $p'_{f,i}$ is computed by:

$$p'_{f,i} = \frac{1}{f - H + 1} \sum_{k=H}^{f} p_{k,i}, \tag{1}$$

where $H = \max\{1, f - W + 1\}$ is the index of the first frame within the smoothing window.

The probability p_f of the keyphrase utterance ending in the frame f is computed with a sliding window of the length S frames, as follows:

$$p_f = \max_{F \le f_1 < f_2 < \ldots < f_n = f} \sqrt[n]{\prod_{i=1}^{n} p'_{f_i,i}}, \tag{2}$$

where $F = \max\{1, f - H + 1\}$ is the index of the first frame within the sliding window, f_i is the index of the frame where the i-th acoustic event has happened according to the model, n is the number of consecutive acoustic events that must happen in order for the whole keyphrase to happen. For example, in order for the work “Alexa” to happen, five following phoneme events must happen: “a”, “l”, “e”, “x”, “a”.

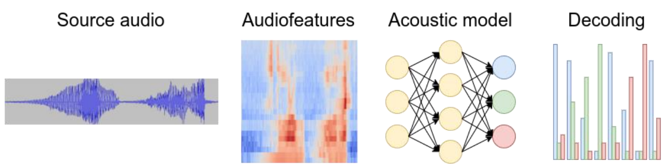

Fig. 1 In the first stage we compute log-mel filterbanks for the source audio. Next we apply neural network. Each output gives the probability of the the specific acoustic event happening in the current frame. Finally we aggregate all these probabilities to get the resulting probability of keyphrase utterance.

3. Acoustic units

In this section we describe all the acoustic unit types we used in our experiments.

3.1 Phonemes

In phonology, a phoneme is a unit of sound that dis tinguishes one word from another in a particular language [6]. For example, in English the words "sin" and "sing" are distinguishable by the phoneme "g". International Phonetic Alphabet is the example of phonetic alphabet suitable for different languages.

Each phoneme of the target keyword can occur not only in the keyword itself, but in the other words. There is a choice of how to handle these occurrences during the training. We denote by "own phonemes" the variant when we optimize our neural network to use only the phonemes in the keyword as targets (and handle other cases as fillers) and by "all phonemes" the case when we optimize the neural network to find the phonemes regardless of whether they are the part of keyword or other word.

"Own phonemes" choice encourages the model to learn the contextual information. It might improve the accuracy of voice activation system, but at the same time the real targets are not phonemes anymore, which may "confuse" the model and thetraining may fail.

3.2 Syllables

A syllable is a unit of organization for a sequence of speech sounds [7]. It is typically made of a syllable nucleus (most often a vowel) with optional initial and final margins (typically, consonants). For this paper we consider the syllable as a sequence of phonemes.

As with phonemes, we have the choices of "own syllables" and "all syllables". The number of syllables per word is almost always less than the number of phonemes per word, so this choice makes a neural network and a decoding a bit simpler, but the duration of syllable is more variable so the distinction task can be more complex.

3.3 Words

As a baseline we can use the whole word as a target. For example we need two neural network outputs for one word keyphrases: the filler probability and the word probability itself.

3.4 Phoneme transitions targets

We tried to use the transition between phonemes as our targets. It reduces the number of targets by one comparing to phonemes. We also distinguish "all" and "own" scenario for this target type.

3.5 Uniform and adaptive targets

The decomposition of words into phonemes is performed with some assumptions based on the linguistic knowledge. It can be argued, that as an every model it has its errors, so it might be profitable to use simple decomposition and let a neural network to deduce actual patterns from data. In order to check this hypothesis we propose two methods of decomposing words into subword targets.

First, we split word into n parts uniformly by the duration of the word. We call this option "uniform targets". n is chosen via hyperparameter search.

The phonemes are irregular in duration. That's why uniform splitting might result in very different types: several phonemes, one phoneme, transition between phonemes. Therefore we propose the second way of splitting the word: "adaptive targets". Here we split the word in n parts minimizing the sum of distances from the frame to the average frame in the split in log-mel filterbank space. This can be done effectively via dynamic programming. As for "uniform target" we choose n via hypeparameter search.

4. Experiments

4.1 Dataset

For our experiments we used our Russian in-house private dataset of 174619 audio files, 139516 were used for training, 17820 for validation and 17283 for testing. We got the phoneme targets via forced alignment with our speech recognition model. The keywords we used for our experiments are shown in Table 1.

Table 1: *The keywords used for our experiments.*

Word	Phonemes	Syllables	Positive samples in the testset
"Алиса" (Alice)	5	3	7455
"Включи" (turn on)	6	2	542
"Тебя" (you)	4	2	462
"Мне" (me)	3	1	889

4.2 Model

We used a time-delay neural network (TDNN) [8] with ReLU non-linearity. The layers specifications are presented in Table 2. The whole receptive field at frame f is made up from the frame $f-28$ to the frame $f+12$. The number of units in the last layer is determined by the chosen targets. For example, if we train model to distinguish phonemes of the word "Alice" we need 6 outputs: one for the filler and 5 for the phonemes.

Table 2: *Specifications of the used neural network.*

Layer	Units	Context
1	192	[-8, 1, 2]
2	96	[-3, 2]
3	192	[-8, 1, 2]
4	96	[-3, 2]
5	192	[-3, 2]
6	96	[-3, 2]
7	-	[0]

4.3 Training

We train all our models with SGD optimizer for per-frame cross-entropy loss. The learning rate and batch size were chosen via random search. The training is performed for 10 epochs. If the validation loss between consecutive epochs differs by less than 0.001 the learning rate is decayed by the factor of 4/3.

5. Results and discussion

25 runs were made for each keyword and each target. We tune the threshold in such a way that false reject rate on the test set is less than 0.1 and the false alarm rate is minimized. The numbers of positive samples are very different for different words, so we report the relative drop of the quality comparing to the best option for the given word. The results are in Table 3. The best options are highlighted in bold. The value n is specified in the brackets, when appropriate.

Table 3: *Drop of the best false alarm rate comparing to the best choice.*

	Алиса	Включи	Тебя	Мне
Own phonemes	5%	1%		54%
All phonemes	36%	**0%**	**0%**	**0%**
Own syllables	17%	150%	114%	141%
All syllables	34%	131%	105%	137%
Own phoneme transitions	49%	24%	123%	88%
All phoneme transitions	22%	53%	91%	102%
Uniform target	**0% (6)**	19% (6)	95% (3)	35% (7)
Adaptivet arget	10% (5)	28% (8)	152% (2)	54% (7)
Word target	80%	733%	176%	139%

We suggest the following points from experiments:

• phonemes are a great choice for all cases, especially when the number of positive samples is small,

• word target gives very bad accuracy comparing to the phonemes,

• when the number of positive samples is big all the options work reasonably, but when the number is small some options are clearly better than other,

• adaptive splitting doesn't give any advantage comparing to uniform splitting.

Our experiments show that phonemes could be used as a baseline for a keyword spotting system. It can be beaten if the dataset is big, but still it shows comparable results. Also it can be seen that “own” options is preferable when the dataset is large, so the model can take advantage of the contextual information. When the dataset is small choosing “own” options greatly reduces the number of positive samples for each target, so the optimization becomes hard. Because of the same reason the “word” target doesn't show good results, because the majority of the examples are negative. We also show that uniform splitting is a simple option that can be tried to outperform the phoneme baseline.

6. Conclusions

We investigated several classical and two new acoustic units for the keyword spotting task. It can be seen from our experiments, that the phoneme target is the best choice as a baseline, but it can be beaten in some cases. Also it's a useful trick to use or don't use the acoustic events similar to target ones, but which occur not in the target keyword. It especially helps when the number of positive examples is not very high.

7. References

1. J. R. Rohlicek, W. Russell, S. Roukos, and H. Gish, “Continuous hidden markov modeling for speaker-independent word spotting,” in *International Conference on Acoustics, Speech, and Signal Processing*, May 1989, pp. 627–630 vol.1.

2. S. Myer and V. S. Tomar, “Efficient keyword spotting using time delay neural networks,” in *Interspeech 2018, 19th Annual Conference of the International Speech Communication Association, Hyderabad, India, 2-6 September 2018*., B. Yegnanarayana, Ed. ISCA, 2018, pp. 1264–1268. [Online]. Available: https://doi.org/10.21437/Interspeech.2018-1979

3. G. Chen, C. Parada, and G. Heigold, “Small-footprint keyword spotting using deep neural networks,” in *IEEE International Conference on Acoustics, Speech and Signal Processing, ICASSP 2014, Florence, Italy, May 4-9, 2014. IEEE, 2014*, pp. 4087–4091. [Online]. Available: https://doi.org/10.1109/ICASSP.2014.6854370

4. M. Wu, S. Panchapagesan, M. Sun, J. Gu, R. Thomas, S. N. P. Vitaladevuni, B. Hoffmeister, and A. Mandal, “Monophone-based background modeling for two-stage on-device wake word detection” in *2018 IEEE International Conference on Acoustics, Speech and Signal Processing, ICASSP 2018, Calgary, AB, Canada, April 15-20, 2018*. IEEE, 2018, pp. 5494–5498. [Online]. Available: https://doi.org/10.1109/ICASSP.2018.8462227

5. A. Kolesau and D. Šešok, “Voice activation systems for embedded devices: Systematic literature review,” *Informatica*, vol. **31**, no. 1, pp. 65–88, 2020.

6. Wikipedia contributors, “Phoneme — Wikipedia, the free encyclopedia,” https://en.wikipedia.org/w/index.php?title=Phoneme&oldid=1006518035, 2021, [Online; accessed 21-February-2021].

7. Wikipedia contributors, “Syllable — Wikipedia, the free encyclopedia,” https://en.wikipedia.org/w/index.php?title=Syllable&oldid=1006686720, 2021, [Online; accessed 21-February-2021].

8. T. Zeppenfeld and A. H. Waibel, “A hybrid neural network, dynamic programming word spotter,” in *[Proceedings] ICASSP-92: 1992 IEEE International Conference on Acoustics, Speech, and Signal Processing*, vol. **2**, March 1992, pp. 77–80.

Seasonal dynamics of plant sediment microbial fuel cell efficiency in a moderate continental climate zone

Rosen Ivanov
Faculty of Geology and Exploration – University of Mining and Geology, Bulgaria
rosen_iv@abv.bg

Abstract: *Plant sediment microbial fuel cells (PSMFC) transform solar energy in an environmentally friendly and efficient way. Their integration in constructed wetlands allows the generation of electricity in parallel wastewater treatment. The work of plant sediment microbial fuel cells is influenced by a number of factors, such as environmental conditions, vegetation type, hydraulic retention time, water flow, the presence of heavy metals and other contaminants in the treated water and others. The purpose of this study is to establish the seasonal dynamics of the effectiveness of PSMFC in Moderate continental climate zone. Seasonal changes in environmental conditions have a significant impact on the generation of energy from the PSMFC in regions with moderate continental climate. With the best electrical parameters the cell is characterized in spring and summer. They are significantly lower in autumn and winter. The effectiveness of PSMFC, both as a treatment facility and as electricity generation is directly related to the vegetation period of the planted vegetation and the effectiveness of the photosynthesis, which are a function of the intensity of the light, the duration of the sunshine and the average daily temperatures.*

Keywords*: PLANT SEDIMENT MICROBIAL FUEL CELLS, SEASONAL EFFICIENCY*

1. Introduction

Electricity production capturing solar energy by living higher plants and in combination with microbial fuel cell is attractive because these systems promise to generate useful renewable energy in sustained manner. [11] These systems are based on natural potential gradient between bottom sediment and upper oxygenic water. Electrons are released by microbial oxidation of organic matter and anaerobic environment of sediment and flow from anode to the cathode through an external circuit. [8] Plants are known to release organics in to soil or aquatic sediments as rhizodeposits, which comprises of carbohydrate, fatty acids, aminoacids, hormones, and organic compounds. This material, rhizodeposits, were then in situ oxidized in the bio anode of the PSMFC and transformed into electrical power. Rhizodeposits account up to 40 % of plants photosynthetic productivity. [7]

Light intensity, quality and photoperiodism are the input signal that can affect the growth of plant and system performace of PMFCs. [2] Effect of an illumination as a light cycle and a power has been studied in the photosynthehtic microbial fuel cell since it is directly linked to the metabolic activity of the microbes. [6] There is an optimal light intensity requirememt for the microbial species and the operational conditions of a system. In addition to this, in PMFCs, light plays an important role for photosynthesis resulting in the concurrent biomass and bioelectricity production. [14] Besides the optimal conditions for the heterogenous microbial community in the rhizosphere, the role of light in maximization of the root exudates with high photosynthehtic activity is an important aspect of research in a PMFC. [13] Therefore, light is not only the limiting factor for power generation while plant physiology also affects the overall performances. Thus, plants having the physiology that can convert the photosynthetic matters in root exudates with the simultaneous absorption by the microbes are well suited to PMFCs since enhanced bioenergy harvest can be achieved. [1] Nevertheless, identification of the optimum light intensity for an efficient photosynthesis, optimum microbial activity, and higher rhizodeposition are the factors that need to be researched intensively within PMFCs. [10]

The species composition of plants depends on climatic conditions and should therefore be carefully selected. The most common aquatic plants are ferns (*Typha latifolia* and *Typha angustifolia)*, reeds (Phragmites), sedges (Carex), peat moss (Sphagnum) and others. In the wetlands there are some algae - *Microspora*, *Oscillatoria*, *Zygnemophyta*. The presence of plants increases bacterial activity as it supplies microorganisms with a source of carbon and energy. [4]

The best prospects for successful energy generation should be in the tropical or subtropical regions of the world, and application of plant sediment microbial fuel cells in frigid climate presents special challenges. Nevertheless, over the past decades, studies in North America and Europe showed that energy generation from PSMFCs may be feasible also in cold climate. [9]

However, there still exists uncertainty about how temperature can affect energy generation processes. In general, plant sediment microbial fuel cells relies largely on biological and biochemical processes, and reliable energy generation is often a function of climate conditions. [5] Nutrient uptake by plants and microbial activity of electroactive bacteria in PSMFC are both directly and indirectly affected by climatic conditions. Direct influence means that the temporal variations in PSMFC performance depend often on the plant physiology, which is governed by solar radiation and temperature. Indirect influence refers to the dependence of biological and biochemical processes on physical conditions; for instance, the low temperature restrains microbial activities and reduces bacterial growth, resulting in low efficiency of PSMFC. [12] These factors make plant sediment microbial fuel cells application more dependent on climatic conditions than standard microbial fuel cells. [3]

As compared to the PSMFC studies in tropical and subtropical regions, there are relatively few published reports in moderate and cold climate. Therefore, this study seeks to highlight the practice, applications, design and operation of PSMFC system in moderate climate. A comprehensive review of the seasonal dynamics of plant sediment microbial fuel cells efficiency in a moderate continental climate zone is presented. The strategies of optimal design and operation of PSMFC for performance intensification in moderate climate are also discussed.

2. Materials and Methods

In order to determine the seasonal dynamics of plant sediment microbial fuel cells efficiency in a moderate continental climate zone, three variants of cells with different vegetation were constructed. The PSMFC consisted of a cylindrical base with a volume of 3650 cm^3.The bottom of the vessel was covered with a layer of gravel with a thickness of 7 cm (≈ 3 kg). The particle fraction was in the range 10-20 mm. In the center of the container was placed a perforated in the base PVC tube with a diameter of 110 mm and a height of 440 mm. At the base of the tube was placed an electrode of stainless steel formed as a spiral whose surface is 400 cm^2 and was covered with a 7 cm layer of gravel. The top the tube was filled with a mixture of sediment and peat in a ratio of 3:1. The device was filled with water and in the surface layer of water was placed a second electrode - the cathode. The cathode was also a spiral and had a surface of 400 cm^2. The first PSMFC was planted with *Carex acuta*, the second with *Carex disticha* and the third with *Typha angustipholia.*

On Figure 1 is shown a scheme of the laboratory model of the PSMFC.

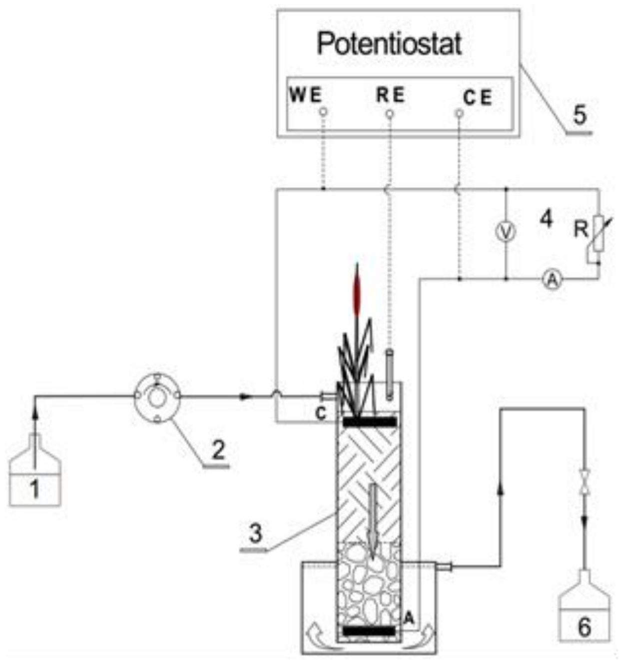

Fig. 1 *Design of Plant sediment microbial fuel cell*
1 – Inflow, 2 – Peristaltic pump, 3 – Plant sediment microbial fuel cell, 4 – Digital multimeter, 5 – Potentiostat, 6 – Outflow, A – Anode C – Cathode

The electrical parameters of PSMFC was measured using portable digital multimeter UNI-T UT33C. A precise potentiometer with maximum value of 13,5 kΩ used for measuring of external resistance.

After stabilization of the electrochemical parameters, the polarization curves of the three variants of PSMFC-s were measured. The best electrical parameters were measured in PSMFC 2 planted with *Carex disticha*, therefore it was selected for further studies. In order to determine the efficiency of the plant sediment microbial fuel cell in a moderate continental climate zone, the electrical parameters of the cell were monitored for one year.

3. Results and Discussion

After a two-month vegetation period, basic electrical parameters were measured in the plant sediment microbial fuel cells. Data for measured electrical parameters of presented on figures 2 and 3. Maximum values of voltage and power density are set in PSMFC 2 - *Carex disticha*. The open circuit voltage in this variant is 791 mV. Maximum power density – 9,2 mW/m^2 is set at an applied voltage of 200 Ω.

Lower values of the above parameters are found in PSMFC 1 planted with *Carex acuta*. In this cell, a maximum open-circuit voltage of 645 mV was measured. The calculated power density reaches 7,27 mW/m^2 at a current density of 23,72 mA/m^2 and an applied resistance of 100 Ω.

PSMFC 3 - *Typha angustipholia* is characterized by the lowest values of the electrical parameters. The open circuit voltage in this variant is 435 mV. The maximum power density of 2,79 mW/m^2 is set at a current density of 10,45 mA/m^2 and an applied resistance of 200 Ω.

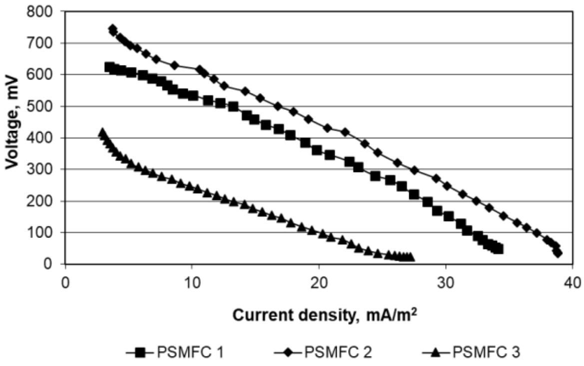

Fig. 2 *Polarization curves of PSMFC-s planted with different vegetation*

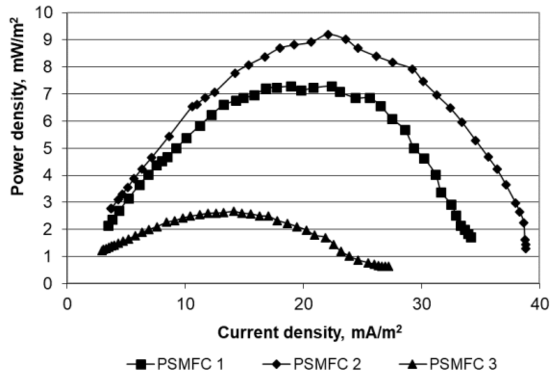

Fig. 3 *Power density of PSMFC-s planted with different vegetations*

Because PSMFC 2, planted with *Carex disticha*. showed the best electrical performance, it was selected for experiments related to the study of the seasonal dynamics of the effectiveness of PSMFC in a moderate continental climate zone. It should also be noted that the vegetation period of *Carex disticha* is about a month longer than *Carex acuta* and *Typha angustipholia*. This would have an additional effect on the seasonal efficiency of the plant sediment microbial fuel cell.

Figure 4 shows the data of the measured open circuit voltage in the cell for one year.

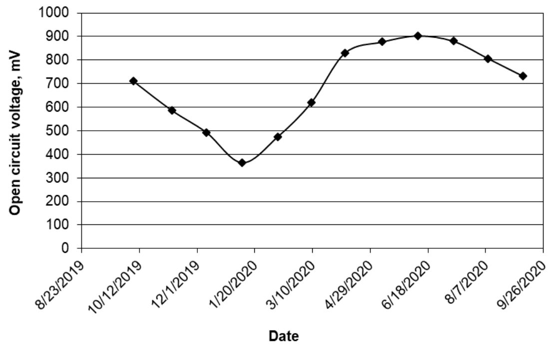

Fig. 4 *Open circuit voltage of PSMFC in different seasons*

The presented data show significantly higher values of voltage in spring and summer, in contrast to autumn and winter. The highest values were measured in the spring, with voltages ranging between 820 mV and 900 mV. Values between 730 mV and 890 mV were measured during the summer. Slightly lower voltage was measured in the autumn. It is in the range of 510 mV - 720 mV. The cell was characterized by significantly lower voltage in winter, with measured values between 380 mV and 580 mV.

Figure 5 presents data on the relationship between open circuit voltage and average daily temperatures for one year.

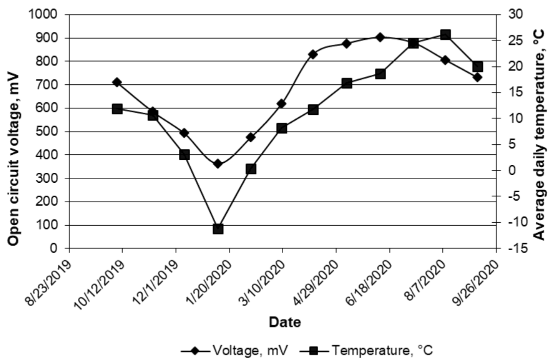

Fig. 5 *Relation between average daily temperatures and open circuit voltage of PSMFC*

The graphs show a clear relationship between average daily temperatures and open circuit voltage. With increasing temperatures in spring and summer, there is an increase in voltage, reaching 890 mV - 900 mV. As the temperatures decrease in autumn and winter, a decrease in the voltage generated by the cell is observed. This dependence is determined by the reduced microbial activity in the anode zone of the plant sediment microbial fuel cell during the cold months. As the temperature increases, the activity of the microorganisms increases, which leads to the generation of a higher voltage in the cell.

As an additional factor should be noted the vegetative period of plants, which through their photosynthesis further increase the voltage of the plant sediment microbial fuel cell.

Figure 6 shows the relationship between the length of the day and the voltage generated by the plant sediment microbial fuel cell.

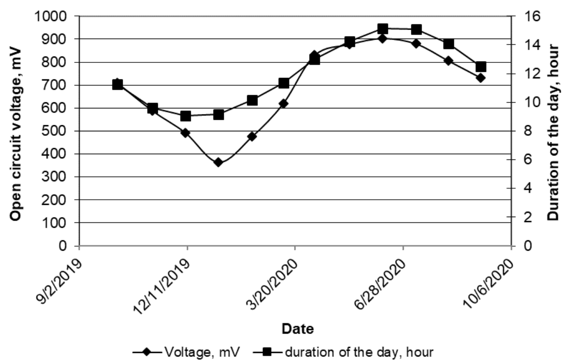

Fig. 6 *Relation between duration of the sunshine and open circuit voltage of the PSMFC*

From the presented data it can be seen that the highest values of open circuit voltage were measured at a day length of more than 12 hours. The generated voltage is in the range 730 mV - 900 mV. In autumn and winter, when the length of the day is less than 12 hours, the values of open circuit voltage range between 380 mV and 700 mV.

The data obtained show a clear relationship between day length and voltage. This indicates that the duration of photosynthesis helps to generate a higher voltage from the plant sediment microbial fuel cell.

Figures 7 and 8 show the measured electrical parameters of the plant sediment microbial fuel cell during the seasons.

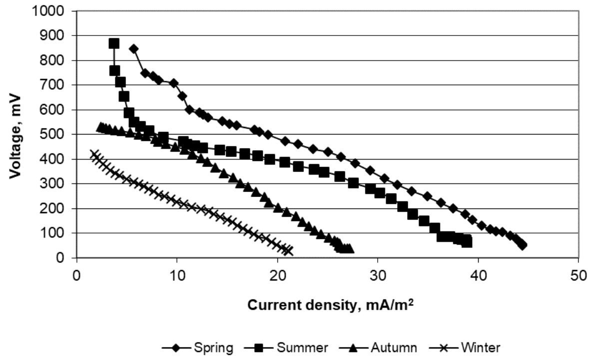

Fig. 7 *Polarization curves of PSMFC in the four seasons*

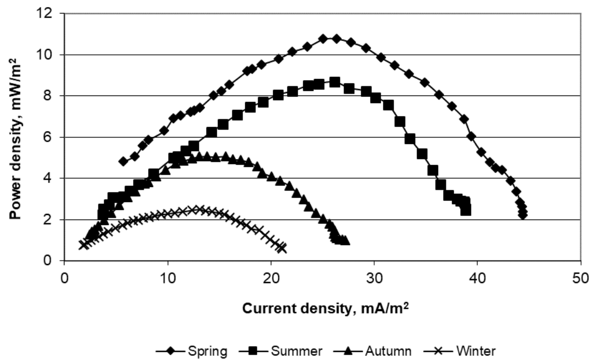

Fig. 8 *Polarization curves of PSMFC-s in the four seasons*

The figures above show that the plant sediment microbial cell showed the highest efficiency in the spring. The voltage in the spring reaches 850 mV. Maximum power density - 10.93 mW m^2 is reached at an applied resistance of 200Ω. The maximum current density reached is 44.5 mA m^2. Slightly lower values of electrical parameters were found in the summer. The maximum power density in summer reaches 8.31 mW/m^2 with a current density of 38.87 mA/m^2 and an applied resistance of 100Ω. The voltage reaches 890 mV.

The plant sediment microbial fuel cell shows significantly lower efficiency in autumn and winter. This shows the significant role of temperature on the activity of microorganisms in the cell, as well as photosynthesis, as factors for higher efficiency of the plant cell.

4. Conclusion

In order to determine the influence of vegetation type on the efficiency of plant sediment microbial fuel cell, three variants with different vegetation were constructed. PSMFC 2, planted with *Carex disticha*, is characterized by the best electrical performance. In this variant, the open circuit voltage of 791 mV was measured, and the maximum power density - 9.2 mW/m^2 was calculated at a load resistance of 200 Ω. Therefore, PSMFC 2 was selected for the next experiments related to the study of the seasonal dynamics of the efficiency of PSMFC-s in a zone with moderate continental climate. Seasonal changes in environmental conditions have a significant impact on the generation of energy from the PSMFC. With the best electrical parameters the cell is characterized in spring and summer, and the maximum power density was reached, respectively 10,71 mW/m^2 and 8,48 mW/m^2. They are significantly lower in autumn and winter. Studies have shown that the effectiveness of PSMFC in a zone with a moderate continental climate is directly related to the vegetation period of the planted vegetation and the effectiveness of the photosynthesis, which are a function of the intensity of the light, the duration of the sunshine and the average daily temperatures.

Acknowledgements

This research was supported by the Karoll Knowledge Foundation, Grant Entrepreneurs in Science

5. References

1. Akratos, C.S., Tsihrintzis, V.A., 2007. Effect of temperature, HRT, vegetation and porous media on removal efficiency of pilot-scale horizontal subsurface flow constructed wetlands. Ecol. Eng. 29 (2), 173–191.
2. Deng H, Chen Z, Zhao F. Energy from plants and microorganisms: progress in plant–microbial fuel cells. ChemSusChem 2012;5:1006–11.
3. Garfí, M., Pedescoll, A., Bècardes, E., Hijosa-Valsero, M., 934 Sidrach-Cardona, R., García, J., 2012. Effect of climatic conditions, season and wastewater quality on contaminant removal efficiency of two experimental constructed wetlands in different regions of Spain. Sci. Total Environ. 437, 938 61–67.
4. Gersberg, R.M., Elkins, B.V., Lyon, S.R., Goldman, C.R., 1986. Role of aquatic plants in wastewater treatment by artificial wetlands. Water Res. 20 (3), 363–368
5. Ham, J.-H., Y, C-G., Hwang, S.-J., Juang, K.-W., 2004. Seasonal performance of constructed wetland and winter storage pond for sewage treatment in Korea. J. Environ. Sci. Health A39 (5), 958 1329–1343
6. Heyvaert, A.C., Reuter, J.E., Goldman, C.R., 2006. Subalpine, cold climate, stormwater treatment with a constructed surface flow wetland. J. Am. Water Resour. Assoc. (JAWRA) 42 (1), 966 45–54.
7. Junttila O. Effect of photoperiod and temperature on apical growth cessation in two ecotypes of Salix and Betula. Physiol Plant 1980;48:347–52
8. Mo Wang, Dong Qing Zhang, Jian Wen Dong, Soon Keat Tan, 2017, Constructed wetlands for wastewater treatment in cold 3 climate — A review, Journal of Environmental Sciences
9. Ng, W.J., Gunaratne, G., 2011. Design of tropical constructed wetlands. In: Tanaka, N., Ng, W.J., Jinadasa, K.B.S.N. (Eds.), Wetlands for Tropical Application. Imperial College Press, 1025 pp. 69–94
10. Rachnarin Nitisoravut, Roshan Regmi, 2017, Plant microbial fuel cells: A promising biosystems engineering, Renewable and Sustainable Energy Reviews 76, 81-89
11. Sani, A., Scholz, M., Bouillon, L., 2013. Seasonal assessment of experimental vertical-flow constructed wetlands treating domestic wastewater. Bioresour. Technol. 147, 585–596
12. Stottmeister, U., Wieβner, A., Kuschk, P., Kappelmeyer, U., K¨astner, M., Bederski, O., M¨uller, R.A., Moormann, H., 2003. Effect of plants and microorganisms in constructed wetland for wastewater treatment. Biotechnol. Adv. 22, 93–117.
13. Takanezawa K, Nishio K, Kato S, Hashimoto K, Watanabe K. Factors affecting electric output from rice-paddy microbial fuel cells. Biosci Biotechnol Biochem 2010;74:1271–3.
14. Timmers RA, DPBTB Strik, Hamelers HVM, Buisman CJN. Long-term performance of a plant microbial fuel cell with Spartina anglica. Appl Microbiol Biotechnol 2010:86

Automation of drilling and blasting passport formation with intelligent algorithms

Evgeniy Nagatkin[1], Evgeniya Volkova[2], Aleksey Druzhinin[3], Evgeniy Kankov[4]
Faculty of Economics and Engineering [1,2,3], Faculty of Mining Technologies [4] – Ural State Mining University, Russian Federation

Abstract: *This article is devoted to the problem of a passport for drilling and blasting operations formation, taking into account the main characteristics. At most mining enterprises, this process is a manual calculation that leads to errors due to human factor and increases the time it takes to generate drilling and blasting passport, and, as a consequence, the time for drilling and blasting.*
The proposed solution is an automated complex that bases its calculations on the data of the cross-section mines shape, the dimensions of the height and width of the mine and the cross-sectional area in the tunnel, the fortress on the scale of prof. M.M. Protodyakonov and the thickness of the host rocks. All geometrical parameters of tunnel face are obtained automatically based on laser scanning. For further calculations, intelligent algorithms are used, implemented using deep learning neural networks (with python tensorflow library). It is worth noting that the final decision on the acceptance of the drilling and blasting passport is made by the person in charge. The result of using the proposed system is automatically generated passport of drilling and blasting operations, including its alternative variations (due to the passport chosen by the person in charge, the system will receive feedback to further improvement of the system algorithm).
***KEYWORDS**: MINE, UNDERGROUND MINING, DRILLING AND BLASTING, NEURAL NETWORK, PYTHON, TENSORFLOW, CALCULATION OF DRILLING AND BLASTING*

1. Introduction

At present, in the mining industry a tendency for a colossal increase in the automation of certain technological processes through the introduction of modern equipment and the usage of innovative technologies can be noticed. But it should be noted that this trend bypasses some mining processes, due to the complexity of their automation in general, the lack of efficiency of existing solutions, or the high cost of equipment. One of these processes is the drilling and blasting passport development.

A large percentage of enterprises engaged in the development of underground deposits use the drilling and blasting method for rock excavation. And these enterprises are obliged to carry out blasting operations using the appropriate documentation, namely, according to the drilling and blasting passport. The efficiency factor of high-quality and modern equipment, when drilling and blasting, directly depends on the correct parameters of the drilling and blasting passport. The drilling and blasting passport must include such parameters as: the layout of the blastholes, the depth of the blastholes, the diameter of the blastholes, the type of cut hole, the consumption of the explosive, the type of explosive, the volume of the blasted rock mass, etc.

A large number of calculated parameters of the drilling and blasting passport, the calculation of which at many enterprises is often performed manually using universal methods, which can lead to errors in the drilling and blasting passport, as well as an increase in the time of its formation for the developed face, due to which there is an increase in the production time and the loss of production pace.

2. Prerequisites and means for solving the problem

The prerequisites for the automation of the process of designing a drilling and blasting passport are many factors. First of all, the wrong, non-optimal drilling and blasting passport development leads to large production losses. For example: non-optimal waste of explosives in excess of the design norm or insufficient level of blasting of the face and, as a consequence, the rework necessity the face by manual methods, which in turn leads to a decrease in production rates, and as a result, failure to fulfill the mining plan. Also, one of the most important prerequisites for the system development is the lack of a unified optimal method for the location of holes, and the consequence of its absence is an increase in the time for building the drilling and blasting passport itself. Often, due to the expenditure of a large amount of time on the design of the blasthole drill, mining enterprises design passports in advance before starting mining operations, and do not change them during the execution of the entire plan, regardless of various changes during the excavation, which is an extremely sub-optimal and costly factor.

The existing digital solutions for a drilling and blasting passport development have an insufficient level of automation, often represent desktop software, where the parameters for generating a passport are entered manually, and it is also a serious disadvantage to cancel the absence of intelligent algorithms for determining suitable methods for generating a drilling and blasting passport. Also, in this type of software there is no feedback from the real object so the parameters of drilling and blasting passport cannot be recalculated based on changed input data in accordance with real values. Thus, the automation of the process of a drilling and blasting passport formation and development is an extremely important problem for many enterprises, which will increase the speed and accuracy of formation of a drilling and blasting passport and the speed of tunnelling.

The current automated systems, as mentioned earlier, are software with no intelligent algorithms and feedback to improve them.[1-3] This is due to the fact that often the specialists of mining enterprises do not have the skills to design intelligent data processing systems, and the data scientists do not have the skills to design drilling and blasting passports and understand the specifics of many processes in mining.

Nowadays, the creation of an automated system for the design of blast-hole passports based on intelligent algorithms has become possible thanks to the development of modern technologies: a reduction in the amount of resources for deploying systems based on intelligent algorithms (the ability to deploy systems of this kind directly in the enterprise infrastructure itself)[4], the rapid growth of the general trend of digitalization of mining operations and the emergence of more specialists in related fields of mining.

3. Solution of the examined problem

The authors of this work propose the following method for constructing the drilling and blasting passport automation:

1. Geometric and working area parameters determination by laser scanning with an automated complex.
2. Type of cut hole determination by geometrical and mining-geological parameters according to the project plan.
3. Module for automatic calculation of explosives development.
4. Methods and module for determining the coordinates of cut holes, contouring and auxiliary holes placement development.
5. Drilling grid method development.

Consider the steps in more detail.

3.1. Geometric and working area parameters determination

Laser scanning technology (LIDaR) is widely used in the construction of digital 3D objects in medicine, architecture, and mechanical engineering. The hardware component of these scanners includes the necessary geodetic instruments such as theodolite and a high-speed and accurate laser rangefinder. These scanners are used to create 3D models of both complex and simple objects. The measurement speed of this type of scanners is high and can reach up to a million iterations per second, and the accuracy reaches up to hundredths of a millimeter.

Laser scanning in this complex is applicable to determine the type of cut hole and geometric parameters of the holes placement surface in the automatic mode. The laser scanners themselves are divided into types depending on the measurement method: pulsed, phase and triangulation. Despite the fact that triangulation scanners have the highest accuracy, scanners using pulsed and phase measurement methods are suitable for scanning incisions, due to the limited effective distance of the triangulation scanner. Regardless of the type of lidar, after scanning the mining face, the coordinates of the points will be obtained at the output - the so-called point cloud, with the help of which an accurate model of the cut will be built, for its further use in calculations for the placement of blastholes. [5]

But lidars have one small drawback, despite measurements, calculations, building a model in automatic mode, this type of device, with each new scan of the face, requires initial orientation in space relative to the required coordinate system, which leads to the intervention of a person placing control points, coordinates which are determined by geodetic methods. Despite this, this type of scanning can significantly speed up the work on measuring the geometric parameters of a face by quickly building an accurate model of it.

3.2. Type of cut hole determination by geometrical and mining-geological parameters.

The location of the holes in the face, the explosion rates, as well as the amount of entry are largely determined by the type of cut hole that used. The choice of the type of cut itself is determined by such indicators as: section of production, rock strength and the type of drilling equipment of a mining enterprise.

By the nature of the action, the cuts are divided into two types: into inclined cuts (cuts with boreholes directed obliquely to the working axis) and cylinder cuts (cuts with boreholes directed parallel to the mine working). Of the inclined cuts, the most common is the wedge cut. Of the cylinder cuts, the most common are: prismatic symmetric, slotted, spiral and double spiral.

Further in the article, the cylinder type of cut will be considered, in particular, the prismatic symmetric cut (Fig. 1) as the basis for further research on this topic, since high efficiency of cuts with the use of inclined holes and the advantages of their usage in comparison with straight ones are achieved only with a certain section of the working and a limited depth of holes.

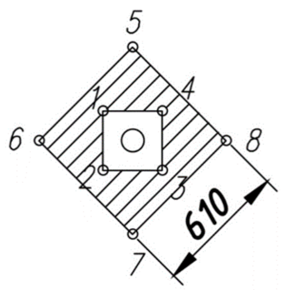

Fig.1. *The prismatic symmetric cut example*

Also, the cylinder type of cut is used both on faces with a cross section of less than 6m2 and more than 6m2, in contrast to the inclined type of cut. Thus, we can say that the most common type of cut is a cylinder cut. Cylinder cut parameters are determined by the following values: the cut construction, the compensating cavity diameter and rocks strength. These parameters are always set initially when designing the production plan, and it can be argued that, in the future, the parameters of the selected cut hole will be entered into the database of the automated complex after creating the project production plan.

3.3. Module for automatic calculation of explosives development.

The amount of explosive required to destroy a unit of rock, or the amount of explosive consumption, depends on such parameters as: the mine rock section strength, the explosive type and the blasting conditions. All calculations are carried out according to formalized formulas. The specific charge when using cylinder cut is recommended to be determined by the modified formula of N.M. Pokrovsky (1):

$$q = (0{,}1 \cdot f \cdot f_1 \cdot v)/e, \qquad (1)$$

Where q is the specific charge of the explosive, kg /m3; f — rock strength coefficient according to M.M. Protodyakonov; f1— rock structure coefficient; v — rock clamping coefficient; e — explosive charge efficiency coefficient.

Cylinder cut require an increased specific explosive charge, and it is calculated only for cut and delineating holes with a rock clamping coefficient v = 1.1 - 1.4.

The amount of explosive per cycle using cylinder cut hole is calculated by the formula (2):

$$Q = Q_{ch} + q \cdot (S_{da} - S_{ch}) \cdot l_{bh}, \qquad (2)$$

Where Qch is the amount of explosive in the cut holes, taken as the sum of the charges of the cut holes. The amount of charge in kg in the cut hole is calculated by the formula (3):

$$q_{ch} = 0{,}785 \cdot d^2 \cdot \rho \cdot \alpha \cdot l_{ch} \qquad (3)$$

where d is the diameter of an explosive cartridge or a borehole, depending on the loading method, m; ρ is the density of the explosive in the charge, kg / m^3; α — filling factor of the cut hole; l_{ch} is the cut holes length.

All these calculations are immediately carried out when designing a drilling and blasting passport, and as practice shows, they do not change in the future, which in turn, under certain conditions of work, leads to overspending and irrational use of explosives. In turn, this can be avoided just by the introduction of an automated system for drilling and blasting passport generating based on laser scanning and intelligent algorithms. Laser scanning after drilling the blastholes using a high-precision point cloud allows determining the actual diameter and length of the blasthole, which may change due to the grinding of the bit and changes in the rock hardness during mining[6].

The intelligent algorithms usage, based on the changed data after scanning, and already existing unchanged coefficients for calculating the amount of explosive, just the same allow to calculate the actual amount of explosive for each cycle.

3.4. Methods and module for determining the coordinates of cut holes, contouring and auxiliary holes placement development.

For the optimal location of auxiliary and cut holes, we propose to use a neural network algorithm, implemented using tensorflow in the python language [7], and based on the solution of the so-called circle packing into an arbitrary area problem [8]. Circle packing problems are a category of geometric problems that consists in placing circles of the same or different diameters in a certain two-dimensional region, touching but not intersecting each other. There are a large number of well-known algorithms for solving this class of problems - from homogeneous mosaics to intelligent algorithms. It should be borne in mind that the zones of influence in the geometric construction of the drilling grid, as a rule, intersect (provided that the radius of the circles is equal to a as zone of influence), but when using the radius equal to a/2, the problem is reduced to the circle packing problem.

One of the algorithms that gives the most qualitative result of mesh generation is the "shaking" method, which consists in the following: each point of the hole placement is shifted in different directions by some randomly selected (and after training the neural network - by a certain) amount (Fig.2). Further, from the options after the shifts, the most optimal is selected, after which the "shaking" is carried out again - until the circles are packed in the most efficient way. In this case, an option is considered to be effective in which there are no or minimized areas that do not fall into the zone of influence of any blasthole, and the number of blastholes also tends to the minimum of the possible number.

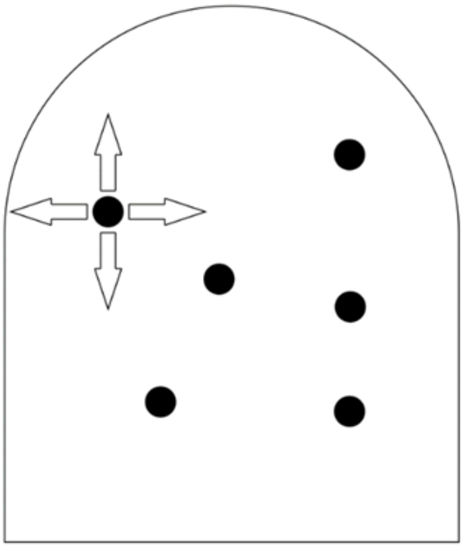

Fig. 2. *The "shacking" algorithm for drilling net design.*

3.5. Drilling grid method development.

After each cycle of drilling and blasting operations in the mine can be so-called bootleg - technological holes formed after blasting, and located in places of cut holes and auxiliary holes. It is prohibited to carry out further drilling operations in these holes, because they may contain explosives. And as practice shows, redesigning of the drilling and blasting passport or making changes to during work is not carried out, drilling continues with an arbitrary displacement of the holes from the bootlegs by 1-2 cm, thus the zones of influence of the holes do not correspond to the initial calculations, which can lead to resource costs and loss of production rates due to insufficient efficiency of further drilling and blasting operations. Repeated laser scanning can avoid this.

The technique is as follows: repeated laser scanning is carried out, as a result of which, using a high-precision point cloud, we can obtain an actual face model, with all the bootlegs located on it. Further, the processing of this model by intelligent algorithms comes into play [9], which displace the cut relative to the axis by a sufficiently effective distance for further drilling operations. After the displacement of the cut on the project of the drilling and blasting passport, the task of circle packing comes is solved, for the subsequent placement of the minimum number of auxiliary holes, corresponding to their zones of influence, without their overlays on the remaining bootlegs but providing full face coverage without spaces free from zones of influence.

Thus, you can quickly and accurately make changes to the current drilling and blasting passport model. Moreover, depending on the displacement of the cut relative to the axis and the bootlegs, you can get several effective drilling and blasting passport models, but the choice of the most effective option is accepted by the person in charge, which in turn will allow further training of neural network algorithms.

4. Results and discussion

As an object for carrying out an experiment using intelligent algorithms, a drilling and blasting passport, already designed for a specific face with a cylinder cut type (prismatic symmetric), was taken. (Fig. 3)

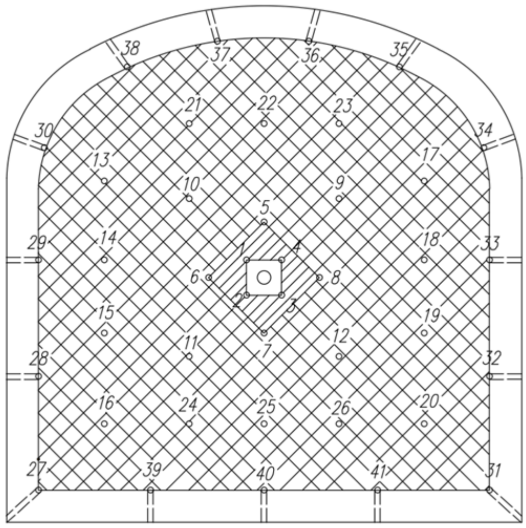

Fig. 3. *Drilling and blasting passport designed manually.*

In the course of the experimental study, markers were imposed on the model of the drilling and blasting passport, indicating the bootlegs remaining after drilling: from cut holes, since they remain always, and randomly located from the auxiliary holes. (Fig. 4)

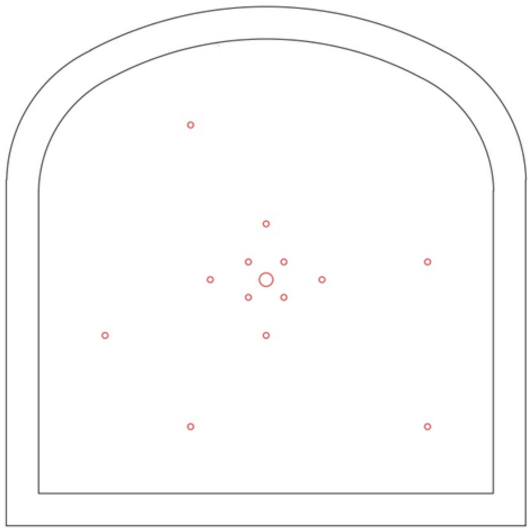

Fig. 4. *Bootlegs model*

Further, using the data from the already designed drilling and blasting passport, with the tensorflow-based neural network, the problem of placing cut and auxiliary holes and constructing their influence zones was solved by displacing the cut relative to the markers of the cutting bootlegs and the most efficient placement of auxiliary holes relative to the bootleg markers of auxiliary holes. (Fig. 5)

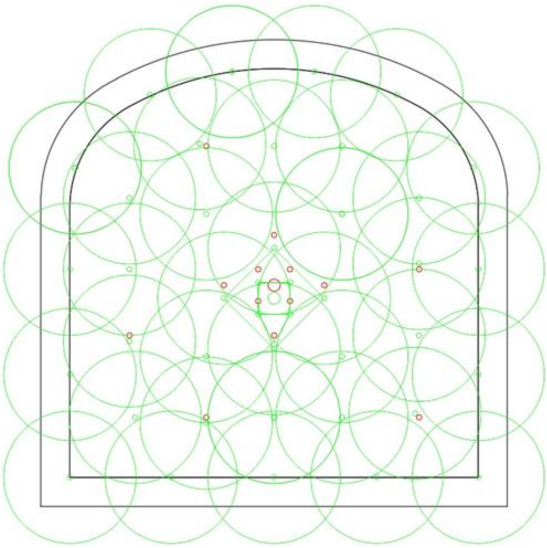

Fig.5. Drilling and blasting passport model designed by neural network

Also, for the design and displacement of the elements of the new passport, algorithms were used to solve the problem of circle packing. (Fig. 6) When solving the problem of circle packing, the circle radius was taken as the zone of influence divided by two (a/2), since the zones of influence must intersect to ensure a high-quality explosion, while the circles during packing do not.

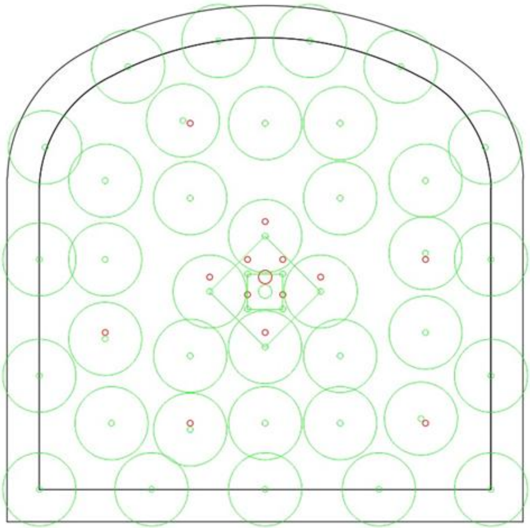

Fig. 6. Circle packing based drilling and blasting passport model

The data obtained is not accurate, due to the initially incorrect design plan of the drilling and blasting passport, the absence of a large dataset for training the neural network, and as a consequence the lack of training, there is a large inaccuracy in providing models with this neural network.

5. Conclusion

Based on the provided models, it can be said that the method of using intelligent and neural algorithms solving circle packing problem are applicable for the automated design of drilling and blasting passports, despite the inaccuracy of the data obtained from the primary experiment, with further training of the neural network on datasets of correctly designed drilling and blasting passports, and also scanned by laser scanning of shaft face models at different work cycles, will allow to train the neural network as efficiently as possible and achieve high accuracy and efficiency in designing drilling and blasting passports.

References:

1. Khomenko O.E., Rudakovv D.V., Kononenko M.N. Autom ation of drill and blast // Technical And Geoinformational Systems In Mining – 2011. – pp. 271-275. DOI: 10.1201/b11586-45.

2. Basargin A.A., Salnikov V.G., Pisarev V. S. Razrabotka me todiki proyektirovaniya burovzryvnykh rabot na otkrytykh gornykh vyrabotkakh s primeneniyem ggis micromine [Development of design methods for drilling and blasting operations in open mine workings using ggis micromine] // Interèkspo GEO-Sibir′ - 2019. - №1. – pp. 249-258. [In Russ].

3. Kozyrev S. A., Fattakhov E. I. Sistema avtomatizirovannog o proyektirovaniya burovzryvnykh rabot dlya prokhodki gornykh v yrabotok v OAO "Apatit" // Gornyj zhurnal. - 2007. №4. – pp. 73-74 [In Russ].

4. Vizilter Yu. V., Gorbatsevich V. S., Zheltov S.Y. Structury-functional analysis and synthesis of deep convolutional neural netw orks. // Computer Optics -2019. - 43(5). –pp. 886-900. DOI: 10.18287/2412-6179-2019-43-5-886-900. [In Russ]

5. Simulation of the preparation and face drilling processes with laser scanning and automated marking of the drilling grid. Evgeniya Volkova, Aleksey Druzhinin, Roman Kuzminykh and Vladimir Poluzadov. E3S Web Conf., 177 (2020) 01010, DOI: https://doi.org/10.1051/e3sconf/202017701010

6. Seccatore, J., Magny, L.; De Tomi, G. Technical and operational aspects of tunnel rounds in artisanal underground mining. // REM - Revista Escola de Minas. - 2014. - v. 67, - n. 3, - pp. 303-310.

7. Sozykin A. V., Obzor metodov obucheniya glubokikh neyr onnykh setey // Vestnik Ûžno-Ural′skogo gosudarstvennogo universiteta. Seria Vyčislitel′naa matematika i informatika. – 2017. – 6 (3), - pp. – 28-59. [In Russ]

8. A. L. Kazakov, P. D. Lebedev. Algoritmy postroyeniya opti malnykh upakovok dlya kompaktnykh mnozhestv na loskosti. // Science journal Numerical Methods and Programming. – 2015. – 16 (2), - pp. 307-317. [In Russ]

9. Procedure of computation and automatic marking of drill hole spacing at excavation of horizontal workings. Maxim Kononenko, Ruslan Ganiev and Roman Kuzminykh. E3S Web Conf., 177 (2020) 01011. DOI:https://doi.org/10.1051/e3sconf/2020 17701011

Optimization of flat solar collector based on the principle of entropy

Marija Chekerovska[1,*], Todor Chekerovski[2], Dalibor Serafimovski[2], Risto V. Filkoski[3]
Faculty of Mechanical Engineering, University "Goce Delcev" – Stip, Str. "Krste Misirkov" No. 10-A[1]
Faculty of Electrical Engineering, University "Goce Delcev" – Stip, Str. "Krste Misirkov" No. 10-A[2]
Faculty of Mechanical Engineering, Skopje, University St. Kiril I Metodij[3]
marija.cekerovska@ugd.edu.mk

Abstract: *This article describes the entropy method optimization based on the approach of minimal increase of entropy in the thermodynamic system. Here is presented the experimental set up of flat plate solar collector with liquid as working medium, effective absorber area of the c ollector 1,4 m^2, absorber plate of aluminum, copper pipes and selective coating. A comparative analysis is conducted between the efficiency of a theoretical model of nonisothermal solar collector and the efficiency obtained by measuring the physical model of a solar collector. Res ults show a general trend of growth the collector efficiency due to the reduction of irreversibility of the represented processes.*

Keywords*: OPTIMIZATION, SOLAR COLLECTOR, ENTROPY*

1. Introduction

Entropy expresses the direction of spontaneous changes in the system. It shows one process irreversibility, and not violating the conservation of energy. This term represents the measure of disorder in one system. Old misconceptions and new breakthroughs of definition of entropy is presented in [1]. The entropy generation analysis as a design tool is presented in [2], where this method is clearly explaining the possibility for designers to conceive more efficient systems.

Entropy generation in simultaneous heat and mass thansfer devices is shown in [3]. In studies of Torres, there are two additional developments: in one is presented the application of the entropy minimization generation in solar collectors for drying processes [4], and another presents the application of the entropy minimization generation to determine the temperature and length of the optimal fluid conduit channel, in solar collectors of different configurations [5].

In this paper the main focus is the optimization of flat plate solar collector based on minimum entropy generation. Analysis presented are comparison between efficiency of a theoretical model of non-isothermal solar collector and the efficiency obtained by measuring the physical model of a solar collector.

2. Optimisation with application of entropy method

The model based on minimisation of the entropy growth rate in this study is built upon the work of Bejan [6,7]. Collector with an effective surface of A_c in stationary conditions at operating temperature T_c, receives solar radiation Q^*, one part part of which is transformed into useful energy (Q_u), and one part is lost to the environment (Q_0):

$$Q^* = Q_u + Q_0 \quad (1)$$

The approach in this work is based on endo-reversible thermodynamics, in which incident radiation energy to the collector is q^* (in W/m^2). The model based is presented with simplified scheme fig. 1. A part of that energy, d$Q(t)$, is received and transmitted by the working fluid, another fraction, d$E(t)$, increases the internal energy of the collector, and the rest, d$Q_L(t)$, is lost in the surrounding ambient.

By setting the energy balance of non-isothermal collector, an expression for heat losses from the collector to the surroundings can be derived. From the Second main law of thermodynamics the following expression for the growth of entropy is derived:

$$\Delta S(\tau) = \int_0^\tau \left[\frac{q*}{T_C(\tau)} - \frac{dQ(\tau)}{T_C(\tau)} - \frac{dQ_L(\tau)}{T_C(\tau)}\right] \geq 0 \quad (2)$$

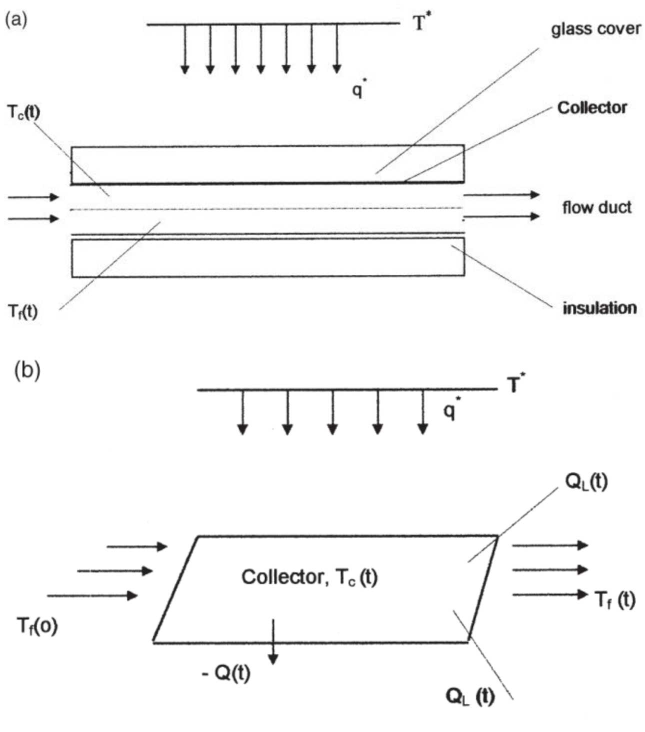

Fig. 1*. Elementary scheme of a solar collector for display of a model based on endo-reversible thermodynamics*

The collector efficiency, through the analyzed variables, can be represented by the following expression

$$\eta = \frac{K[T_c(\tau) - T_f(\tau)]}{q^*} \quad (3)$$

Previous expressions make it possible to optimize the operation of the solar collector in terms of minimum increase in entropy. Moreover, on the basis of the further analysis carried out in the thesis, expressions are derived for optimal output temperature and the corresponding value of the optimal flow of working fluid in terms of minimum increase in entropy.

Optimal time τ needed for transfer of certain amount of heat, can be obtained by the following expression

$$\tau = \frac{2C_f}{K} \ln\left[2 - \frac{T_f(0)}{T_c(0)}\right] \quad (4)$$

The diagram in Fig. 21 shows the time τ necessary to transfer a certain amount of heat, as a function of the ratio of the initial temperatures of the fluid t_f and the absorber t_c.

3. Results from the thermodynamic optimisation

The diagram in Fig. 2 shows the time τ necessary to transfer a certain amount of heat, as a function of the ratio of the initial temperatures of the fluid T_f and the absorber T_c.

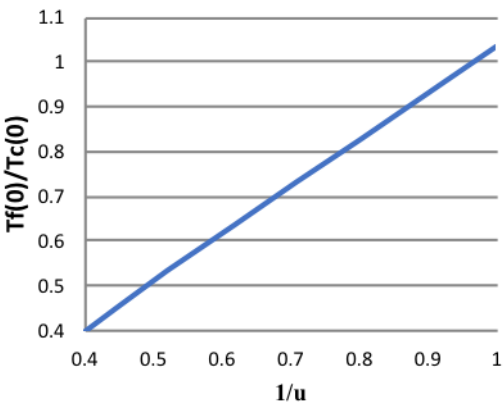

Fig 2. *Dependence between the ratio (1/u)=$T_f(\tau)/T_c(\tau)$ and $T_f(0)/T_c(0)$*

The diagram in Fig. 3 represents the time required to transfer a certain amount of heat, as a function of the ratio of the initial temperatures of the fluid and the absorber.

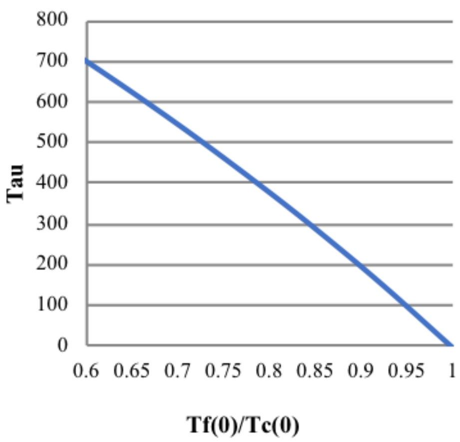

Fig 3. *Optimal duration of the process τ as a function of the ratio $t_f(0)/t_c(0)$*

The total increasing rate of entropy is a function of the parameters of the environment, q^* and T_a, the initial temperature conditions expressed by the ratio $T_f(0)/T_c(0)$, the conductivity K and the mass flow of working fluid m. Figure 4 shows the change of the increasing rate (generation) of entropy as a function of the mass flow of working fluid.

In Tables 1 and 2 are given results from experimental measurements, as well as results of calculations using the relations concerning non-isothermal model of the solar collector.

The basic specification of the test facility is given below:

- Individual flat plate solar collector with liquid as working medium;
- Absorber plate of aluminum, copper pipes, selective coating;
- Effective absorber area of the collector A_c = 1,4 m^2;
- Location - Shtip, Republic of N. Macedonia (latitude 41^o 45' and longitude 22^o 12');
- $\tau\alpha$=0,82, F_RU_L=7,78 W/m^{2}C, $F_R(\tau\alpha)$=0,64.

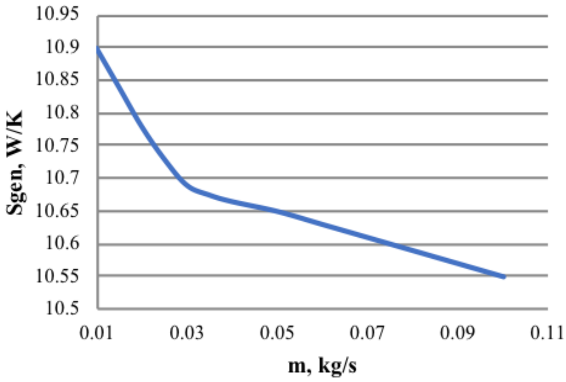

Fig. 4. *Relationship between the entropy growth rate (generation) and mass flow of working fluid*

In Table 1 and Table 2 are presented experimental results obtained on the static collector experimental set-up.

Table 1*: Results obtained on the static collector experimental set-up*

N	Time	Temp. t_a	Temp. t_{in}	Inc. thermal power q^*, W/m^2
1	10.30	15	40	780
2	11.00	15	41	855
3	11.30	16	42,5	893
4	12.00	16	44	890
5	12.30	17	45	875
6	13.00	17	46	825
7	13.30	18	47	775
8	14.00	18	48	705

Table 2*: Results obtained on the static collector experimental set-up*

N	Time	t_{out}, ^{o}C	θ_{out}	M	$N_s + 1/\theta^*$
1	10.30	43,5	2,90	2,348	0,649
2	11.00	47	3,13	2,142	0,436
3	11.30	48	3,00	2,188	0,514
4	12.00	50	3,13	2,195	0,457
5	12.30	52	3,06	2,373	0,366
6	13.00	53	3,12	2,442	0,340
7	13.30	54	3,00	2,836	0,291
8	14.00	53,5	2,97	3,118	0,386

Results concerning the efficiency of the collector, obtained experimentally using the theoretical model presented in this material are given in Table 3.

Table 3. *Results for the collector efficiency obtained experimentally and with the theorethical model*

$(t_i-t_a)/q^*$	η_{exp}	η_{th}
0	0,68	0,65
1	0,675	0,64
2	0,67	0,63
3	0,665	0,62
4	0,65	0,61
5	0,645	0,6
8	0,62	0,58
10	0,605	0,56
15	0,585	0,54
16	0,584	0,525
20	0,58	0,51
22	0,57	0,495
25	0,56	0,48
26	0,55	0,47
30	0,54	0,46

Diagram in Figure 5 shows the comparative results for the efficiency of the collector as a function of ($t_{in} - t_a$)/q^*, obtained by experimental research and by the theoretical analysis, by applying the model for minimization of the increase of entropy. They show a general trend of growth the collector efficiency due to the reduction of irreversibility of the represented processes.

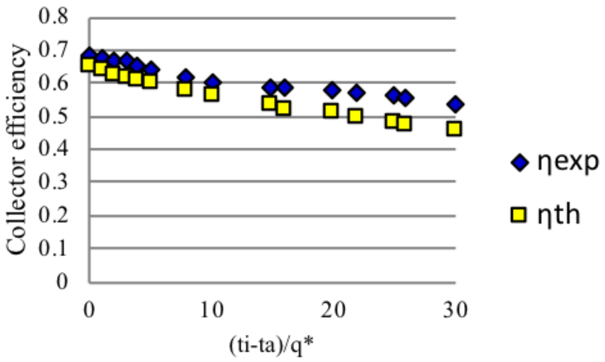

Fig. 5*. Change of the collector efficiency as a function of (t_i - t_a)/q* obtained by applying the model for entopy growth minimization*

4. Conclusion

In the section on thermodynamic optimization, a model for optimization of solar collector based on the principle of minimizing the growth of entropy is presented. A comparative analysis is conducted between the efficiency of a theoretical model of non-isothermal solar collector and the efficiency obtained by measuring the physical model of a solar collector.

By the conducted analysis, optimal regime parameters of the collector are obtained - optimal operating temperature of the collector, the intensity of useful heat extraction, optimal flow of working fluid etc. From the deduced results it can be concluded that the performance of the collector shows a tendency to decrease with increase in the value of the ratio (t_i - t_a)/q^*.

5. References

1. Martyushev, L., Entropy and entropy production: old misconceptions and new breakthroughs, Entropy, 15(4), pp. 1152-1170, 2013. DOI: 10.3390/e15041152
2. A. Sciacovelli, V. Verda, and E. Sciubba, Entropy generation analysis as a design tool - A review, Renew. Sustain. Energy Rev., **43**, pp.1167-1181, (2015).
3. G. Prakash, J. Lienhard, and S. Zubair, Entropy generation minimization of combined heat and mass transfer devices, Int. J. Therm. Sci., **49**(10), pp. 2057-2066, (2010)
4. E. Torres., J. J. Navarrete, and B. A. Ibarra, Thermodynamic method for designing dryers operated by flat-plate solar collectors, Renew. Energy, **26**, pp. 649-660, (2002)
5. E. Torres, J. Navarrete, A. Zaleta, and J. G. Cervantes-de Gortari, Optimal process of solar to thermal energy conversion and design of irreversible flat-plate solar collectors, Energy, 28(2), pp. 99-113, (2003)
6. A. Bejan, D. W. Kearne, F. Kreith, Second law analysis and synthesis of solar collector systems, Journal of Solar Energy Eng, **103**:23–8, (1981)
7. A. Bejan, *Entropy generation minimization*. 2nd ed. CRC Press, Boca Raton, (1995)
8. S. K. Saha, D. K. Mahanta, Thermodynamic optimization of solar flat-plate collector, Renewable Energy 23 (2001), 181-193
9. S. Fischer, W. Heidemann, H. Muller-Steinhagen, B. Perers., P. Berquist, B. Hellstrom, Collector test method under quasi-dynamic conditions according to the European Standard EN 12975-2, Solar Energy **76**, pp. 117-123, (2004)
10. D. Rojas, J. Beermann, S. A. Klein, D. T. Reindl, Thermal performance testing of flat-plate collectors, Solar Energy **82**, pp. 746-757, (2008)

Investigation of hollow ceramic structures by contactless computer-tomographic non-destructive method

Lyuben Lakov[1], Nikolay Stoimenov[2], Mihaela Aleksandrova[1]
[1]Institute of Metal Science, Equipment and Technologies with Hydro- and Aerodynamics Centre “Acad. A. Balevski”, Bulgarian Academy of Sciences, Shipchenski Prohod Blvd. 67, 1574 Sofia, Bulgaria, e-mail: mihaela.krasimirova@mail.bg
[2]Institute of Information and Communication Technology, Dept. Distributed Information and Control Systems – BAS, Sofia
e-mail: nikistoimenow@gmail.com

Abstract: *This article deals with the study of the cavity of ceramic constructional elements for the construction of beehives and carriers for electric furnace heaters. Unlike the traditional practice of performing tomography studies to determine the structure and harmful defects in the interior and surface of specimens, in the present studies, the non-destructive non-contact method is used to assess the nature and volume of deliberate fulfilled cavities in ceramic specimens. The role of well-shaped and regulated cavities is to reduce the coefficient of thermal conductivity in the hives to the inside, and in the carriers for heaters to the outer walls of the furnace, i.e. heat loss. The cavity samples are obtained from an aqueous dispersed colloidal system based on patent-protected quartz glass-ceramics by the "pouring" method. The obtained structural details are fireproof, thermally stable and with high physical and mechanical characteristics. They are composed of amorphous* SiO_2*, mullite and cristobalite. The study of the cavity at different beam depths was performed using a NIKON XTH 225 device, and the data processing Volume Graphic, My VGL.*

Keywords: *HOLLOW CERAMIC CONSTRUCTIONS, WATER DISPERSION COLLOIDAL SYSTEMS, NON-CONTACT NON-DESTRUCTIVE METHOD, TOMOGRAPHIC METHOD*

1. Introduction

The hollow ceramic constructions (plates for beehives and supports for heaters for electric furnaces) obtained, studied and presented in this article consist of three layers - two dense outer and an intermediate air layer formed between the two dense layers. Of importance for the practice are the thicknesses of the two supporting thick layers, the top and the one of the air cavity in order to provide the necessary thermal insulation. Achieving the necessary requirements is associated with the combination of different factors determining the construction of the individual layers in the molding process. The first factor is the composition of the solid phase in the aqueous dispersed colloidal system, from which the samples are made in gypsum molding equipment. From this composition depends, the molding, as well as physical and mechanical properties of ceramic products. The second factor is the amount of water, the added liquefied separators, and mainly the residence time of the system in the molds. The evaluation of the obtained details after drying and firing at 1240°C is realized by evaluating the cavity and the thickness of the bearing layers. One of the analysis methods is destructive, which is expensive, inefficient and time consuming. A promising maximum automated and undamaged method of ceramic constructions is the Tomography method, which has not yet been used for the comprehensively analysis of the described specimens as well as the other similar samples.

It is known that tomography comes from the word "tomo", which means "cut" or the basis of absorbent X-rays, which allows the visualization of the internal micro and macro structure of the materials. CT scanning and cavity assessment technology can also be used by evaluating the size and properly shaping the cavities in the samples.

Computed tomography is a method by which from multiple X-ray images of the object, taken from different angles, a three-dimensional image is obtained by computer processing, and the examination is performed in successive sections [1, 2, 3, 4]. The Micro CT system consists of an X-ray source, a sample rotation stage and a detector. The X-rays that are received by the detector are directed to certain places in the sample. They have a high resolution, which depends on the specimen size. In the process of the sample scanning, it is rotated 360 degrees and the resulting 2D images are recorded. These images are processed with specialized software to obtain 3D images from for volume pixels.

Due to its powerful and precise equipment, CT scanning technology is a very useful research technique with very wide possibilities in the field of ceramic production.

2. Experimental part

The article presents the study of the macrostructure of 6 separate ceramic parts - carriers of the heaters building the working space of a furnace for melting aluminum alloys. (fig. 1, 2, 3, 4, 5, 6, 7) and part of constructional details (fig. 8) (ceramic beehive plate) similar in structure for all walls making the fruit tree, the shop and the drawer of the beehive (fig. 9). The material from which both types of details are made is quartz glass-ceramics, which is one of the most thermally resistant ceramics with CTE $5.10\text{-}7K^{-1}$. The fire resistance is particularly important in carriers and according to the claims used is 1450°C. The compressive and tensile strength is 500 MPa and the bending strength is 70 MPa [5]. The composition includes 70% amorphous SiO_2 and 30% washed kaolin.

The non-destructive mapping of the internal structures of the cavities in the ceramic products provides information about the perfection of the air intermediate layer and possible imperfections in the two outer dense supporting layers, such as cracks, inhomogeneities, etc.

Experimental studies to determine the structure of kitchen products are carried out on real ceramic kitchen products. CT allows the study of a wide range of materials and sample sizes with a range from 20 to 225 kV. CT tomography is equipped with a five-axis positioning system. The maximum weight of the sample is 15 kg, and the maximum dimensions are 15x15x15 cm. The obtained maximum resolution of the detector is 1900x1500 with an active area of 467 cm and an accuracy of 3μm. The system is equipped also with specialized software for reconstruction of the internal structure of the sample in 3D [6].

3. Results and Discussion

The experimental studies were performed in the Smart Lab laboratory, Institute of Information and Communication Technologies at the Bulgarian Academy of Sciences, Sofia.

Tests were performed on 7 samples described above. The thicknesses of the supporting layers and cavities were measured. Defects in the dense layers have been identified, such as cracks, damages, cavities and inadmissible deviation in the construction of the elements.

Each sample is scanned and reconstructed by 3D. The inside structure is also presented. The descriptions of the cartographies are presented from detail 1 up to detail 7.

Detail 1.

From fig. 1 it is obvious that the cavity of the material is uniform for the most part. The walls of the part have an average size of 8 to 16 mm. The walls have a porous structure. An exemplary pore size is shown in fig. 2.

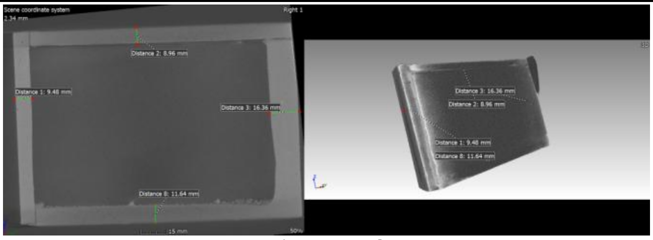

Fig. 1. *Detail.*

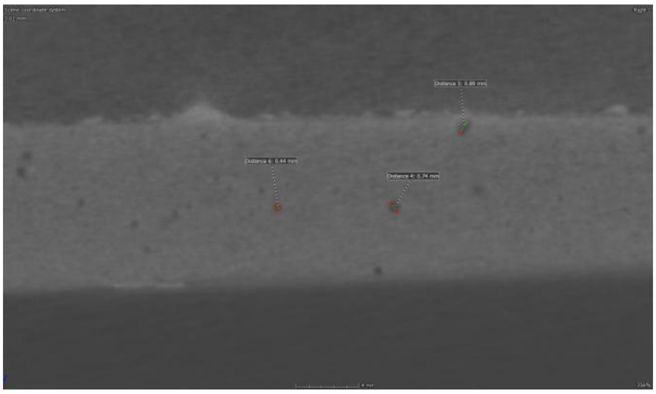

Fig. 2. *The porosity of the walls.*

Detail 2.

In fig. 3 the cavity of the detail is shown, as for the most part it is homogeneous. In the middle of the detail, there is an artifact (hollow/additional material) with a size of 1.71 mm in its most protruding part.

In fig. 4 the dimensions of the walls of detail 2 are shown. The average dimensions are in the range of 7.85 mm to 9.62 mm. Due to the specific of the detail (ribbing) for one wall are given 2 sizes.

In fig. 5 is shown part of the porosity of the walls of the detail. The pore sizes are in the range from 0.69 to 1.17 mm.

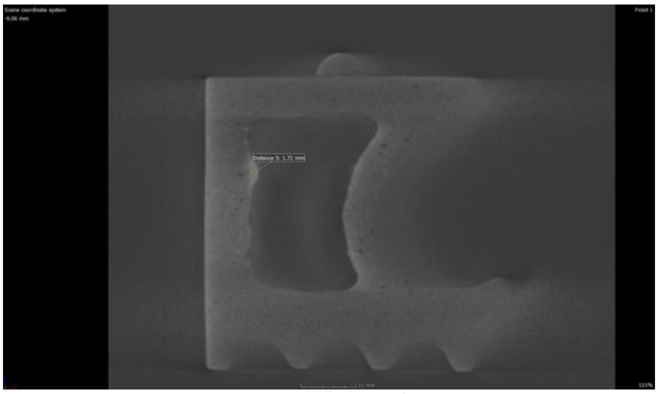

Fig. 3. Hollowness of the part.

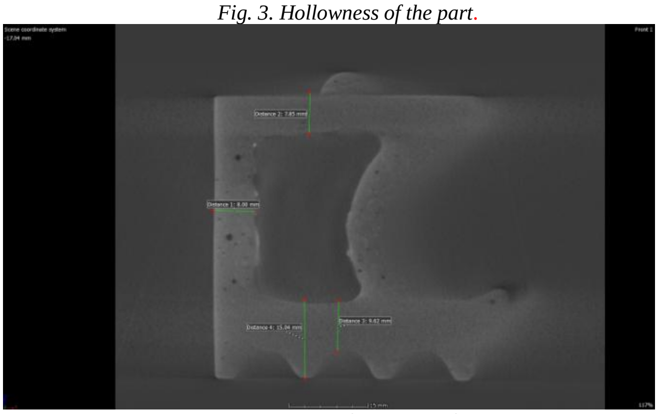

Fig. 4. *Dimensions of the walls of detail 2.*

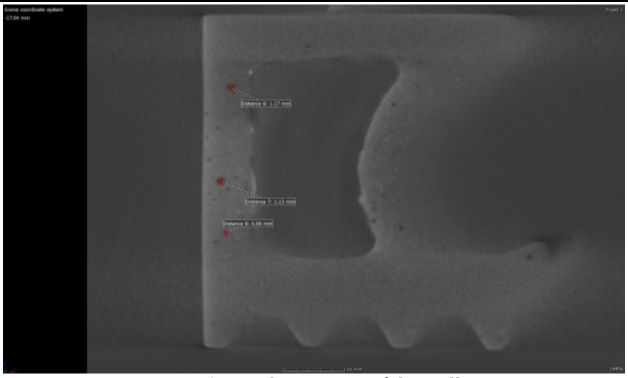

Fig. 5. *The porosity of the walls.*

Detail 3.

Uniformity of the cavity is observed for the most part. During the ribbing, an unevenness is observed in the cavity following the ribbed wall, shown in figures 6 a) and b).

In fig. 7 is shown the average dimensions of the walls in the range from 4.22 mm to 8.33 mm, and due to the specific of the detail (ribbing) for one wall are given 2 sizes.

The average size observed at the porosity of the material is in the range from 0.5 to 2.08 mm, shown in fig. 8. They are most strongly exhibit expressed in the beginning - fig. 8 a) and in the end of the detail -fig. 8 c).

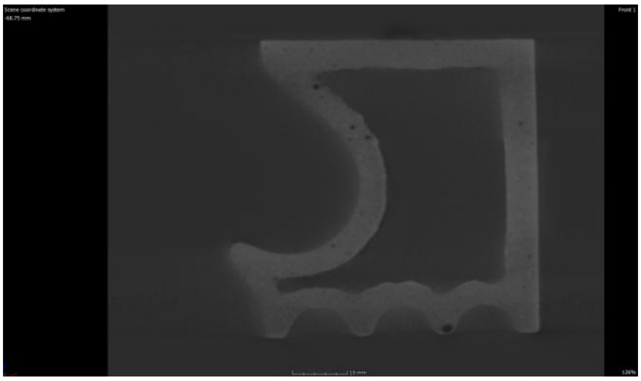

a)

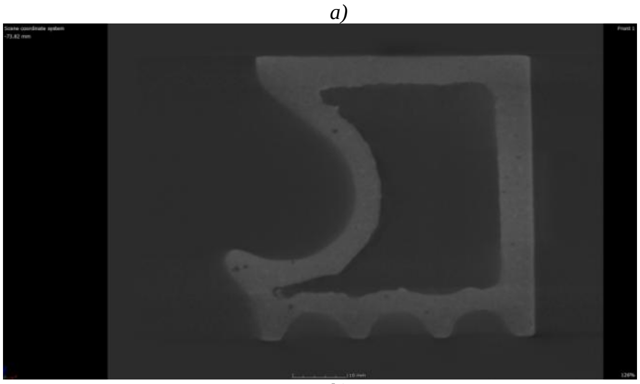

b)

Fig. 6. *Hollowness of the detail.*

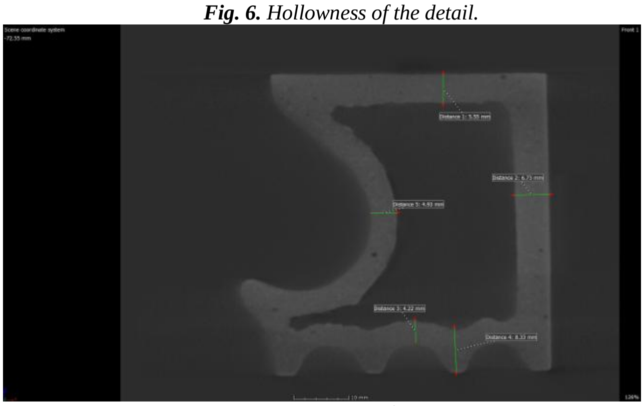

Fig. 7. *Dimensions of the walls.*

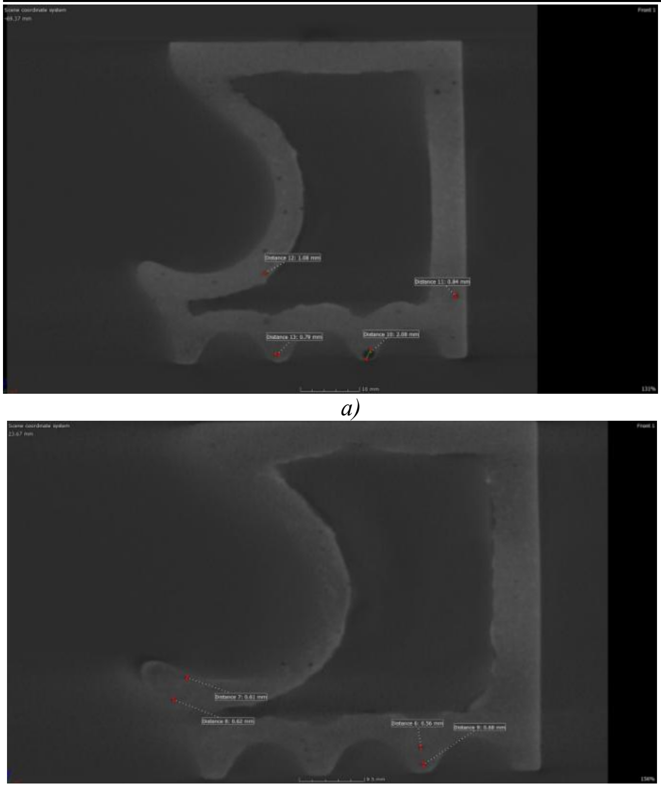

a)

б)

***Fig. 8.** The porosity of the walls.*

Detail 4.

Homogeneity of the cavity part is observed in detail 4.

In fig. 9 is shown the average dimensions of the walls in the range from 4.39 mm to 8.17 mm, and due to the specifics of the detail (ribbing) for one wall are given 2 sizes.

The average size observed in the porosity of the material is in the range of 0.26 to 0.8 mm. Shown in fig. 8, being most strongly expressed at the beginning of fig. 8 a) and the end of the detail - fig. 8 c).

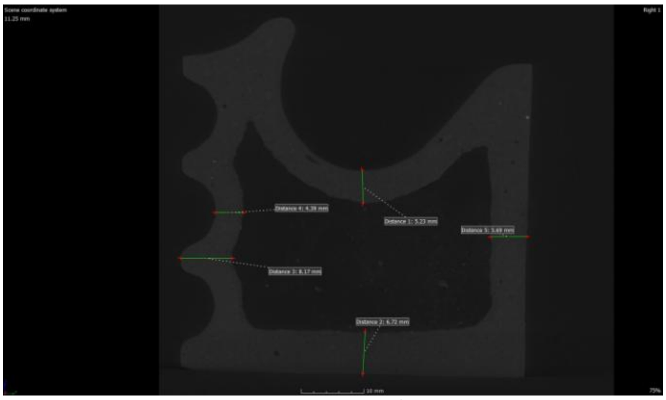

***Fig. 9.** Dimensions of the walls.*

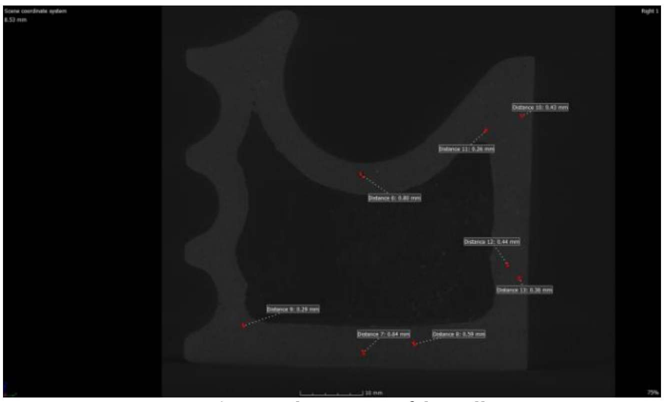

***Fig. 10.** The porosity of the walls.*

Detail 5.

In detail 5, the uniformity of the cavity part is shown in fig. 11. A slight form of porosity of the material is also observed

Fig. 12 shows average wall sizes in the range from 3.42 mm to 4.8mm. Due to the specifics of the part (ribbing), additional dimensions are given, including the ribbing. The dimensions range is from 6.03 to 6.88 mm.

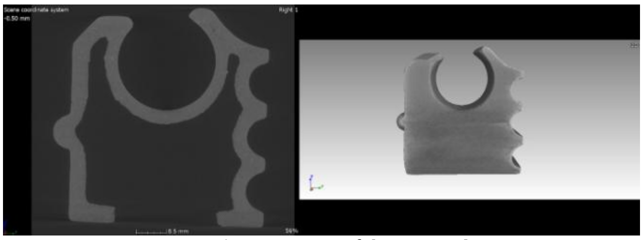

***Fig. 11**. Cavity of the material.*

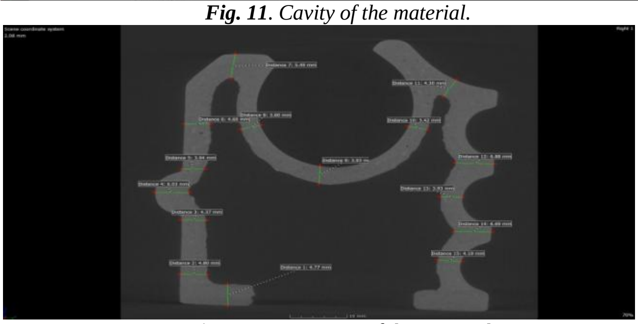

***Fig. 12.** Dimensions of the material*

Detail 6.

Homogeneity of the cavity part is observed in detail 6, except for the area at the heater trap shown in fig. 13. In fig. 13 a) is shown the cavity at the beginning of the part, 13 b) - the middle and 13 c) the end of the detail. A slight form of porosity of the material is observed. The left part of the images shows the section in which the cavity is located, and the right part shows the location on the 3D part with a line.

In fig. 14 is shown average wall sizes in the range from 3.42 mm to 4.8 mm. Due to the specifics of the part (ribbing), additional dimensions are given, including the ribbing. The dimensions range is from 6.03 to 6.88 mm.

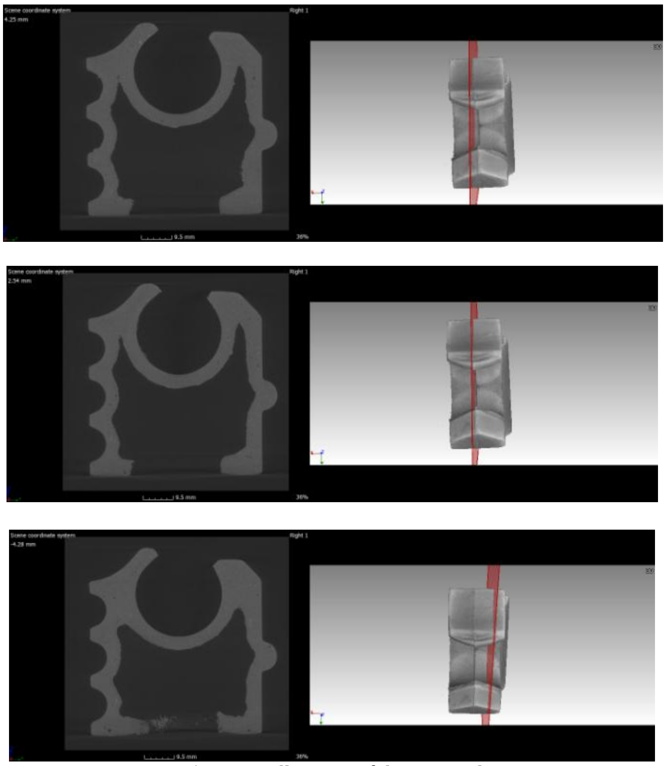

***Fig. 13.** Hollowness of the material.*

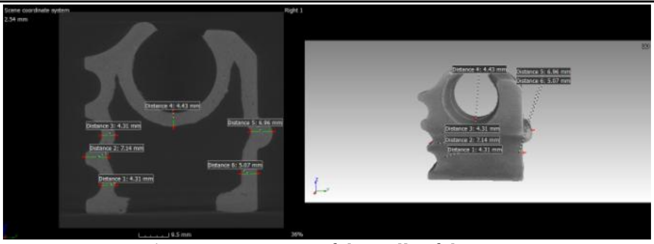

Fig. 14. *Dimensions of the walls of the part.*

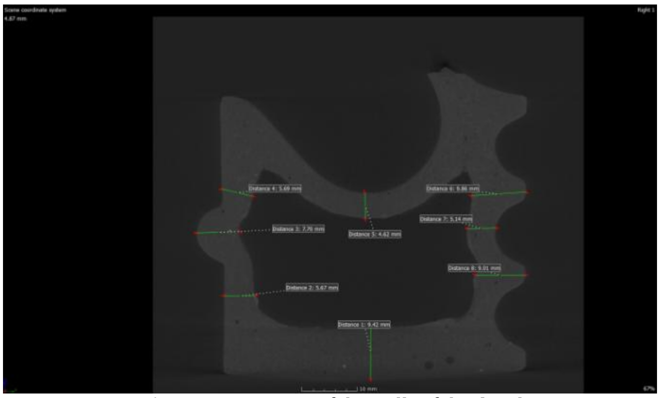

Fig. 15. *Dimensions of the walls of the detail.*

In detail 7 (presented in fig. 15) the dimensions of the walls of the detail are shown.

Pores with dimensions (up to 10 mm) larger than those in the other details are observed in fig. 16

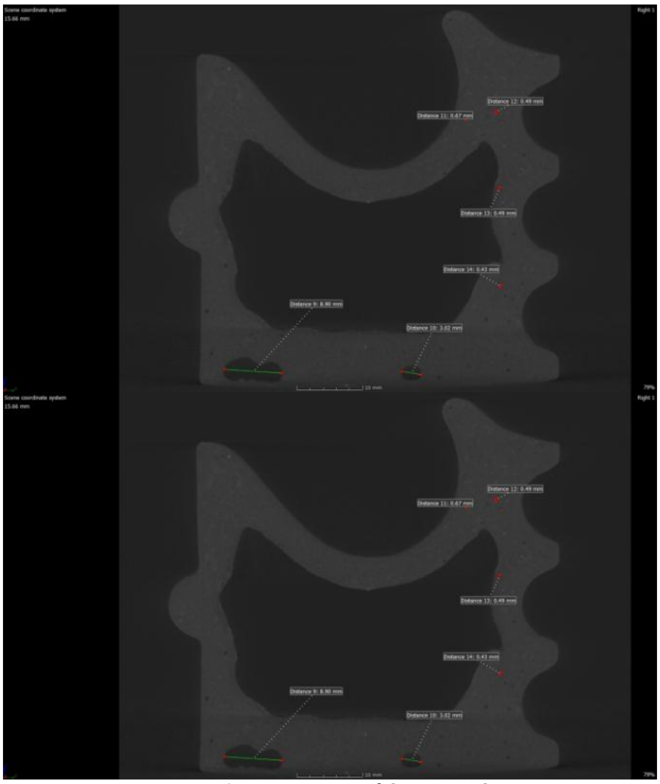

Fig. 16. *Porosity of the material*

4. Conclusions

From the analyses realized by the method of non-destructive 3D examination of the internal structure of the details, it can be concluded that in most details there is a porosity of the walls of the details. The cavity is homogeneous. In the future it is planned to measure the volume of the hollowness of the details, to determine the minimum, average and maximum sizes of the porosity of the material of the details as a result of the performed analyzes.

Studies show that computed tomography is effective in assessing, monitoring and diagnosing the actual condition of hollow ceramic products. Quality images suitable for processing are obtained. The main disadvantage is the requirements for the size of the tested samples and the time for collecting data for large images.

5. References

1. H. Marta, G. Roberson, M. Skente, D. Schneberk, S. Azevedo, “Computerized tomography studies of concrete samples, Nuclear instruments and Methods in Physics”, Research Section B: Beam Interactions with Materials and Atoms, Volume 58, Issue 2, June (1991), pp. 216-226.

2. H. Marta, D. Schneberk, G. Roberson, p. Monteiro, “Computerized Tomography Analysis of Reinforced Concrete”, Materials Journal, Volume 90, Issue 3, (1993).

3. K. Orhan, Micro-computed Tomography(microct) in medicine and Engineering Springer, 2020.

4. L. Liu, T. Guo, “Seismic non destructive testing and a reinforced concrete bridge column using, tomographic imagingtechniques”, Journal of Geofhysics and Enginering, volume 2, Issue I, march 2005, pp. 23-31.

5. Svetlan Bachvarov at al., “Ceramic Technology”, Carasvati, Sofia, 2003.

6. Kazakova S., Kamenova I., Klochkov L., Stoimenov N., Popov B., Sokolov B. Application of 3D Industrial Tomography In Dental Medicine.. International Scientific Conference “Industry 4.0”, 13-16 December 2017, Borovets, Bulgaria,, Scientific Technical Union of Mechanical Engineering Industry – 4.0, 2017, ISSN:2535-0021, 187-1

Mathematical analysis of an electrical circuit

Stela Todorova, Mladen Proykov
University "Prof. d-r Asen Zlatarov", 1 "Prof. Yakimov" bul, 8010 Burgas,, Bulgaria
rector@btu.bg

Abstract: *There are some research about mathematical analysis of electrical circuits. In time when the scientists are in a deep search of invention new alternative ways for producing renewable energy, mathematic postulates and analysis can help optimize the construction of electrical circuits and prevent lost of energy. By themselves, the electrical schemas that represent Electrical circuits are a combination of interconnected electronical elements (components). According to the characteristics of the elements of Electrical schemas they are divided into the following groups: Passive and Active, Linear and Nonlinear, Bipolar and Multipolar. In our research we are going to switch from high to low power and vice versa, so we are going to us the abilities of diodes that switch from on to off state. The different values of low and high power of the electrical circuit will be represented programmatically with a cross-platform application - Arduino Integrated Development Environment and programmable language C++.*
***KEYWORDS**: ELECTRICITY, PROGRAMMING, ELECTRICAL CIRCUIT*

1. Introduction

According to the definition, the electrical network is a combination of elements of interconnected circuits. The network may or may not provide a closed path to the flow of electricity. But an electrical circuit can be a combination of one or more networks that gives a closed path to the electric current. This means that when one or more networks are connected to each other to complete one or more current paths, an electrical circuit is formed.

An electrical circuit consists of the following topological elements: node, branch and contour. A node is a point where two or more circuit topological elements are connected together. Node is a point of connection in the circuit. When a structural element of the circuit is connected to the circuit, it is connected through its two terminals to be part of a closed path. When a structural element exists between two nodes, the path from one node to another through this element is called a chain branch. If it starts from one node and after passing through a set of nodes returns to the same initial node without crossing two of the intermediate nodes, it travels through one node contour of the circuit. [2]

2. Representation of electrical circuit with Arduino Uno and Breadboard

We are going to analyze an electrical circuit programmatically with the microcontroller development board Arduino Uno and Breadboard that is shown in Fig. 1.

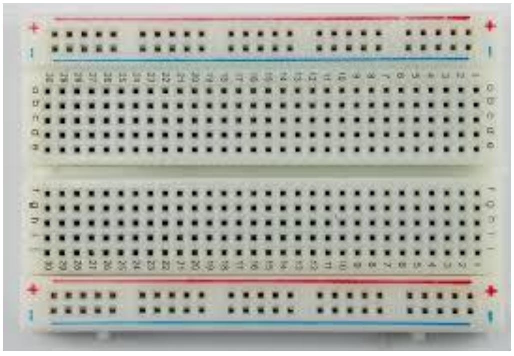

Fig. 1 *Breadboard.*

Breadboard is a patch panel with pins which will play the role of nodes of the electrical circuit and where it will be possible connecting structure elements and components, which will create branches. The structure elements that we are going to use in our electrical scheme, that is are shown in Figure 2 are: resistors, Tilt switch and LED diodes, which purpose is to assure one direction flow of electricity from one input node to end node through one contour. [1]

It is possible to make a table and represents each pin of Breadboard as a member of two - dimensional array, which first dimension is formed by the ordered set of a, b, c, d and second dimension includes the integer numbers from 1 to 30.

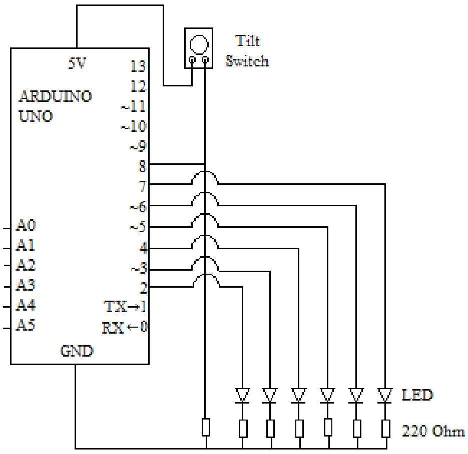

Fig. 2 *Electrical scheme.*

As Microsoft Excel name each cell of its tables, we are going to name the pins as a combination of the elements of the first dimension and second dimension that is illustrated in Table 1. [1]

Table 1. A table that represents each pin of Breadboard as a member of two - dimensional array.

	a	**b**	**c**	**d**	**e**
1	a1	b1	c1	d1	e1
2	a2	b2	c2	d2	e2
3	a3	b3	c3	d3	e3
4	a4	b4	c4	d4	e4
5	a5	b5	c5	d5	e5
6	a6	b6	c6	d6	e6
7	a7	b7	c7	d7	e7
8	a8	b8	c8	d8	e8
9	a9	b9	c9	d9	e9
10	a10	b10	c10	d10	e10
11	a11	b11	c11	d11	e11
12	a12	b12	c12	d12	e12
13	a13	b13	c13	d13	e13
14	a14	b14	c14	d14	e14
15	a15	b15	c15	d15	e15
16	a16	b16	c16	d16	e16
17	a17	b17	c17	d17	e17
18	a18	b18	c18	d18	e18
19	a19	b19	c19	d19	e19
20	a20	b20	c20	d20	e20
21	a21	b21	c21	d21	e21
22	a22	b22	c22	d22	e22
23	a23	b23	c23	d23	e23
24	a24	b24	c24	d24	e24

25	a25	b25	c25	d25	e25
26	a26	b26	c26	d26	e26
27	a27	b27	c27	d27	e27
28	a28	b28	c28	d28	e28
29	a29	b29	c29	d29	e29
30	a30	b30	c30	d30	e30

Moreover, it is possible to form another table, that is shown in Table 2 which values will be the Volts digital pins 2, ~ 3, 4, ~ 5, ~ 6, 7 and 8 of Arduino Uno that connects with each pin of Breadboard, according to the names and rules of the two - dimensional array that we illustrated in Table 1. [1]

Table 2. A table which values are the Volts of digital pins 2, ~ 3, 4, ~ 5, ~ 6, 7 and 8 of Arduino Uno that connects with each pin of Breadboard.

	a	**b**	**c**	**d**	**e**
1	0	0	0	0	0
2	0	0	0	0	0
3	0	0	0	0	0
4	0	0	0	0	0
5	0	0	0	0	0
6	0	0	8	0	0
7	0	0	0	0	0
8	0	0	0	0	0
9	7	0	0	0	0
10	0	0	0	0	0
11	~6	0	0	0	0
12	0	0	0	0	0
13	0	0	0	0	0
14	0	0	0	0	0
15	0	0	0	0	0
16	0	0	0	0	0
17	~5	0	0	0	0
18	0	0	0	0	0
19	0	0	0	0	0
20	0	0	0	0	0
21	4	0	0	0	0
22	0	0	0	0	0
23	0	0	0	0	0
24	0	0	0	0	0
25	~3	0	0	0	0
26	0	0	0	0	0
27	0	0	0	0	0
28	0	0	0	0	0
29	2	0	0	0	0
30	0	0	0	0	0

The digital pins of Arduino Uno, that is illustrated in Fig. 3, define the output voltage level of the pins of the Breadboard. Also, the digital pins of Arduino Uno and the pins of the Breadboard forms a separate contour which activation depends entirely programmatically through the functions: digitalWrite(pin, value) and digital Read (pin). [1]

Fig. 3 *Arduino Uno.[5]*

The Volt of digital pin 8 of Arduino Uno is the OUTPUT point of the circuit and the other 6 a the INPUT points of the circuit. [1]

3. Analysis of electrical circuit with Arduino Uno and Breadboard

The digital pins of Arduino Uno define the input and output voltage level of the pins of the Breadboard. Also, the digital pins of Arduino Uno and the pins of the Breadboard forms a separate contour which activation depends entirely programmatically through the functions: digital Write (pin, value) and digital Read (pin). According to this it will be possible to be created a dashboard time - table and the activation of each contour will be illustrated with "1" and the lack of voltage with "0". It can be named as A dashboard time - table of activating contours, that is shown in Table 3, which will be switched on in a time span of 600 000ms that each digital pin of Arduino Uno will be set programmatically. [1]

Table 3. A dashboard time - table of activating contours.

	2	**3**	**4**	**5**	**6**	**7**
10 min	1	0	0	0	0	0
20 min	1	1	0	0	0	0
30 min	1	1	1	0	0	0
40 min	1	1	1	1	0	0
50 min	1	1	1	1	1	0
60 min	1	1	1	1	1	1

5. Conclusion

With programmable dashboard time - table it will be possible electricity suppliers to monitor the current consumption of their subscribers, and in addition if it is implemented a controller with a combination with a trigger will provide less voltage to a household, which at some time point in the day does not consume full capacity of electrical appliances. With the software program it will be possible to change the input and output nodes and not only change the active contours, but also to control the flow of current in one or another circuit, which if implemented in the electricity network, it will reduce unnecessary energy consumption and unnecessary maintenance of resources to supply electricity that is not used and consumed. This would reduce the use of natural resources as such as the vital factor for life - water that is used by thermal power plants and the cost of electricity supply to both suppliers and consumers of electricity.

6. References

1. Scott Fitzgerald, Michael Shiloh, Arduino Projects Book, (2015)
2. Riverglennapt, Nodes, branches and loops of a circuit, Available: https://riverglennapts.com/bg/circuit-and-network/172-nodes-branches-and-loops-of-a-circuit.html
3. Svetlin Nakov, Fundamentals of Computer Programming with C++, Available: https://introprogramming.info/english-intro-csharp-book/
4. Boris Estatiev, Basic Laws in Electrical Circuits Available: https://www.uni-ruse.bg/disciplines/TE/
5. ARDUINO UNO REV3, Available: Arduino Uno Rev3 | Arduino Official Store

Reducing the catastrophe risk in coastal areas: risk management at fsru terminals

Filip Jovanović, Mirano Hess
University of Rijeka, Faculty of Maritime Studies, Croatia

Abstract: *Today, coastal areas are among the most densely populated and busiest places in the world, with an extremely important economic and social value. With those areas being very intensely exploited, there is a strong possibility of different accidents and catastrophes occurring. Therefore, it is a matter of great importance to implement timely and quality measures to minimize the risk of negative consequences. This research explores the theories of coastal area management and risk management, while focusing on the synthesis of both of them on FSRU terminals. Given the fact that this special type of LNG terminals is becoming more and more present in the coastal areas of the world, this paper implements analysed theories and proposes risk minimising and safety measures for reducing the catastrophe risk with FSFRU terminals and thus contributing to the preservation of the coastal area.*
Keywords*: COASTAL AREA MANAGEMENT, LNG TANKER, FSRU TERMINAL, RISK MANAGEMENT, SAFETY*

1. Introduction

This research focuses on risk analysis, risk management techniques and methods to reduce risks to acceptable levels in an extremely rich but also sensitive coastal area. It should be appreciated at the outset that risk can never completely disappear, it always exists, but it is possible to reduce it and reduce it to the level of acceptable risk [1, 2]. What is the acceptable level of risk depends on the situation and various factors, and this is one of the items that need to be defined during the risk management process. The entire risk management process can be divided into two main segments. The first is risk assessment, and the second is action to reduce it.

As there are many possible scenarios for various ventures and projects in the coastal area, the number of potential disaster risk reduction measures is exponentially higher. Each individual project that begins carries certain risks, and therefore for each of them it is necessary to develop and apply a system of disaster risk reduction measures, and apply theories of coastal zone management and risk management [3]. A large number of countries use FSRU terminals (Floating Storage and Regasification Unit) for transhipment of liquefied natural gas and one of these countries is the Republic of Croatia, where preparations are currently underway for the construction of such a plant in Omišalj on the island of Krk [4]. Ship-to-ship transfer, which is one of FSRU transhipment methods is shown on Figure 1.

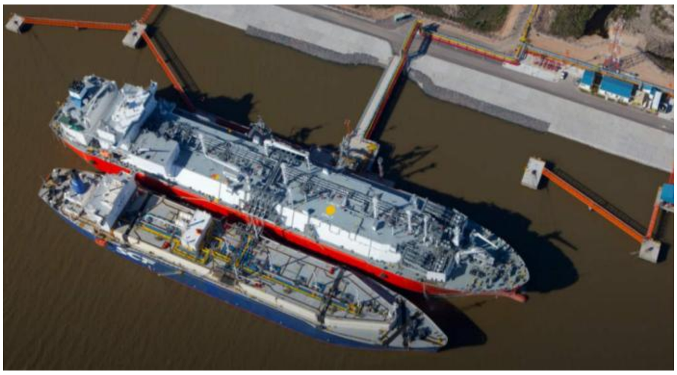

Fig.1 *Ship-to-ship transfer. Source: MFAME, Excelerate Energy: All Set for 1000th Ship-to-Ship Transfer of LNG Celebration, 05.08.2016., https://mfame.guru/excelerate-energy-set-1000th-ship-ship-transfer-lng-celebration/ (27.07.2020.)*

It is important to note at the outset that the floating terminal for the import of liquefied natural gas is actually a ship connected to the onshore pipeline through which natural gas is further transported to end consumers [5]. Once the liquefied natural gas is unloaded at the FSRU terminal, a regasification process needs to begin before the natural gas can be sent further to the onshore pipeline network to supply consumers. The regasification system can be considered the main functional system of each FSRU terminal, since it is in this system that the conversion of gas from liquid to gaseous state takes place [6]. Figure 2 shows a schematic of the regasification process at the FSRU terminal.

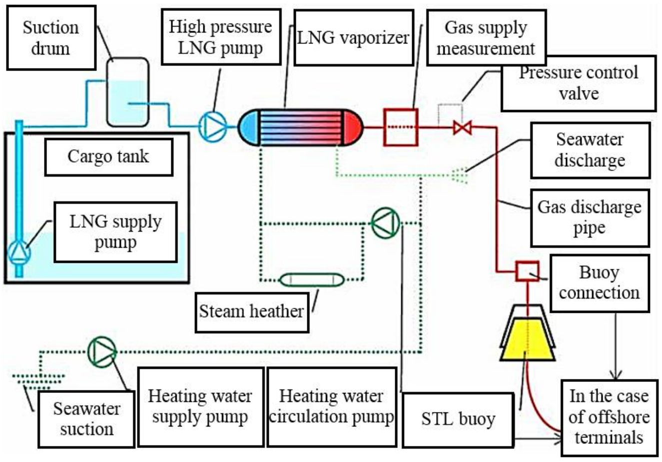

Fig.2 *Schematic of the regasification process. Source: authors on the basis of Janssens, P., Energy Bridge: The World's First LNG Offshore Solution, Gastech, Bilbao, Spain, 2005.*

When conducting a risk assessment related to the import of liquefied natural gas through the FSRU terminal, the analyses must include the FSRU ship, incoming LNG tankers, other coastal infrastructure and the terminal, location and local meteorological and oceanographic conditions, traffic in the waters and the surrounding area.

Four categories of factors influence risk assessment [7]:
- location, specific local conditions, LNG imports, importance for the region
- potential threats, potential accidents, possible accidents, critical coastal infrastructure and FSRU ship, incoming LNG tankers
- risk management objectives, identification of consequences to be avoided (e.g. injuries or damage to property), importance of LNG supply
- possibilities of protective mechanisms, safety measures, warning and alarm systems, reaction measures in case of accident

These categories must be taken into account when determining whether the implemented safety measures can successfully achieve the desired level of risk management for a particular project in a particular area. Hazardous projects such as liquefied natural gas imports should be regularly re-evaluated, in order to reassess the adequacy of the safeguards applied because conditions may change frequently. For example, changes in the context of facilities, coastal infrastructure, the emergence of new threats, changes in risk management objectives and many others.

2. Methodology of risk assessment

When joining each project, some benefit is expected from it for a certain cost. However, each project carries with it certain risks, and it is often necessary to implement certain risk reduction measures, which also represents additional costs. It is for this reason that this analysis is done, which determines the methods that can be used to keep the project profitable in the end. In this way, a balance is sought between the costs caused by the implementation of risk reduction measures and the residual level of risk. As pointed out earlier, the risk can never be completely eliminated, but only reduced to an acceptable level, and this is exactly what this method seeks to achieve, taking into account cost-effectiveness and potential benefits. As part of this method, the so-called cost-benefit balance is often used to determine the balance between costs and benefits, the ALARP principle. This principle is based on reducing the risk as much as reasonably possible by rational use of available resources. Therefore, if the implementation of some measures would slightly reduce the risk given the high costs of the measures, it is concluded that the implementation of such measures is not justified. Conversely, if the risk were significantly reduced for a reasonable cost of measures, enforcement is justified. From this it can be concluded that for the costs of implementing risk reduction measures and the risk reduction itself, it is desirable to be proportional in size. The ALARP principle is often displayed graphically, with three different fields representing risk levels. Figure 3 provides a pictorial representation of this principle.

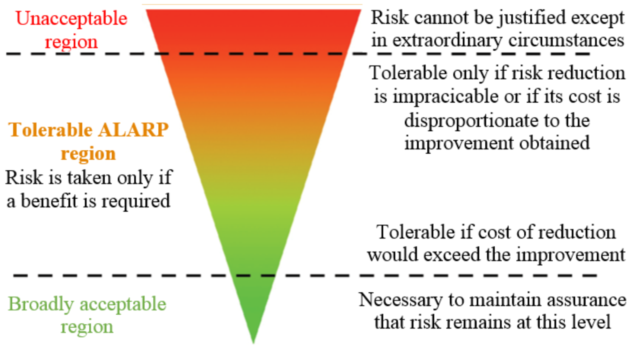

Fig.3 *Scheme of ALARP (As Low As Reasonably Practicable) system.*

The uppermost field represents an unacceptable risk, and it is mandatory to implement risk mitigation measures in order to reduce it to an acceptable level. The middle field represents an acceptable risk and the implementation of measures is not necessarily necessary, but it is desirable if an additional significant risk reduction would be achieved for a reasonable cost. The lower field represents a negligible risk that is so low that it is insignificant and can be ignored. Cost-benefit analysis together with the ALARP principle is almost always used when planning all projects in coastal areas.

The context of the FSRU facility such as location, micro location, specific local conditions, meteorological and oceanographic conditions, and desired cargo operations must be identified for risk assessment. Information that must be taken into account are:

- neighbouring surrounding area: distance from other port areas and facilities, distance from residential, commercial, industrial facilities, or other infrastructures such as tunnels, bridges, etc., as well as distance from regular traffic lines and flows
- prevailing weather conditions: wind direction and speed, possibility of particularly dangerous weather conditions such as hurricane or hurricane wind, sea currents, wave height, seismic activity, type of sea bottom, proximity of river estuaries, possibility of ice, etc.
- cargo operations: size and design of the FSRU ship, expected frequency of delivery, size of tanks, regasification capacity, seasonal needs for LNG, required quantity of supply

In the process of identifying potential hazards and threats to the FSRU ship and the surrounding area, it is necessary to take into account "unexpected" accidents, but also the possibility of intentionally caused accidents such as in the case of terrorist attacks [8]. Potential accident scenarios include: leakage from tanks or pipelines, rupture of tanks or pipelines, collision with an incoming LNG tanker, oil spill due to damage to the hull, accidents with ballast system, shipboard accidents, fires, explosions, interruption due to significant worsening of weather conditions, danger of terrorist attacks, robberies, kidnappings, etc. It is important to emphasize that in case of operation of FSRU ship as a receiving LNG terminal, there is no danger of pollution of the marine environment with ballast water, since LNG tankers arrive with full cargo and without ballast. As they discharge the cargo, they take ballast from the local area, so there is actually no discharge of ballast water into the local waters.

3. Risk management objectives

This phase involves determining the objectives of risk management and the level of severity of the consequences of accidents during LNG operations, including potential property damage, potential injuries, potential damage to public safety, etc. Setting goals is done in close cooperation with owners and managers, experts and scientists. The task of this step is actually to determine the acceptable risk, i.e. the extent to which it is acceptable to perform a process given the severity of the consequence that is potentially possible. It is impossible to reduce the risk to zero, but it is possible to reduce it to the extent that it is acceptable for a certain project and a certain area.

It is common for the following important factors to be taken into account when setting risk management objectives [9]:

- consequences in the event of a collision with an LNG ship
- consequences in case of spillage of LNG into the sea
- hazards caused by the spillage of LNG into the sea (damage to the environment, risk of fire and explosion, danger to the health of human, animal and plant organisms)
- hazards arising from spills from propellant tanks into the sea
- acceptable duration of the interruption of the FSRU ship
- speed of resumption of operation of the FSRU ship after a temporary interruption of operation
- consequences in case of operations' termination of the FSRU

4. Protective and safety measures to reduce risk

This phase includes the identification of all safeguard operations to reduce potential risks and the safety and security measures of the FSRU ship and the surrounding terminal area. The general items covered by the risk mitigation safeguards is listed here, and the next chapters will describe in more detail the specific implementation of some of safety and security measures on FSRU ships [9]. Thus, safeguards that mitigate potential risks on FSRU ships include:

- safety measures for gas supply systems, pipelines, tanks
- regasification and distribution
- availability of medical, fire, police services and SAR services
- availability of a sufficient number of adequate tugs
- warning and alarm systems
- the possibility of rapid, efficient cessation of cargo operations
- safety aspects of FSRU ship design (double hull, fireproof, etc.)
- safety distance from other port areas and facilities, residential, commercial, industrial facilities and the like
- pollution prevent measures in the event of an LNG spill
- measures in case of fire, explosion
- measures in the event of a collision with an LNG ship on arrival
- measures for termination and commencement of cargo operations
- measures of reaction in case of war or siege
- evacuation plan
- security systems of the FSRU ship and the surrounding area of the terminal (protective fences, security guards, video, etc.)

5. Monitoring, evaluation and modification of measures

Once safety and security measures have been in place, all for the purpose of mitigating risks, their effects need to be regularly monitored and evaluated during their implementation. It is necessary to evaluate their success in maintaining pre-defined risk management objectives, and to react if it is concluded that there is still room for improvement of the system. It is also important to regularly update and modify the existing risk management system, as there may be a change of context in terms of changing delivery volumes, construction of new facilities near the terminal, changing requirements related to international conventions, etc. Regular evaluations of the existing system and the application of new, updated safety and security measures increase the safety of people, property and the environment, and reduce risk, which is exactly what it aims to achieve.

6. Risk reduction measures

Regarding the system of measures to reduce the risk of accidents and catastrophes during the operation of a floating terminal for the import of liquefied natural gas (Figure 4 shows an example of an LNG spill), as well as the general protection of the terminal and the surrounding area, three main components are distinguished: safety, security and corrective measures in case of an accident. These measures will be described and explained in more details. Here, it is important to mention conventions and regulations that apply to this type of ship, and which actually serve as a basis for good practice in achieving security and protection of FSRU terminals.

Fig.4 *An example of an LNG spill. Source: Hine, L., MOL outlines lessons learned from LNG ship cargo release, 21.07.2016.*

FSRU terminals are adapted to special local conditions and legal regulations, and are subject to the national standards of the country in whose territory the exploitation takes place [10]. It is important to note once again that FSRU ships are subject to all the classic classification requirements for ships dealing with the cargo of liquefied natural gas. Therefore, FSRU ships, just like conventional LNG ships, must comply with the following conventions, codes and regulations of the International Maritime Organization (IMO):

- International Convention for the Safety of Life at Sea (SOLAS)
- International Convention for the Prevention of Pollution from Ships (MARPOL)
- International Code of the Construction and Equipment of Ships Carrying Liquefied Gases in Bulk (IGC)
- International Ship and Port Facility Security Code (ISPS)
- International Safety Management Code (ISM)
- International Convention on Standards of Training, Certification and Watchkeeping for Seafarers (STCW)

In addition to the above conventions, it is clear that FSRU ships must comply with all other conventions in the maritime world. Furthermore, it is necessary to have valid certificates and documents in accordance with these conventions, and to meet all appropriate safety requirements prescribed by classification societies, flag state and the state in which the terminal is operated. In addition, these ships are required to comply with regulations related to the construction and equipment of ships performing regasification processes (Guide for Building and Classing LNG Regasification Vessels) and special instructions for LNG ships issued by the Society of International Gas Tanker and Terminal Operators (SIGTTO) [11]. Of course, in terms of ship construction, FSRU ships, as well as all new tankers being built today, must meet the standards of double hull construction, which is one of the most important safety measures to prevent accidents and catastrophes [11].

7. Safety measures

The term safety of the FSRU terminal refers to the day-to-day operations performed on it, and they can be related to cargo and cargo operations or any other area such as mooring or unmooring. Emphasis was placed on their proper execution and implementation of precautionary measures, as well as reaction measures in case of potential accidents during the execution of these operations. Several standardized safety systems are used, which are in fact the most common for all types of LNG ships, and their primary goal is to increase the safety of terminals, crew, property and the environment, and accordingly, reduce the risk of accidents and disasters.

ESD system

An emergency shutdown system (ESD) is a system that has the important task of stopping all cargo processes active at the terminal in the event of an emergency. The system must therefore include all parts of the process at the terminal, namely: FSRU ship, LNG ship reloading cargo, tugs that must be on standby to access and tow the ship to a safe distance from the terminal in time and the onshore pipeline infrastructure and safety valves. Since this system is mainly used during cargo transhipment operations, in order to be functional, the system must be synchronized with the land infrastructure and other ship with which the transhipment is performed. After activating the system, the automatic shutdown of cargo pumps and compressors begins and certain safety valves are closed by the system. Also, in many strategically placed locations on the terminal, switches for manual activation of the system can be found, however, the main purpose of the system is that it is activated independently and automatically in certain emergency situations, thus preventing potential negative consequences. Some of the activation factors of the system are: exceeding the limit values of pressures in cargo tanks, land and ship pipelines or pumps, fire detection on FSRU ship, LNG ship reloading cargo or anywhere else in the terminal area, interruption of synchronization with other ship or land infrastructure and power outage. Before starting the process of reloading cargo from the LNG ship to the terminal, the entire system undergoes a thorough check to determine the state of readiness, after which transhipment operations can begin after it is clearly established that the synchronization of all parts is successful and the system is in standby mode.

HIPPS system

The High Integrity Pressure Protection System (HIPPS) system is responsible for preventing excessive pressures in any part of the operating system during liquefied natural gas cargo operations [10]. The basic mode of operation of the system is to eliminate the source of overpressure by closing the predefined safety valves, shutting off the pumps or acting preventively by opening the vents before excessive pressures occur and rise above the maximum allowable values, thus preventing potential accidents. It usually works in combination with the aforementioned ESD system, and is activated as one of the safety factors of the system.

Pressure control and exhaust valve system

The system has an important function of optimizing the pressures in the tanks and pipelines of the FSRU terminal in case of exceeding the previously set limit values, with the aim of safety of the terminal and its surroundings [11]. The system determines the minimum and maximum allowable pressure values, and in case of increase above the upper limit value, gas is released through vent valves and pressure is reduced, while in case of decrease below the lower limit value, additional gas enters and pressure increase occurs. This prevents potential damage to tanks and pipelines due to too high or too low pressures within the system. The system works by having the valve of each tank connected to its vent mast. In addition, each tank is connected to a main vent tank in which evaporated gas is collected before being discharged through the main vent mast, which is usually located somewhere on the bow of the FSRU ship [10]. As a flammable atmosphere is created when the gas comes out of the vents when the gas comes into contact with oxygen from the air, it is necessary to constantly treat the vents with nitrogen, which creates an inert or non-flammable atmosphere. At the bottom of each vent mast there is a valve that regulates the release of nitrogen into the vent line, for the reason already stated that when the vent valve is opened, gas is released into the atmosphere, which leads to a potential risk of ignition when leaving the vent mast. Namely, in this situation, two of the three factors required for the fire, i.e. the closure of the burning triangle (heat source - flammable substance - oxygen) are met, and in that case even the smallest spark, which is the heat source, is sufficient for the fire. The presence of nitrogen in this mixture of gases, therefore, acts in a way that dilutes the flammable mixture of natural gas, and at the same time reduces the proportion of oxygen in the atmosphere immediately at the exit of the gas from the vent.

PERC system

The Powered Emergency Release Coupling (PERC) is a system responsible for acting in an emergency situation by quickly and efficiently stopping cargo transhipment processes and releasing all transhipment pipes with the help of specially designed safety hooks that are located at the junction of the terminal pipeline and the cargo LNG pipeline of the ship [11]. Also, the system can release the mooring ropes so that in the event of an emergency, the ship can be removed to a safe distance as soon as possible, either with its own propulsion or with the help of tugs. This applies to both the LNG transhipment vessel and the FSRU vessel. A PERC system arrangement is illustrated on figure 5.

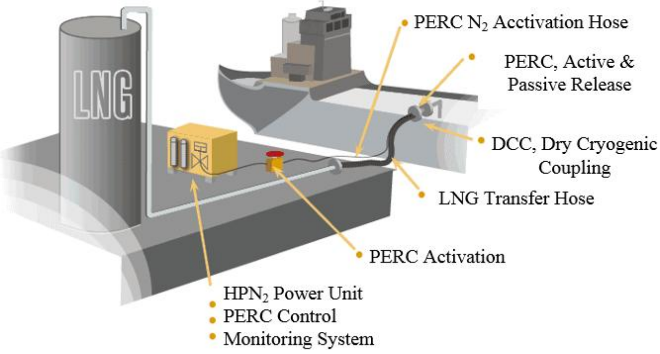

Fig.5 *PERC system arrang. Source: MannTek LNG Solutions, 21.10.2020.*

The system is connected to the aforementioned ESD system and is usually activated automatically as part of the safety factors of that system.

8. Security measures

When it comes to securing the FSRU terminal, emphasis is placed here on measures to prevent unauthorized persons from entering the ship and the surrounding area of the ship, to prevent possible acts of terrorism and to prevent other potential illegal actions related to terminal property such as vandalism, burglary, theft, damage, unauthorized drone shooting, unauthorized use of infrastructure, etc. [12].

The most important framework of measures in securing terminals is the application of the International Ship and Port Facility Security Code (ISPS), which sets a standard of preventive measures for protecting both the ships themselves and the ports or terminals. The basic goal of the code is proper protection, timely identification of threats and taking preventive measures to eliminate potential security threats, as well as the correct response in case of adverse events.

Also of great importance in the overall security of each FSRU terminal is the proper application of the International Safety Management Code (ISM). This code covers ships and companies at the same time, thus ensuring the necessary synchronization between ships and companies. Based on this code, a ship safety management system (SMS) is adopted, which prescribes safety management methods for each individual ship, and there is a specific person ashore who is in charge of the connection between the ship and the company on ISM issues and SMS, as well as to control the implementation of security measures.

4. Conclusion

Coastal areas around the world today are among the most important areas on Earth. Not only does an extremely large proportion of the world's human population live here, but the same is true for many plant and animal species. In addition, these areas represent an extremely valuable resource for all coastal states that have the ability to exploit it.

As in practice there are many cases in which the application of protective measures is required in the coastal area, this paper focuses on analysis of and practical application of safety and security measures of the floating terminal for the import of liquefied natural gas. This analysis illustrates how the proper implementation of safeguards can decrease the risks of negative consequences and disasters to the lowest possible level. No serious incidents have been reported since these terminals operate worldwide, as is the case in the entire LNG industry, due to the fact that the highest standards of safety and security in maritime affairs are present here, and the adopted protection measures are properly and timely implemented and, if necessary, improved. This is the main proof that a properly adopted system of coastal zone management and risk management, if adequately adapted to the specific problems that occur in the area, can result in the desired way, which is to reduce the risk of disasters in the coastal area.

The design, construction, operational procedures, and control of other coastal exploitation systems can be similarly organized. If problems are anticipated, noticed and identified in time, and approaches to solving them, by applying adequately adopted measures, the coastal area can certainly be positively affected in the long run. In this way, it is possible to reduce the risks of negative consequences and disasters, and preserve the coastal area, so that future generations can also engage in activities in this area. Respect for the principles of sustainable development, coastal zone management and risk management is the only correct path to be followed in any activity in extremely rich, but equally sensitive, coastal areas.

10. References

1. FAO, Integrated coastal management law: Establishing and strengthening national legal frameworks for integrated coastal management, FAO Legislative Study, no. 93, Rome, Italy, 2006.
2. United Nations, United Nations Conference on Environment & Development - Agenda 21, Rio de Janeiro, Brazil, 1992.
3. Post, J.,C., Lundin, C.,G., Guidelines for Integrated Coastal Zone Management, Environmentally Sustainable Development Studies and Monographs Series No. 9, The World Bank, Washington, D.C., 1996.
4. Paltsev, S., Economics and Geopolitics of Natural Gas: Pipelines versus LNG, Massachusetts Institute of Technology, Cambridge, MA, USA, 2015.
5. Songhurst, B., The Outlook for Floating Storage and Regasification Units (FSRUs), The Oxford Institute for Energy Studies, Oxford, UK, 2017.
6. Hochung, K., JungHan, L., Design and Construction of LNG Regasification Vessel, Gastech, Bilbao, Spain, 2005.
7. Hightower, M., Luketa-Hanlin, A., Gritzo, L., Covan, J., Review of the Independent Risk Assessment of the Proposed

Cabrillo Liquefied Natural Gas Deepwater Port Project, Sandia National Laboratories, CA, USA, 2006.
8. Janssens, P., Energy Bridge: The World's First LNG Offshore Solution, Gastech, Bilbao, Spain, 2005.
9. McGuire, G., White, B., Liquefied Gas Handling Principles On Ships and in Terminals, Third Edition, Witherby & Company Limited, London, 2000., p.57-73.
10. International Chamber of Shipping, Tanker Safety Guide (Liquefied Gas), Second Edition, Edward Mortimer Ltd, London, 1995., p.11-20.
11. McGuire, G., White, B., Liquefied Gas Handling Principles On Ships and in Terminals, Third Edition, Witherby & Company Limited, London, 2000.
12. World Bank Group, Environmental, Health, and Safety Guidelines for Liquefied Natural Gas Facilities, IFC, Washington, D.C., 2017.

Innovative business development and the startup ecosystem in the era of the fourth industrial revolution

Galyna Zhavoronkova, Vladimir Zhavoronkov, Vusala Nagieva,
National Aviation University,
Kyiv, Ukraine
zhavor@ukr.net

Annotation. *The study of the theoretical aspects of the development of innovative business has proved that the most effective form of innovative business, which can create and implement the final product, is a startup. The environment and infrastructure of a startup form its ecosystem. An innovation ecosystem includes economic agents, as well as an innovation environment consisting of ideas, rules of the game, social interactions, and culture. The state of the innovative business and the startup ecosystem of Ukraine behind its main components and institutions are analyzed, and the factors of the development of the startup ecosystem for its competitiveness among the world are determined. Government measures and initiatives should promote the emergence of a community of startup founders who will work closely with other actors in the private sector of the economy and the public sector. At the same time, the state should not assume the role of a leader, but only an initiator.*

KEYWORDS: *INNOVATIVE BUSINESS, MODEL, STARTUP, ECOSYSTEM, DEVELOPMENT FACTORS.*

1. Introduction

The fourth industrial revolution means more and more automation of absolutely all processes and stages of production: from digital product design, creating a virtual copy of it – to remote configuration of equipment in production under the technical requirements for the release of a specific "smart" product. This revolution is unique in terms of the pace, dimension, and consistency of transformations. It was driven by digitalization and networking. It blurs the boundaries between the physical, digital, and biological spheres while changing entire systems, basic concepts (money, power, partnership, property, identity) [1].

Innovative business is based on the constancy of the external environment, understanding it as a necessary condition for a stable organization and effective functioning of the economic system as a whole. It should be noted that most countries face the problem of lack of investment resources necessary for the development of innovative business, there is a structural imbalance between supply and demand in the field of financing innovative projects.

In the economic context, the concept of "ecosystem" is considered as a concept that describes the evolution of the nature of the interactions of economic agents, the models of their innovative activity, and their relationship with the operating environment [2]. The innovation ecosystem includes economic agents, as well as an innovative environment consisting of ideas, rules of the game, social interactions, and culture [3].

Consequently, innovative business turns into a strategic growth factor, affects the structure of social production, changes the economic organization of society, and stabilizes the social situation in the country.

2. The model of the startup ecosystem in innovative business

A distinctive feature of the startup ecosystem from the environments for other types of business is the close relationship with applied science. Naturally, in regions where leading universities, research institutes, scientific and technological parks operate, innovation ecosystems are more developed, which increases the success of the startup implementation [4]. The size and maturity of the startup ecosystem are determined by its ability to provide opportunities for the launch, development, and successful implementation of startup projects, as well as the further development of innovative companies.

A startup ecosystem (hereinafter referred to as SE) is an innovative and developed region where a set of institutions operates, in particular research institutes, the best technical universities, technology parks, giant firms in the field of information and communication technologies, organizations whose activities are aimed at supporting business initiatives in the technology and innovation sector. The basis for the functioning of the SE is the movement of venture capital, intellectual and human resources, the purpose of which is to introduce innovations [5]. The peculiarity of the organized SE is that the resources necessary for the introduction of innovations should be supplemented from the commercial sector [6].

The first and most developed ecosystem is considered to be Silicon Valley in California, whose progress is stimulated by giant IT firms, as well as advanced universities. Boston and Berlin are also considered the most progressive SE, where one of the largest technoparks WISTA is located, where numerous enterprises in the field of creative industries and innovative business also operate [7].

PHASE #1. OCCURRENCE	**PHASE #3.1. NATIONAL INTEGRATION**
Characteristics: accumulating resources; founding the first startups; the emergence of a community of innovative entrepreneurs **Initiatives:** organization of conferences and meetings	**Characteristics:** implementation of a significant number of startups – the rapid growth of CE capitalization; active receipt of foreign resources; increasing CE competetiveness; the emergence of an innovative brand in the country; strengthening the relationship between research institutes and businesses **Initiatives:** reducing tax pressure on venture projects
PHASE #2: ACTIVATION	**PHASE #3.2. GLOBAL INTEGRATION**
Characteristics: combining the efforts of startup leaders and authorities to raise capital and strengthen interregional ties; adapting fo-reign experience; increase productivity by using resources in the work of start-up teams. **Initiatives:** state support programs, establishing ties with global SE.	**Characteristics:** **i**mplementation of large projects (more than $ 500 million); the startups-the primary engine of the economy; active immigration: personnel, entrepreneurs; fixing the connection with other CE; SE is the main business platform in the country. **Initiative:** flexible immigration policies, the content of the low cost of living
PHASE # 4: MATURITY	
Characteristics: slowing growth rates; balancing all areas; strengthening business and research links at the global level; expanding the differentiation of areas in the startup sector. **Initiatives:** active investment in R & D, development of effective implementation practices	

Figure 1. Startup ecosystem lifecycle

The startup ecosystem evolves at the macro level, overcoming certain phases. The Startup Genome organization, which studies the evolution of dozens of startup ecosystems over several years and publishes annual reports on the state of the SE of mainly developed countries, has proposed a model for the development of an ecosystem consisting of four phases (Fig.1).

To determine the phase of SE development, the organization uses a set of metrics that allow assessing the pace of ecosystem development, their relationships at all levels, the state of funding, state support, infrastructure, etc. The phases of ecosystem development do not have clearly defined timelines. For example, for almost 30 years, the Israeli SE has reached the last phase, while the Berlin one is in "world integration", and the Hong Kong one is only "activation".

Advanced organizations and institutions offer various models of CE, but, according to the author, the most complete model is that proposed by the Netherlands accelerator and its research institute Startup Delta [7] (Fig. 2). The region in which all these elements and institutions are present is considered a "strong" or full-fledged CE. The complex infrastructure of a startup provides its comprehensive support at all stages of development.

Networks		**Expertise**	**Education**
Support in entering the local market	Competitions	Transfer of knowledge and technologies	Innovation Business Centers
Cooperation	Co-working space	Industry development	Support for student entrepreneurship
Events	Startup-media	Education	Science parks, research institutes
Capital		**Support**	
Investing at the pre-seed stage	Alternative financing	State	Incubators& Accelerators
Angels	Government funding	Development of the concept	Organizations that exercise social influence
Corporate and venture capital	Private and venture capital funds	Scaling a startup	Developing a venture business

Figure 2. Startup ecosystem model based on the startup Delta Institute

The state of the spheres in these five categories (networks, expertise, etc.) is studied based on the analysis of the state of commercial and non-commercial structures operating in these spheres.

1. Science parks. The main function of science parks is a mechanism for commercializing R & D results. A science park is defined as an organization established by a VSO or research institute based on a Cooperation agreement to transfer scientific knowledge to commercial structures.

2. Technology transfer. This is the process of transferring scientific achievements/discoveries from one organization to another for further development and commercialization. The sequence of the provision of technology transfer services can be considered as its life cycle.

3. Venture capital. The venture capital market is defined as a set of economic relations between buyers (innovative enterprises) and sellers (venture capitalists) regarding the movement of venture capital, reflecting the economic interests of market participants and ensuring the exchange of innovative products [8].

4. Business incubators are defined as structures that help projects at the initial stages to develop their idea, identify the target audience, build a team, get customers and feedback from them. **Accelerators** invest in startups by providing mentoring support and charge for their services, not money, but a share in the project [9].

5. State support. State support plays an important role in the creation of the SE. Examples of effective state support for innovative enterprises are the Netherlands and Ireland, which is a relatively short period have caught up with large countries thanks to the active policy of the state in this direction [10].

3. State of innovative business in Ukraine

In most cases, the activities of most science parks in Ukraine do not meet either the set priorities or the needs of the market, so these structures do not bring sufficient economic results. The state of science parks, research institutes, Western military districts and other institutions related to scientific activities has a steady tendency to decline (table. 1). There is a turnover of scientific personnel, a decrease in spending on science and innovation, a reduction in the share of innovative products, and R & D in GDP.

Table 1. *State of Science, Technology, and innovation in Ukraine 2010-2017*

Year	Number of organizations in the field of research and development	Number of scientists	Total innovation costs, mln UAH	Share of enterprises engaged in innovation, %	Share of innovative products sold in industry, %	Share of R&D GDP, %
2010	1303	89564	8045,5	13,8	3,8	0,90
2011	1255	84969	14333,9	16,2	3,8	0,79
2012	1208	82032	11480,6	17,4	3,3	0,80
2013	1143	77853	9562,6	16,8	3,3	0,80
2014	999	69404	7695,9	16,1	2,5	0,69
2015	978	63864	13813,7	17,3	1,4	0,64
2016	...	...	23229,5	18,9	...	0,48
2017	...	...	9117,5	16,2	0,7	0,45

Due to the weak interaction of Science and business, technology transfer has not found its development in Ukraine, which is due to the peculiarities of the state's economic development and legal aspects of intellectual property protection [12]. Nevertheless, since 2015, there has been a jump in the commercialization of R & D in Ukraine (fig. 3-4). The graphs show a tendency for technology imports to prevail over exports, especially until 2015, which indicates a relatively low competitiveness of the innovation sector of the Ukrainian economy. In Ukraine, the total amount of venture capital as of 30.06.2016 amounted to UAH 235.46 billion, which is 4.4% (or UAH 9.92 billion) more than in 2015.

Ukrainian investors and funds invested. 68 million in startup projects in 2015. This is three times more than in 2014 and 25% more than in 2013. The share of funds of Ukrainian investors during 2013-15 consistently exceeded the share of foreign investors, and in comparison with 2010 it increased more than 5 times (from 10% to 52%) (Fig. 5) [13].

During 2010-15, the IT sector showed a positive average annual growth trend of 80%, despite the decline in investment activity in 2014 (-55% compared to 2013). According to a study by the Ukrainian capital and private equity Association (UVCA), there are currently 17 active venture funds, 6 private equity funds and 1 corporate fund (HP Tech Ventures) operating in Ukraine. The portfolio of funds averages 20 companies; funds provide from 20 thousand to several million dollars; 16 funds are ready to invest in startups at the sowing stage, 10 funds at Rounds A and B, and 7 each at the pre-sowing growth stage, respectively [14].

Most incubators and accelerators have been operating in Ukraine since 2012 (foreign or domestic branches), which has led to a sharp increase in the number of startups launched and successfully implemented. The volume of attracted investments for the year of operation ranged from 500 thousand hryvnias (Polyteco) to 15.5 million US dollars (GrowthUP). The largest institution among the accelerators and incubators available in Ukraine is GrowthUP, which has been operating since 2007, accepting from 200 to 600 startup projects per year. The amount of funding for the project in these institutions ranges from several to 50 thousand dollars (most of the funds are provided by GrowthUP) [15]. Incubation and acceleration conditions in Ukraine differ somewhat from organization to organization, although they are similar in some aspects.

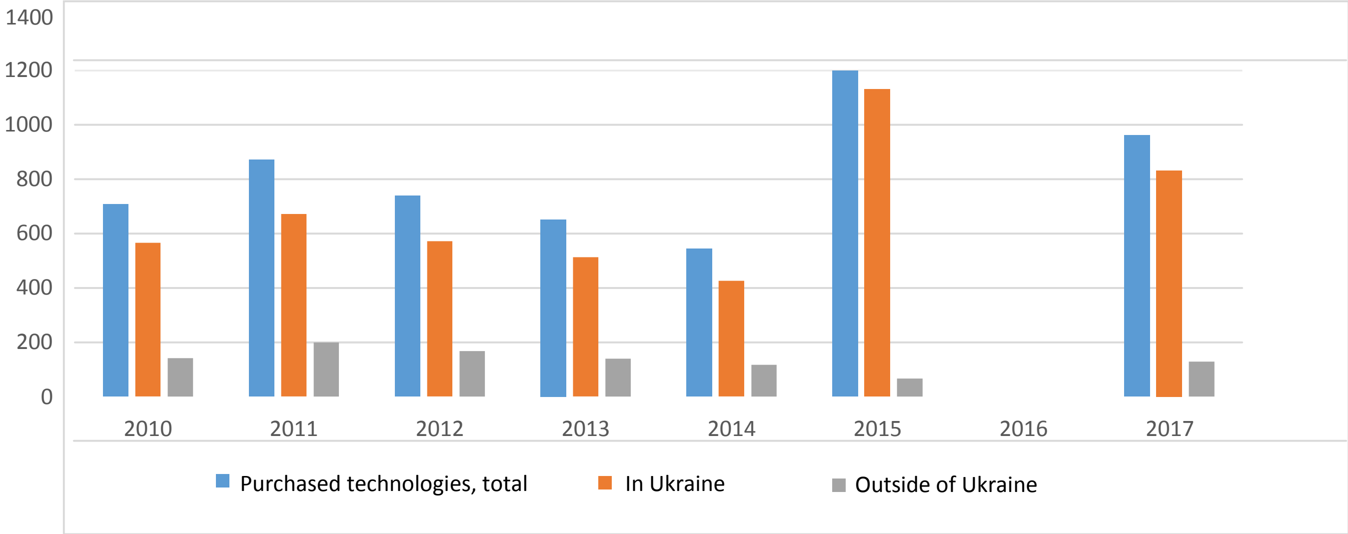

Figure 3 Dynamics of the number of purchased technologies in Ukraine (unit)

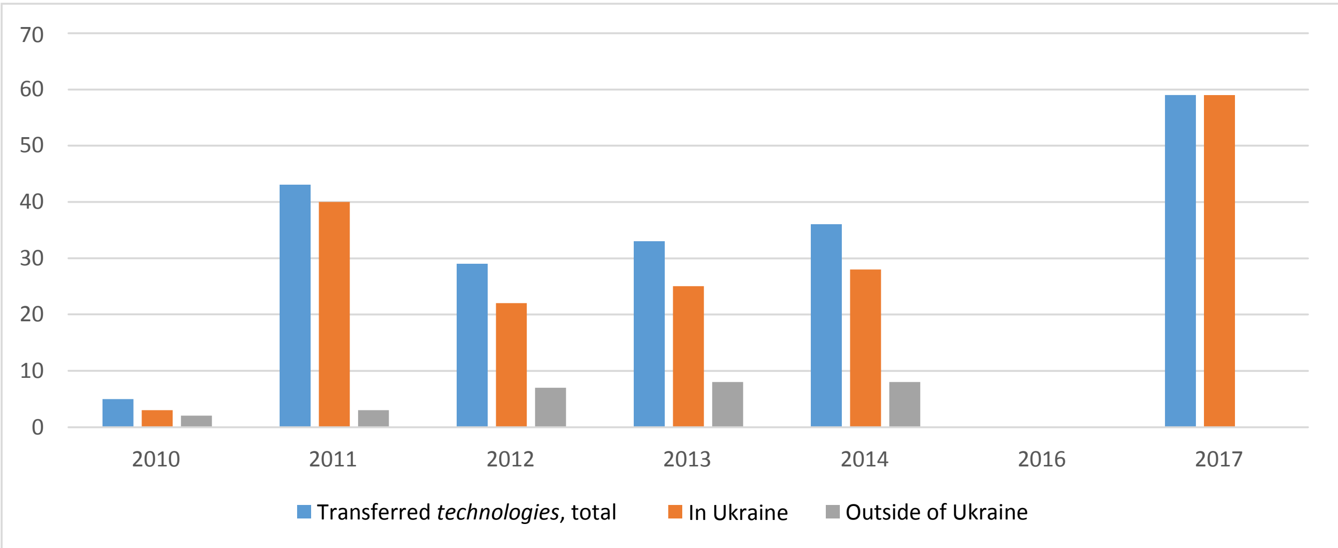

Figure 4. Dynamics of technologies transferred in Ukraine and abroad (unit)

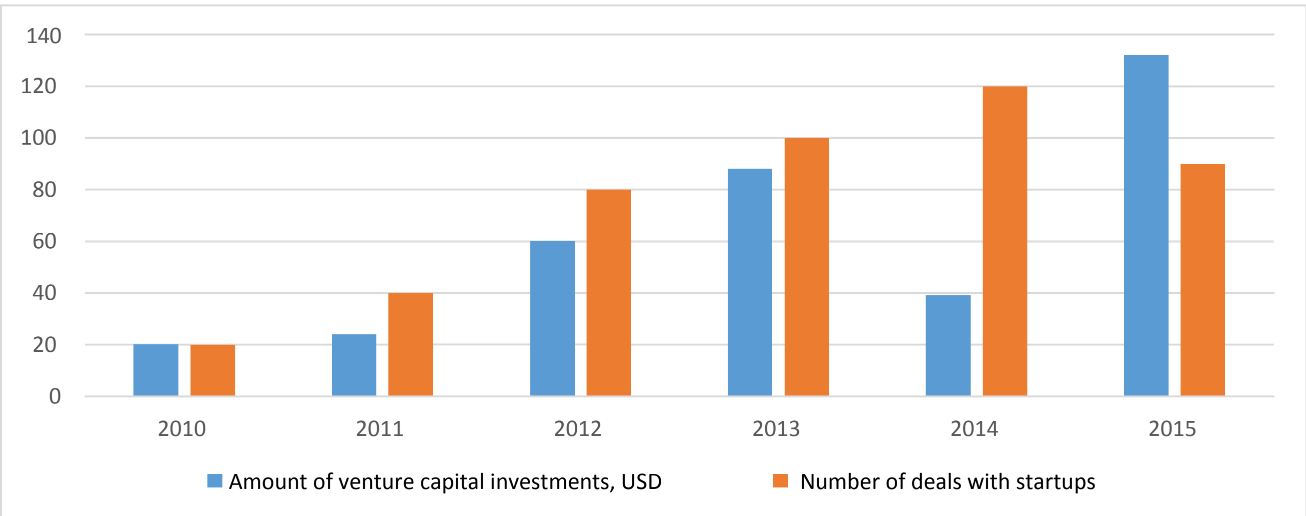

Figure 5. Dynamics of venture capital investments in Ukraine (unit)

The state policy in the field of innovation in Ukraine is regulated by the Law "On Innovation Activity". For the systematic development of the innovative sector of the economy, several state measures are envisaged, which, in particular, include: financial support for innovative projects and the establishment of preferential taxation of innovation entities. To provide financial support for the innovative activities of business entities of various forms of ownership, the Cabinet of Ministers of Ukraine established a State Innovative Financial and Credit Institution to provide repayable or non-repayable loans under certain conditions.

4. Assessment of the attractiveness of the Ukrainian SE.

At the moment, there are several methods for evaluating the startup ecosystem in the world. The assessment of the ecosystem, by main components, industries, categories, is carried out to determine its state, phase, level of development and develop a strategy or program for the development of the SE. The need for startups, large firms, and the state to focus on the market of innovative business in the conditions of its dynamic development, determines the importance of conducting analysis and a comprehensive assessment of the startup ecosystem. To determine the appropriate approach for assessing the Ukrainian SE, the existing methods were considered (Table 2).

Table 2. Methods for evaluating the startup ecosystem

Methodology	Sequence of actions	Result
I. Methodology of the American startup accelerator Founder Institute	1. Choosing the optimal model for CE. 2. Collecting data on institutions in relevant industries. 3. Creating a complete CE structure of institutions in stages.	The complete structure of the national or regional SE.
II. Startup Genome organization methodlogy	1. Collect data by Category (productivity, State of industries, knowledge and talent base, funding, etc.). 2. Statistical analysis of data by Category. 3. Determining the development phase	The phase of CE development is defined.
III. Global Innovation Index	1. Collection of statistical data on 80 indicators of various categories (state institutions, infrastructure, human capital, and research, etc.). 2. Normalization of indicator values on a 100-point scale. 3. Aggregation of normalized values	The index that reflects the state and level of development of the country's innovation sector
IV. Startup Friendliness Index	1. Collect statistics related to categories. 2. Normalization of indicator values on a 100-point scale. 3. Aggregation of normalized values	The index that reflects the attractiveness of the ecosystem

Therefore, the existing methods for evaluating startup ecosystems are fragmentary, since they study ecosystems only from separate positions. Based on the considered methods and features of the Ukrainian economy, the following methodology for the assessment of the SE is proposed (Table 3).

The selection of indicators by categories and spheres was carried out, the normalization and aggregation of indicators were carried out according to the formulas (Table 4).

Table 3. A comprehensive methodology for assessing SE

	Sequence of actions
1. Determining the phase of SE development	1. Collection of data on relevant indicators for Ukraine and, for comparison, other ecosystems in different stages of development. 2. Comparative data analysis and conclusion.
2. Evaluating the attractiveness of the SE	1. Selection of indicators by category and area. 2. Normalization of indicator values. 3. Calculation of the SE score. 4. Comparison of ecosystems and innovation sectors of countries to determine Ukraine's position on the global innovation market.
3.1 Research of the state of science, science parks	1. Collecting data on indicators for recent years 2. Analysis and conclusion regarding the dynamics of indicator values.
3.2 Technology transfer	1. Data collection on technology transfer. 2. Analysis and conclusion regarding the dynamics of indicator values.
3.3 Venture capital	1. Collecting data on the state of venture fund assets, the number of transactions and investment volumes, and key internet segments. 2. Analysis and conclusions.
3.4 Incubation	1. Comparative analysis of programs.
3.5 State influence	1. List of the main state measures in this area.
3.6 Generalizations and conclusions	

Table 4. Normalized indicators by category and area

Scope/category	0-100	Scope/category	0-100
1. MARKET	34,9	4. INFRASTRUCTURE	36,9
1.1 Performance	30,6	4.1 Transport	30,6
1.2 Attractiveness	39,3	4.2 Energy and ecology	39,9
2. FINANCE	32,3	4.3 Information and communication technologies	40,2
2.1 Resources	23,2	5. HUMAN CAPITAL	41,6
2.2 System	41,4	5.1 Education and standard of living	32,7
3. "SPACE" FOR STARTUP DEVELOPMENT	32,1	5.2 Labor market	50,5
		6. STATE INFLUENCE	24,8
3.1 technology and science	32,1	6.1 Policy aspects	27,3
3.2 Business environment	32,1	6.2 Crime	22,3

On a 100-point scale, the overall attractiveness of the startup ecosystem in Ukraine is 33.7 / 100, inferior to most ecosystems in the world. It can also be noted that in countries with a high level of development of the innovation sector, SE is also more formed and stable.

4. Factors of development of the startup ecosystem in Ukraine.

The creation of a competitive SE is associated with many political and economic aspects. The formation of an appropriate environment for the development of startups should be part of an integrated long-term strategy for economic development and be based on the strengths and prospects of the Ukrainian economy, the scientific environment, the fiscal and educational systems [16]. Planning the development strategy of the Ukrainian SE can be based on the experience of successful countries in this aspect and should take into account the combination of the most influential factors (Table 5).

Table 5. Factors in the development of SE in different categories

Factors by level	The factors that determine the success (advanced) SE	Basic concepts for the development of SE
Level 1. Contextual factors: a) political and legislative, b) cultural and institutional; c) national and regional ***Level 2.*** Government support for research, funding, industry; personal support and support for organizations	- availability of the right personnel in the labor market; advanced technologies; access to capital; high-quality services of incubators and accelerators; corporations with open innovations; - culture of entrepreneurship; - promotion of business development; - well-established intellecttual property mechanisms; - access to the markets on an international scale and connectedness.	1) the concept of state impact: the availability of specialized; 2) the concept of free development

The promotion of systemic changes by the public sector in the organization of a competitive ecosystem should take place by international practice, and either the state or, by agreement, a set of private structures should initiate the formation of the SE. Most of the world's ecosystems have developed both under the influence of the state (especially in the phase of emergence) and based on entrepreneurial initiatives. At the same time, the absolute majority of ecosystems (including Silicon Valley, the ecosystems of Beijing, Tel Aviv, Berlin, Stockholm, Moscow, etc.) began to form on the state initiative [17].

Government measures and initiatives should promote the emergence of a community of startup founders who will work closely with other actors in the private sector of the economy and the public sector. At the same time, the state should not assume the role of a leader, but only an initiator. In Ukraine, the government has developed some initiatives to support startups, but they do not perform their functions properly. To bring coherence, organization, and transparency to the SE of Ukraine, the state should identify target groups and direct the available tools and possible measures to stimulate their development.

6. Conclusions

A startup can be started, but it cannot be implemented without the necessary infrastructure and comprehensive support at all stages of development. In Ukraine, the innovation sector is stagnating, but the startup ecosystem in the private sector of the economy is gradually growing.

The directions of stimulating the development of the startup ecosystem should be on the state initiative, which provides for a set of measures for five components. As a result of their implementation, a well-formed and controlled network of commercial and non-commercial structures that form the ecosystem of startups in Ukraine will be formed. In turn, this will allow the state to cooperate in a coordinated and effective manner with these structures, which will contribute to raising the Domestic SE to a new level of development.

7. References

1. Schwab k. The Fourth industrial revolution: K. Shvab. - M.: Publishing House "E", 2017 – 208 p.

2. Mercan B, Gortas D. Components of Innovation Ecosystems: A Cross-Country Study // International Research Journal of Finance and Economics, Vol. 76, 2011.

3. Smorodinskaya N. V. Network innovation ecosystems and their role in the dynamization of economic growth // Innovation. - 2014. - No. 7. - pp. 27-33.

4. Launchopedia financial direction web portal / launch of lifecycle financing. [Electronic resource]. - Access mode: https://fundingsage.com / startup-financing-tour-and zhy`ttyevogo life cycle financing / seed-stages/

5. Official web portal of the international research organization in the field of innovation Startup Genome. [Electronic resource]. - Access mode: https:// www.startupgenome.com/

6. The official web portal of the international research organization in the field of startup innovation is flashing. [Electronic resource]. - Access mode: https://www.startupblink.com/

7. Web portal of the Dutch Research Institute and accelerator startup Delta. [Electronic resource]. - Access mode: https://www.startupdelta.org/

8. Pilipenko B. venture capital as a source of financing for innovation processes. / B. Pilipenko-Kiev, 2015. - 273 P.

9. Web portal of a media resource Hubs.ua by business direction / Accelerator vs business incubator. [Electronic resource]. - Access mode: http://hubs.ua/starter/akselerator-vs-biznes-inkubator-21224.html

10. Official web portal of the state program of support for the development of startups of the Republic of Ireland Enterprises Ireland / support for startups from the Enterprise Ireland. [Electronic resource]. - Access mode: https://www.enterprise-ireland.com/en/Start-a-Business-in-Ireland/Startups-from-Outside-Ireland/Funding -and-support-for-startups-in-Ireland / government-support-through-enterprises-Ireland.html

11. Official web portal of the state statistics service of Ukraine. [Electronic resource]. - Access mode: http://www.ukrstat.gov.ua/

12. Zhavoronkova G. V. Tekhnologicheskaya bezopasnost Ukrainy I mirnoe Rynok tekhnologii [technological security of Ukraine and the world market of technologies]. – №4 (32). 2011 pp. 3-7.

13. Kvasova O. Razvitie Ven'churny bankovy investitsii V Ukrainy [development of venture banking investment in Ukraine]. – 2014. – №1 (66). - P.107

14. Web portal of the economic media resource Ekonomicheskaya Pravda Ukrainska Pravda / the first catalog of investors in Ukraine has been published [Electronic resource]. - Access mode: https://www.epravda. com.ua/rus/news/2017/04/5/623518/

15. Web portal of a media resource Ain.ua / Ukrainian startup incubators: what do they represent and what do they want in return? [Electronic resource]. - Access mode: https://ain.ua/2013/01/29/ukrainskie-startap-inkubatory-chto-predostavlyayut-i-chto-xotyat-vzamen/

16. Web portal of the American accelerator Found Institute/how to build your Local Startup Ecosystem. [Electronic resource]. - Access mode: https://fi.co/insight/how-to-build-your-local-startup-ecosystem

17. Official web portal of the European Union Innovation Support Program Horizon 2020. - Access mode: https://ec.europa.eu/programmes/horizon2020/en

A cybersecurity risk assessment

Valentina Petrova
Nikola Vaptsarov Naval Academy, Varna, Bulgaria
vmb75bg@gmail.com

Abstract: *The main purpose of this paper is to offer a data-driven approach to assess cyber risk and to ensure appropriate confidentiality, integrity, and availability. A study presents the decision hierarchical model of cyber security risk assessment based on AHP methodology and describes a quantitative measure for evaluating and ranking security incidents. It can be used to conduct cost-benefit analysis, design and optimize cybersecurity in the systems.*

KEYWORDS: CYBERSECURITY, AHP

1. Introduction

Cyber risk assessment requires defined and objective methodologies; otherwise, its results cannot be considered reliable. Too much subjectivity in the risk assessment process can weaken the credibility of the assessment results and compromise risk management programs [7, 13].

Defining reliable models for the cyber risk exposure is still an open problem. Existing models [1, 12] suffer from some important concerns that, for example, prevent the insurability market development [1].

This study presents a cybersecurity model to conduct a cybersecurity risk assessment. It demonstrates how to use AHP to perform risks assessment to prioritise risks in the systems. AHP risk assessment methodology is discussed extensively including how to structure risks in a hierarchy, make pair wise comparison to assess which cybersecurity risk is more important and calculate priority weight of the risks to organize risk ranking.

AHP methodology produces quantitative cybersecurity risk ranking which helps to prioritise the components of a system in terms of their level of vulnerability to an attack, and threats in terms of the danger they pose. Risk assessment assists the engineers with the development of security policies, with the design of secure system and with the rational allocation of scarce resources. It facilitates the communication between security, business and experts.

2. A multi-criteria decision-making approach

Cyber risk evaluation and the study of its related impact are performed mostly in qualitative ways, which are usually affected by errors and misrepresentations of the risk. They also exhibit several disadvantages, such as the approximate nature of the achieved results and the difficulty of performing a cost-benefits analysis [7]. The lack of quantitative data can be dangerous: if the assessment is entirely qualitative, subjectivity will loom large in the process [13].

This has created a multi-criteria problem, which can be solved using a multi-criteria decision making approach (MCDM) [4].

Table 1 Summary of applications of the DM techniques [3]

Method	Application	Percentage
AHP	128	32,57%
ELECTRE	34	8,65%
DEMATEL	7	1,78%
PROMETHEE	26	6,62%
TOPSIS	45	11,40%
ANP	29	7,38%
Aggregation DM methods	46	11,70%
Hybrid MCDM	64	16,28%
VIKOR	14	3,56%

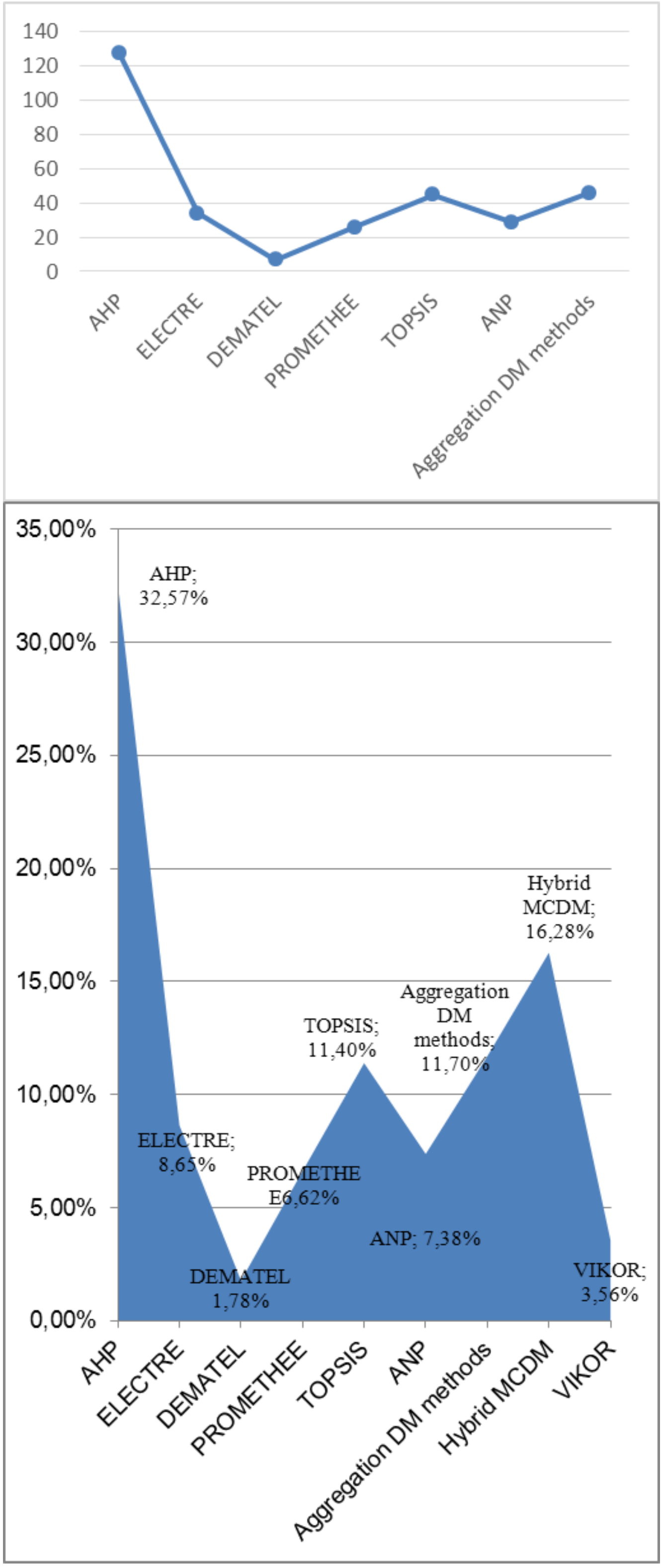

Fig. 1 Frequency of MCDM techniques and approaches

The selection process is based on a literature review and classification of international journal articles [3]. MCDM provides strong decision making (DM) in domains where selection of the best alternative is highly complex. MCDM method has been applied to many domains to choose the best alternatives. Where many criteria have come into existence, the best one can be obtained by analysing different scopes of the criteria, weights of the criteria, and the selection of the optimum ones using any MCDM techniques. Table 1 shows frequency of MCDM techniques and approaches. Based on the results presented in this table, a total of 393 studies have employed DM techniques and approaches. Table 1 and fig. 1 shows that AHP method (32.57%), and its applications have been used more than other tools and approaches.

AHP uses objective mathematics to process subjective preferences of a risk manager or a risk management group in determining the relative importance of risks [11].

3. An Analytical Hierarchy Process for cyber security risk assessment.

The process of risk assessment and treatment is fundamental to the implementation of an effective cyber security program and plays a crucial role for the national and international regulations in the field of data protection [7, 13].

The confidentiality, integrity and availability are considered the core underpinning of cyber security and the steps for achieving them are: determination of the affecting criteria, questionnaire collection and statistical analysis, weighting these criteria, evaluation of the entire performance according to these weighted criteria. The evaluation criteria used in this study are: attacks, vulnerabilities, penetration testing, threats, assets, security measures, unauthorized access, and security alerts. According to giving priority to criteria weight, the application allow to find best choice (Availability) and worst choice (Integrity) from all results shown in fig. 2.

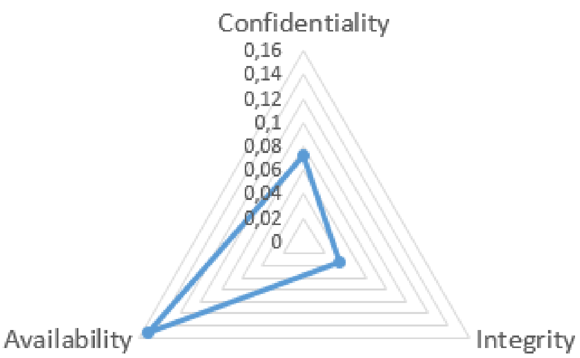

Fig. 2 Comparison of the alternatives

If the stakeholders' answers are evaluated with a more objective process, this will result in a more objective profiling of the company [7, 13]. This is the aim, which the author pursue by introducing the use of some data-driven key risk indicators.

Data-driven key risk indicators suppose that the author disposes a tool that monitors the company and returns a sufficient amount of quantitative evidences such as malicious code / software activity (i.e., malware, ransomware, botnet evidences); insecure / unencrypted / vulnerable protocols usage (i.e., P2P, vulnerable SSL, etc.); deep web exposure (company targeted by criminals); data breaches due to human errors, third parties, or hacking activity; software / infrastructure vulnerabilities [7, 13].

Quantitative risk assessments based on subjective criteria are effective when experts use:

- indicators and incidents to feed data into models;
- a vulnerability scale assesses and indicates how well prepared we are for a cyber risk event;
- measures for following factors: availability, frequency, confidentiality, integrity, and probability of a cyber risk occurring.

Cyber risks will be quickly rated on their potential impact.

An Analytical Hierarchy Process (AHP) represents the field of science called MCDA (Multi Criteria Decision Analysis), which is intended to assist the users in making decisions, defined as a subjective measurement of various preferences [9]. The main goal of the AHP method is dealing with complex decisions by giving them a rational structure, calculating the weight of the criteria and alternatives.

The AHP method is composed by the following stages:

Stage 1: The AHP was used to determine critical and vulnerable cyber security risks within systems based on a decision goal, criteria list and alternatives. The situation is to assess all cyber security risks and to prioritise inherent risks.

Goal: Identifying critical substations and estimating cyber security risks.

Criteria: The author proposed eight criteria named attacks, vulnerabilities, penetration testing, threats, assets, security measures, unauthorized access, and security alerts.

Alternatives: The alternatives are Confidentiality, Integrity, and Availability.

The confidentiality, integrity and availability are considered the core underpinning of cyber security. Security control and vulnerability can be viewed in light of one or more of these key concepts.

Stage 2: The decision hierarchical model of cybersecurity risk assessment

The criteria and alternatives are organized in a hierarchy. The hierarchy has three levels. The first level is the decision goal, the second level is the risks and the third level is the alternatives.

The hierarchical structure is defined and described to support cyber security. The complete hierarchical structure is illustrated in Figure 3:

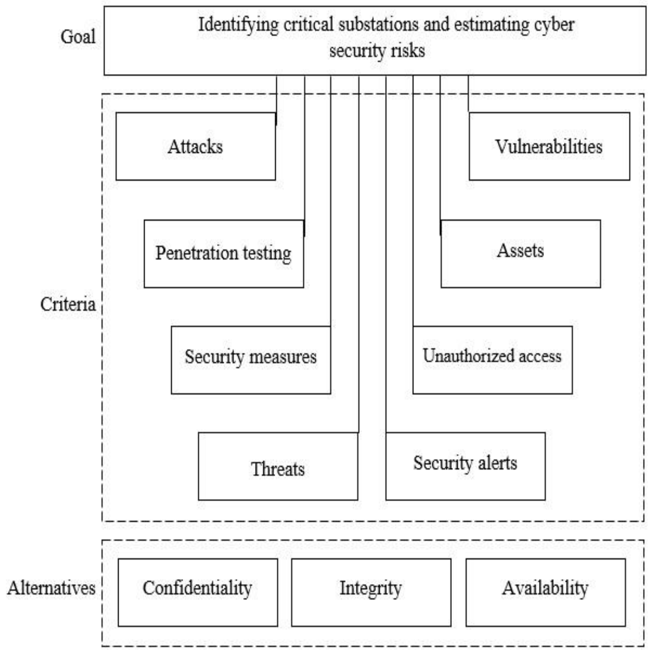

Fig. 3 The decision hierarchical model of cybersecurity risk assessment

The author presents the decision hierarchical model of cyber security risk assessment to evaluate and rank security incidents using the AHP whereby the eight decision criteria were the likelihood of an event and its consequences. The model reduces the number of risks and allows security analysts to focus on a critical incidents, which reduces the time and resources.

Stage 3: Mathematical implementation of the method Analytical Hierarchy Process.

Analytic hierarchy process (AHP) is a method of decision making using objective calculations based on evaluation of several criteria [10]. The AHP defines some stages of analysis [2, 6]: the hierarchical structures formulation, prioritization, priority weight calculation of each criteria or alternative, and consistency checking. The hierarchical structure is defined by considering the scope, objectives, criteria, relevant actors, and alternatives [10]. Priority is a value that determines the level of importance of an alternative or criteria [2]. AHP uses pair wise comparisons to assess the cybersecurity risks. The AHP defines pairwise comparison to determine priorities using a matrix to compare variable of the same level in pairs. Risk assessors decide which risk is more important and decide the strength of importance using a scale of 1 to 9. Comparisons were implemented using the Saaty preference scales [10]. Table 2 presents the comparison scale.

Table 2 Scale of the AHP Method [9]

Verbal Expression	Explanation	Scale	Reciprocal values
Equal importance	Two activities contribute equally to the objective.	1	1.000
Moderate importance	Experience and judgment slightly favour one activity over another.	3	1/3 (0.333)
Strong importance	Experience and judgment strongly favour one activity over another.	5	1/5 (0.200)
Very strong importance	An activity is favoured very strongly over another.	7	1/7 (0.143)
Extreme importance	The evidence favouring one activity over another is of the highest possible order of affirmation.	9	1/9 (0.111)
Intermediate values	The values are compromises between the previous definitions.	2	1/2(0.500)
		4	1/ 4 (0.250)
		6	1/6 (0.167)
		8	1/8 (0.125)

Priority weighting of each criteria or alternative is calculated using the Eigen value principle [4]. This can be defined as a geometric mean method. The accuracy of the decisions is measured by computing consistency ratio (CR) and Consistency Index. Consistency checking is performed to determine the likelihood of conflicting inputs. The inconsistency value should not be more than 10% [10].

All proposed criteria were accepted as important, but four of them were ranked above the average mark. These criteria are: attacks, vulnerabilities, threats, and assets. The final ranking of alternatives are shown in structured evaluation of confidentiality, integrity, and availability relative to the importance of the criteria in Figure 4.

According to some criterion, confidentiality is more advantage than the other alternatives. The result demonstrates that confidentiality is the most appropriate that meets the criteria.

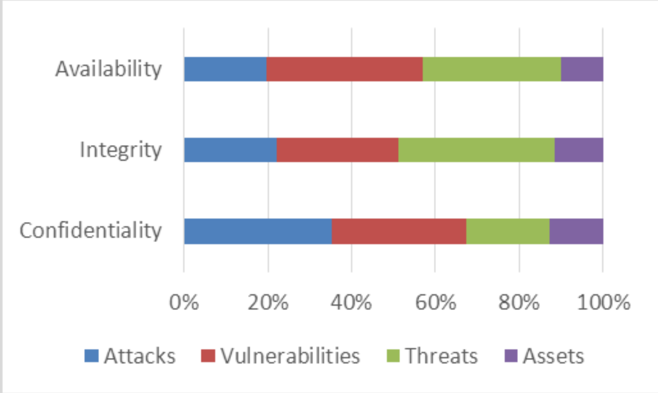

Fig. 4 Structured evaluation of confidentiality, integrity, and availability relative to the importance of the criteria

4. Conclusion

The author introduced the ASP methodology and described how it could be used to derive a quantitative measure for the cybersecurity risk assessment.

AHP methodology quantifies a cybersecurity risk assessment, helps to prioritise the components of a system in terms of their importance to the successful operation of the system, and improves subjective judgement by providing consistency in the cybersecurity risk assessment process.

A cyber security risk assessment methodology that may be exploited in the process of the design of instrumentation and control systems is suggested. The methodology outlines eight criteria that must be undertaken in order to conduct cyber security risk assessment during the system and component design, and equipment supply three stages. The paper describes the activities that must be undertaken during each stege.

This research recommends using more criteria in the future, and further integration of the method with other MCDM techniques and fuzzy methods to select and rank the best alternatives based on the identified criteria.

As subjects of future work are: vulnerabilities within the system will be identified and quantified using the Fuzzy Evaluation Method. An attack graph will be designed and used in order to find cyber scenarios, the probabilities of which will be also calculated.

5. References

1. Biener, C. ,M. Eling, and J. H. Wirfs, "Insurability of cyber risk: an empirical analysis," The Geneva Papers on Risk and Insurance—Issues and Practice, vol. 40, no. 1, pp. 131–158, 2015.

2. Ishizaka A., P. Nemery, Multi-criteria decision analysis methods and software, Chichester: John Wiley and Sons, (2013).

3. Mardani A., A. Jusoh, K. Nor, Z. Khalifah, N. Zakwan, A. Valipour, Multiple criteria decision-making techniques and their applications – a review of the literature from 2000 to 2014, Economic Research-Ekonomska Istraživanja, 2015.

4. Muhammad N., N. Cavus. Fuzzy DEMATEL method for identifying LMS evaluation criteria. 9th International Conference on Theory and application of Soft Computing, Computing with Words and Perception, 2017.

5. Naumov S. and I. Kabanov, "Dynamic framework for assessing cyber security risks in a changing environment," in Proceedings of the 2016 International Conference on Information Science and Communications Technologies (ICISCT), pp. 1–4, Tashkent, Uzbekistan, November 2016.

6. Petrova V., Using the Analytic Hierarchy Process for LMS selection, CompSysTech '19: 20th International Conference on

Computer Systems and Technologies, June 2019, Ruse, Bulgaria, Pages 332–336, ISBN: 978-1-4503-7149-0.

7. Rot, A., "IT risk assessment: quantitative and qualitative approach," in Proceedings of the World Congress on Engineering and Computer Science 2008 (WCECS 2008), San Francisco, CA, USA, October 2008.

8. Saaty, T.L., 1980. The Analytic Hierarchy Process. McGraw-Hill, New York.

9. Saaty T., Theory and Applications of the Analytic Network Process, RWS Publications, 2005.

10. Saaty T., L. Vargas, Models, methods, concepts, and application of the analytic hierarchy process, New York: Springer, 2012.

11. Sum, R., Risk Prioritisation Using The Analytic Hierarchy Process. Innovation and Analytics Conference and Exhibition (IACE 2015)AIP Conf. Proc. 1691, 030028-1–030028-8; doi: 10.1063/1.4937047

12. Ugur Aksu M., M. Hadi Dilek, E. Islam Tatli et al., "A quantitative CVSS-based cyber security risk assessment methodology for IT systems," in Proceedings of the 2017 International Carnahan Conference on Security Technology, pp. 1–8, ICCST, Madrid, Spain, October 2017.

13. https://doi.org/10.1155/2019/6716918